Department of Water Resources Engineering
Lund Institute of Technology
Lund University
Master Thesis
Report TVRL 2006:10

Climate Change Impacts on Groundwater Recharge in Gulf Islands, Canada

Emmanuel Kwame Appiah-Adjei
Lund, 2006

Supervisor:
Dr. Diana Allen
Department of Earth Science, Simon Fraser University, Canada

Report TVRL 2006:10

Master of Science Thesis in Water Resources

Department of Water Resources Engineering

Lund Institute of Technology, Lund University

Box 118

221 00 Lund

Sweden

Phone: +46 46 222 000

ABSTRACT

With significant changes expected in the earth's global climate over the next century, due to global warming, and its resulting changes in the frequency and amount of precipitation, there has been growing concerns on climate change impacts on water resources. Especially concerned to water managers and governments is the potential impacts on groundwater aquifers since they are the main available source of potable water supply worldwide.

This research, therefore, investigates the potential impact of climate change on groundwater recharge to the fractured bedrock aquifers, which serve as the main source of potable water supply to the inhabitants of Gulf Islands in BC, Canada. Using Statistical DownScaling Model (SDSM) in combination with the LARS-WG stochastic weather generator, daily current and future (i.e., 2010-2039, 2040-2069, and 2070-2099) climate data were generated from CGCM1 predictions of the study location. These predictions were used as input to the HELP hydrologic model for estimation of recharge for the different climate change periods. The main properties of the aquifer -soil permeability, aquifer permeability and water table depth- used for recharge modeling were linked to ArcGIS for generating recharge zones, which allowed spatial and temporal integration of the recharge results.

The combination of SDSM and LARS-WG in downscaling and predicting both the observed monthly temperature and precipitation was very successful. Mean annual precipitation downscaling with SDSM is predicted to increase by 52%, 65% and 88% relative to the observed for 2020's, 2050's and 2080's, respectively. On the other hand, the mean monthly temperature is predicted to rise by 1.14^{o}C in 2020's, 2.05^{o}C in the next 30 years and up to 3.5^{o}C by the end of the century. According to HELP, the current mean annual recharge is about 44 % of the annual precipitation and is predicted to increase progressively by 7%, 8% and 9% in the 2020's, 2050's and 2080's, respectively, from the current.

ACKNOWLEDGEMENTS

Sincere thanks to my supervisor, Dr. Diana Allen, of the Department of Earth Sciences at Simon Fraser University (SFU), Burnaby, BC, Canada, for the motivation, advise, explanations and all the materials made available to me in bringing out this thesis. I appreciate, very much, the time spent on me and the opportunity to experience a different culture and acquire new knowledge in my graduate studies.

Heartfelt gratitude is also expressed to the administrative staff, computer technicians and the graduate students, especially my colleagues at Dr. Allen's laboratory, for their support in various ways throughout my stay at the department. Special thanks to Mike Toews and Jessica Liggett for your wonderful assistance with my numerous questions, computer problems, and giving me the needed introduction to the use of ArcGIS. I am also grateful to Mary Ann Berg for offering me free initial accommodation on arrival at SFU.

My deepest appreciation and thanks go to the administrative staff -Dr. Joakim Malm, Prof. Rolf Larsson and Anna Carlqvist- and fellow students of the Water Resources programme in Lund University, Sweden for their support and encouragement in my decision to travel this far, Canada, for my thesis. Special thanks to Dr. Cintia Uvo for accepting to be the examiner of this thesis work.

Lastly, my sincere gratitude to my family and all friends back home, Ghana, and abroad who contributed in diverse ways towards the successful completion of this thesis and my entire graduate studies. I am especially grateful to Mr. Solomon Asomaning, my uncle, for all his concern and willingness to support me financially whenever needed. God richly bless you all.

Emmanuel Kwame Appiah-Adjei
May 2006, Lund

TABLE OF CONTENTS

LIST OF FIGURES

LIST OF MAPS

LIST OF TABLES

CHAPTER 1. INTRODUCTION

1.1 BACKGROUND

Projections from the Intergovernmental Panel on Climate Change (IPCC) experiment in 1995 and other widely respected Global Climate Models (GCMs) shows significant global warming and alterations in frequency and amount of precipitation from year 2000 to 2100 (Hengeveld, 2000; Mearns *et al*., 2001). These changes in global climate, expected to affect the hydrological cycle, may alter surface water levels and groundwater recharge to aquifers with various other associated impacts (e.g., sea water intrusion, water quality deterioration, potable water shortage, etc.) on natural ecosystems and human activities (Mearns *et al*., 2001). Although the most noticeable impacts of climate change could be changes in surface water levels and quality (Winter, 1983), the greatest concern of water managers and governments is the potential decrease and quality of groundwater supplies, as it is the main available potable water supply source for human consumption and irrigation of agriculture produce worldwide (Bear and Cheng, 1999). The groundwater aquifers are recharged mainly by precipitation or through interaction with surface water bodies; hence climate change influence on these (i.e., precipitation and surface water) ultimately affects groundwater systems.

Aside climate influence, recharge to aquifers is very much dependent on the characteristics of the aquifer media and the properties of the overlying rocks and soils. Several physical, chemical, and modeling approaches can be used to estimate recharge on the basis of surface water, unsaturated zone, and groundwater data (Scanlon *et al*., 2002). Among these approaches, modeling is the only tool that can predict recharge, and it is also extremely useful in isolating the relative importance of different controls on recharge, provided that it properly accounts for the all process involved. The accuracy of recharge estimations depend largely on the availability of hydrogeologic and climatic data. However, the heterogeneous nature and, often, less knowledge of the recharge flow paths makes recharge estimation through modeling very challenging and a difficult task (McCarthy *et al*., 2001; York *et al*., 2002). Notwithstanding these problems, modeling has been used to study recharge rates and patterns reasonably well in porous aquifer media (Scalon *et al*., 2002; Allison, 1988). On the other hand, quantifying recharge rates and patterns in fractured systems are less studied and poorly understood (Cook and Robinson, 2002; Scalon *et al*., 2002).

A Canada-wide evaluation of climate change and variability showed significant expected impacts on hydrologic systems (GCSI and Environment Canada, 2000). In British Columbia (BC), groundwater management is among the most important water issues. Although the province is one of the largest users of groundwater, not enough research has been undertaken to determine the sensitivity of groundwater systems to changes in critical input parameters like precipitation and runoff (e.g., Whitfield and Taylor, 1998). More so, the few research studies in the province dealing with groundwater sensitivity to climate change have been conducted on alluvial aquifers (e.g., Allen *et al*, 2004a; 2004b), with relatively little research on fractured aquifers, which serve the water needs of a very significant amount of the populace in the province.

1.2 PURPOSE AND OBJECTIVES

The main purpose of this thesis is to investigate the potential impacts of climate change on groundwater recharge to the aquifers of Gulf Islands in BC, Canada. Groundwater aquifers located in fractured bedrock on the islands provide the main source of sustainable potable water supply for the inhabitants. However, the potential impacts of climate change may pose a threat to the sustainability of the groundwater. With increasing development -both permanent and temporary residences for recreational purposes during summer seasons- on the islands, there is a need to investigate how future climate change patterns could affect the islands' groundwater systems. The outcomes of such an investigation could aid in efficiently managing the water resources of the islands, and allow for mitigative action to avoid future water problems.

Therefore, the objectives of this research are to:

- Analyze the historical climate data for the Gulf Islands and identify a representative climate station;
- Quantify how the climate of the islands would change in the next 100 years according the Canadian Global Coupled Model 1 (CGCM1) time period predictions on the islands;
- Quantify how the change in climate for the different CGCM1 predictions would affect recharge to islands' aquifers; and
- Assess the impacts that climate change would have on groundwater systems of the islands.

1.3 SCOPE OF WORK

The scope of work involves generating daily current and future climate data and using these data to drive a recharge model -US Environmental Protection Agency's Hydrologic Evaluation of Landfill Performance (HELP) model (Schroeder *et al*., 1994). Spatially-distributed current and future recharge is mapped in GIS for both current and future climates. The methodology employed is similar to that used for modeling recharge to the Grand Forks aquifer by Allen *et al*. (2004b), but with some modifications, specifically with regard to consideration of fractured rock in the recharge models. A detailed overview of the methodology is presented below.

Observed climate

1) Download daily precipitation (P) and temperature (T) data from the Environment Canada website for the major weather stations on the Gulf Islands and nearby Vancouver Island (e.g., Victoria International Airport).
2) Quality check and verify data for missing values. Insert missing dates and pad missing values with 999.

3) Calculate and graph monthly normals of P and T for the weather stations.
4) Compare graphs and select a representative station for the Gulf Islands.
5) Obtain sunshine hours directly from Environmental Canada for the representative station. No solar radiation data are available on-line.

Statistical DownScaling Model (SDSM) – downscaling

1) Download, install, register and learn SDSM.
2) Download CGCM1 data sets comprising National Centre for Environmental Prediction (NCEP) re-analysis calibration data and all the CGCM1 scenarios from the Canadian Institute for Climate Studies (CICS) website.
3) Reformat the observed P and T data to .DAT format files as is required for SDSM analysis.
4) In SDSM, verify the quality of the data.
5) In SDSM, analyze and generate statistics for P and T.
6) Screen variables for regression with P and T, correlation matrix (conditional for P, unconditional for T).
7) Calibrate model to P and T separately using predictor variables from the NCEP data set.
8) Analyze calibration results and compare to observed historical climate in terms of: mean, min, max, median, variance (and for P only: % wet days, dry and wet spell lengths) at each step a file is generated.
9) Generate weather data using the CGCM1 predictors for each CGCM1 time period (i.e., current, 2020s, 2050s, and 2080s).
10) Analyze all outputs in SDSM (i.e., compute statistics in SDSM).
11) Import all analysis results to Excel spreadsheet and compare output results.

12) Export all P and T SDSM downscaled output to separate files for use in LARS-WG. These include shift factors for future climate scenario generations.

LARS-WG: stochastic weather generator

1) Download, install, register and learn LARS-WG.
2) Reformat observed P, T and sunshine hours to the form required by LARS-WG.
3) Reformat P and T data from SDSM outputs for use in LARS-WG.
4) Calibrate LARS-WG to observed historical data.
5) Test model fit to observed historical data using statistics.
6) Set up current and future time period scenario files from the SDSM results.
7) Generate weather data for current and future time periods using the scenario files.
8) Export data to SDSM and perform statistics similar to that performed on original SDSM output. The statistical analysis can also be performed in Excel Spreadsheet.
9) Compare statistical results of LARS-WG output with SDSM output and the observed data.
10) Reformat LARS-WG outputs for use in the HELP model.

HELP

1) Compile and reclassify soil, aquifer permeability, slope, and water table depth information previously collected for the Gulf Islands.
2) Create representative vadose zone columns for the Gulf Islands from a combination soil class, aquifer media class and water table depth class.
3) Run the WGEN weather generator in HELP, but replace generated weather with the formatted LARS-WG output. Note WGEN was previously found

to be inferior to LARS-WG for generation of representative stochastic weather (Allen *et al*., 2004b).

4) Run HELP model, and evaluate output (graphs and statistics).

5) Repeat steps 1 to 4 for all climate time periods.

ArcGIS

1) Create recharge zones in ArcGIS to reflect the different combinations of soil type class, aquifer permeability class and water table depth class for the Gulf Islands, based on GIS datasets and a water well database.

2) Develop a spreadsheet for analyzing recharge results and formatting to the requirements of ArcGIS.

3) Link the recharge tables (monthly) to polygons of recharge zones, and map recharge monthly and annually for all climate scenarios (i.e., CGCM1 time periods).

1.4 THESIS OUTLINE

This thesis consists of six main chapters. Chapter 1 discusses the background and purpose of the thesis, as well as provides an outline of the methodology used. Chapter 2 describes the general setting and physiography, bedrock geology and surficial material, hydrogeology and recharge, and climate of the Gulf Islands. Also, a comparison of the climate data from all the islands is undertaken, and a representative weather station chosen for the Gulf Islands. Chapter 3 focuses on downscaling and generating daily precipitation and temperature values for current and future time periods from their corresponding CGCM1 scenarios. A description of the weather inputs generation, using LARS-WG, and the aquifer inputs derived from the available well database of the study area for HELP recharge estimations are presented in Chapter 4. Recharge results are discussed in Chapter 5. Finally, some concluding remarks are provided in Chapter 6.

CHAPTER 2. THE GULF ISLANDS STUDY AREA

2.1 GENERAL SETTING AND PHYSIOGRAPHY

The Gulf Islands, Canada, are located to the southeast of Vancouver Island, BC and lie to the north of the Canada-United States international border adjacent to the San Juan Islands, USA (Figure 2-1). The islands, comprising Mayne, Gabriola, Pender, Galiano, Saturna, Saltspring, and other smaller islands, are situated in the Nanaimo Lowland subdivision of the Georgia physiographic unit (Holland, 1976).

The islands (359.1 km^2 in area) cover about 3.8% of the total land area of the entire province of BC, and have a total population of 14,622, representing 0.3% of the total BC population (BC STATS, 2004). Majority of the population lives along the coast of the islands, which is more highly developed relative to the inland areas. Land use during the time of early settlement was predominantly agriculture, but has changed to dominantly residential in recent years, with only a few areas supporting agricultural activities. The population on the islands increases significantly during the summer months, and on weekends, as part-time residents and tourists arrive for vacation and recreational purposes. Public access to the islands from the surrounding cities, and between islands, is mainly by ferry; other private means of transportation like canoes, powerboats, kayaks, water taxis, and airplanes are also used.

Topography and landforms of the area are a general reflection of the underlying bedrock structure and the various surficial and geological processes that have occurred in the area in past geologic times (Figure 2-2). Common landforms include ridges, separated by narrow valleys, which were created by intense folding and differential erosion of the underlying bedrock formations. Generally, the ridges have steep descents on one side and gentle slopes on the other side, and are capped by more resistant rock formations (sandstone and conglomerate), whereas the valleys have been eroded out of the least resistant mudstone formations.

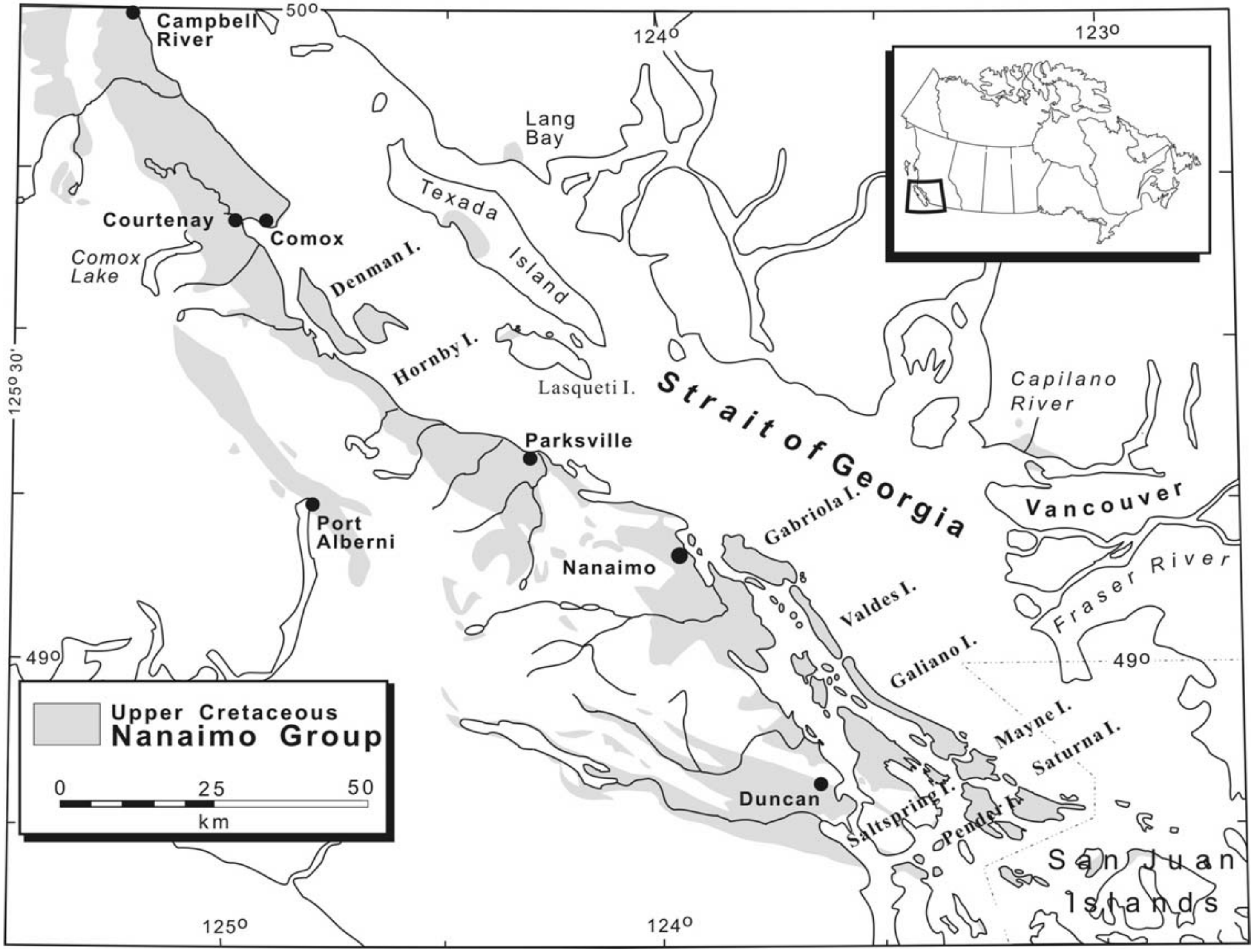

Figure 2-1: Location map of the Gulf Islands showing the exposure of the Nanaimo Group. Geology from Mustard, 1994.

Elevation of the region ranges from sea level to 450 m in the southern portion (e.g., Saturna Island and Saltspring Island), and to 150 m in the northern portion (van Vliet *et al*., 1987; 1991).

Figure 2-2: Aerial photo of the Gulf Islands illustrating the topography, which is a reflection of the underlying bedrock structure and the various surficial and geological processes that have acted in the past.

2.2 CLIMATE

The climate of Gulf Islands region is strongly influenced by the rain-shadow effects of the Olympic Mountains to the south in Washington, USA, and by the mountains of Vancouver Island to the west, and is moderated by the ocean (Holland, 1976). The climate is characterized by cool, dry summers and humid, mild winters (van Vliet *et al*., 1987; 1991).

Historic weather data, comprising observed daily and monthly temperature and precipitation values from weather stations situated on the major islands in the study area were analyzed for the purpose of finding a weather station that is representative of the islands' climate. Adequate data (i.e., data with a long period of record (POR)) were required for comparison to downscaled climate data. Observed historic data from the weather stations, assumed to be representative of each of the islands, were downloaded from the Environmental Canada website (2005). A summary of the weather station information is provided in Table 2-1. Initial analysis of the raw data showed that there was either too short a POR (less than 30 years of continuous data) or too many missing data, and in many situations, both. Thus, for the purpose of this study, there was a need to explore nearby weather stations with climatic conditions similar to Gulf Islands.

Table 2-1: Weather station information on the islands.

Station Name	**Latitude**	**Longitude**	**Climate Identifier**	**Elevation (masl)****
Galiano North	48° 99'	-123° 57'	10130MN	6.0
Saturna Island CS	48° 78'	-123° 05'	1017101	24.4
Saltspring Island SM	48° 89'	-123° 55'	1016995	45.7
Mayne Island	48° 84'	-123° 32'	1014931	28.0
North Pender	48° 81'	-123° 32'	1015638	15.0
Gabriola Island	49° 15'	-123° 73'	1023042	6.0
*Victoria Int'l Airport	48° 65'	-123° 43'	1018620	19.2

*representative weather station

** metres above sea level

Figures 2-3 and 2-4 show graphs of calculated mean monthly temperature and precipitation, respectively, for the various stations. Mean monthly temperature and precipitation were calculated based on a 15 and 20 year period, respectively, rather than the standard 30 years period (Environment Canada climate normals), due to many years of missing data. Average monthly temperature and average monthly precipitation were also calculated for all islands combined, and are shown on these graphs for comparison.

Mean monthly temperature on the islands generally ranges between 3.66°C to 4.23°C in the winter season (i.e., November, December and January), increasing to a range of 16.98°C to 18.39 °C during the summer months (June, July and August). January is the coldest month on the islands, with a mean minimum temperature of 3.66°C, whereas the warmest month is August, with a maximum mean temperature of 18.39°C. Gabriola Island has slightly lower temperature conditions throughout the year, whereas Saltspring Island experiences warmer temperature conditions compared to the other islands (Figure 2-3).

Mean annual precipitation on the islands ranges from 658mm to 983mm, with the lowest annual precipitation recorded at Saturna Island and the highest on Saltspring Island. Monthly minimum precipitation (23 mm on the average) on the islands falls in July, whereas the monthly maximum (143 mm on the average) mostly falls in November each year (Figure 2-4). About 80% of the mean annual precipitation falls in the months of October to April, and less than 10% of the mean annual precipitation falls during the summer period. The reduced precipitation in the summer season is partly attributed to the 'rain-shadow effect' created by the Olympic Peninsula of the USA to the south and the mountains of the Vancouver Island, BC to the east.

The Victoria International Airport station was selected as the most representative of the islands because it has a good historic dataset, with only few missing values. A general comparison of the temperature conditions at Victoria Airport to that of the islands' average shows a similar pattern (Figure 2-5), but is up to about 5% lower than islands' average. Average monthly temperature for the islands in the first half of the year (January to June) approximately matches that of Victoria, but is slightly higher than Victoria in the latter half (July to December). The mean monthly temperature at the Victoria Airport during the winter season ranges between 4.23-4.89°C, increasing to a range of 14.73-16.67°C in the summer months.

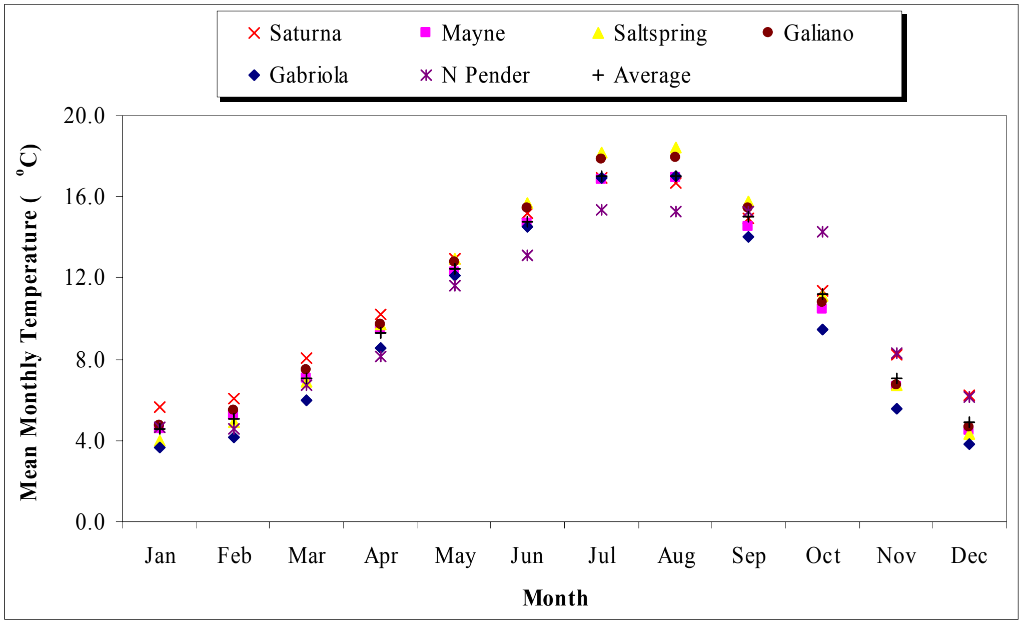

Figure 2-3: Calculated mean monthly temperature for the POR 1985-2000.

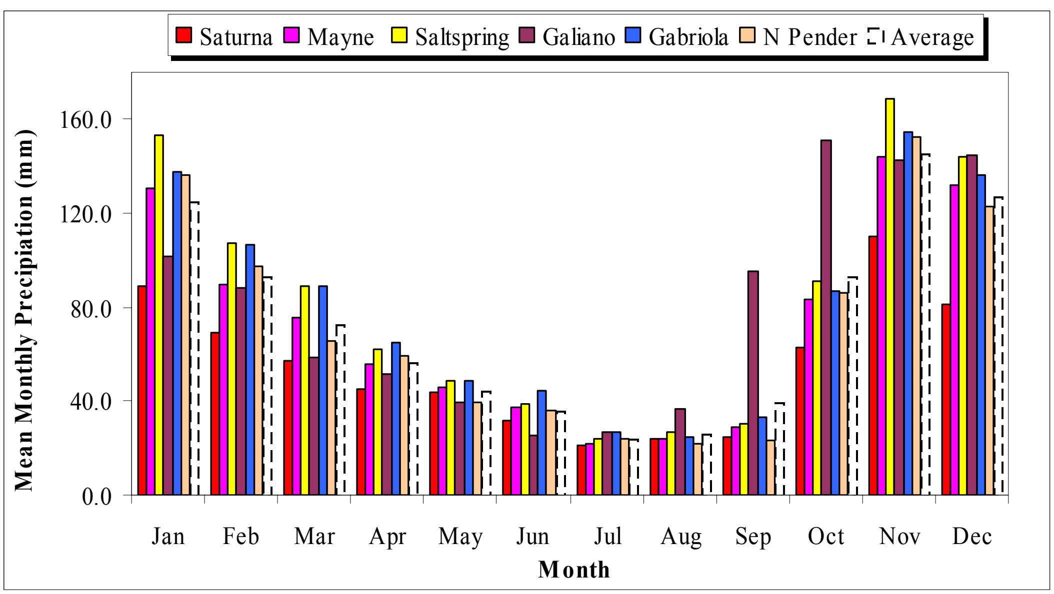

Figure 2-4: Calculated mean monthly precipitation for the POR 1981-2000.

The mean annual precipitation at Victoria is 891mm, and is about 10% higher than that of the islands' average. Mean monthly precipitation from April to October on the islands is higher than in Victoria, whereas it is the reverse from November to

March (Figure 2-6). The above analysis clearly indicates that the climatic conditions of Victoria Airport are similar to that of the Gulf islands, with some minor variation. Hence the daily weather data from the Victoria Airport was used to represent the Gulf Islands for climate scenario generation and recharge modeling.

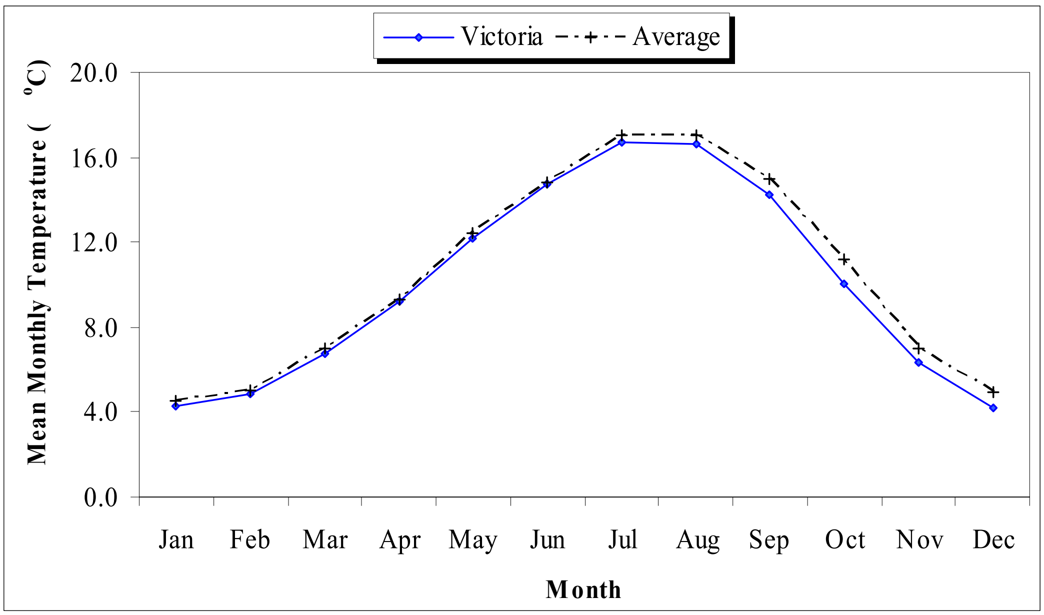

Figure 2-5: Mean monthly temperature at Victoria Airport compared to the average monthly temperature for all islands combined.

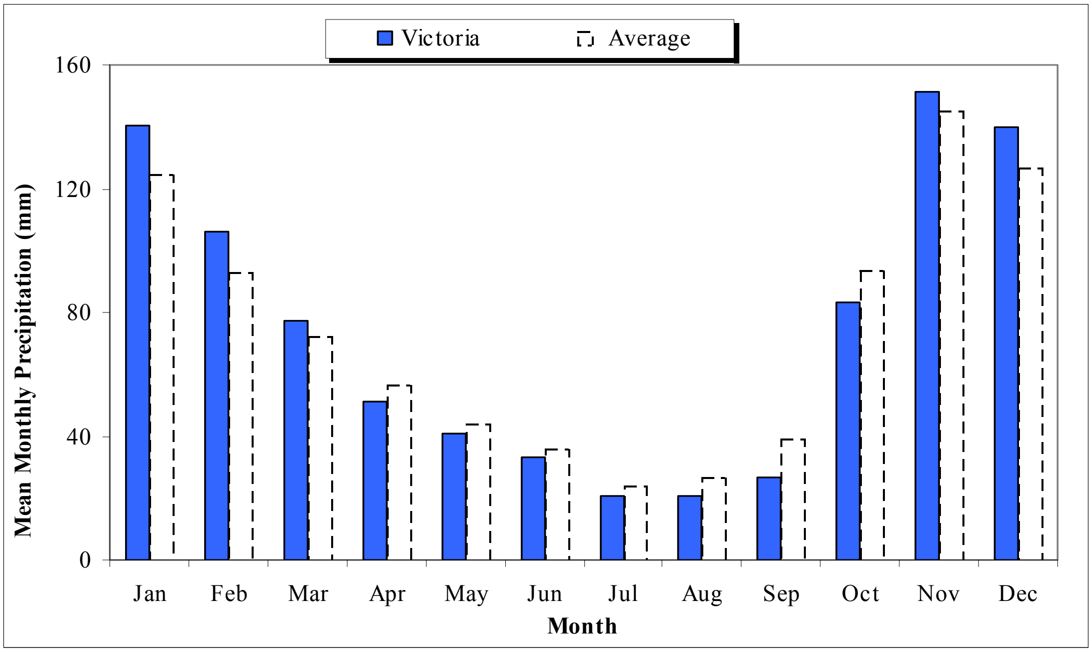

Figure 2-6: Mean monthly precipitation at Victoria Airport compared to the average monthly temperature for all islands combined.

2.3 BEDROCK GEOLOGY AND SOILS

The Gulf Islands are underlain by a conformable sequence of marine and non-marine sedimentary formations of Late Cretaceous age, known as the Nanaimo Group (see Figure 2-1). The Nanaimo Group formations consists of sandstone, mudstone (commonly referred to as shale), siltstone, conglomerate, and, very rarely coal (Muller, 1977; van Vliet *et al.*, 1991). Commonly exposed on the islands are the conglomerates, sandstones, mudstones and siltstones (Figure 2-7 and 2-8). The Nanaimo Group underwent a series of compressional deformations, uplift and differential erosion during the Middle Eocene and Neogene geologic periods, which resulted in the formation of fractured syncline and anticline combinations as well as regional faults. Evidence of these past geologic activities is seen in the commonly-exposed alternating layers of sandstone, siltstone and some conglomerate on the side slopes of ridges. The bedrock strata dip gently, but steeply in fault zones (Figure 2-9), in the northeast direction. Most folds on the islands are associated with longitudinal and cross faulting (Muller and Jeletzky, 1970; Mustard, 1994).

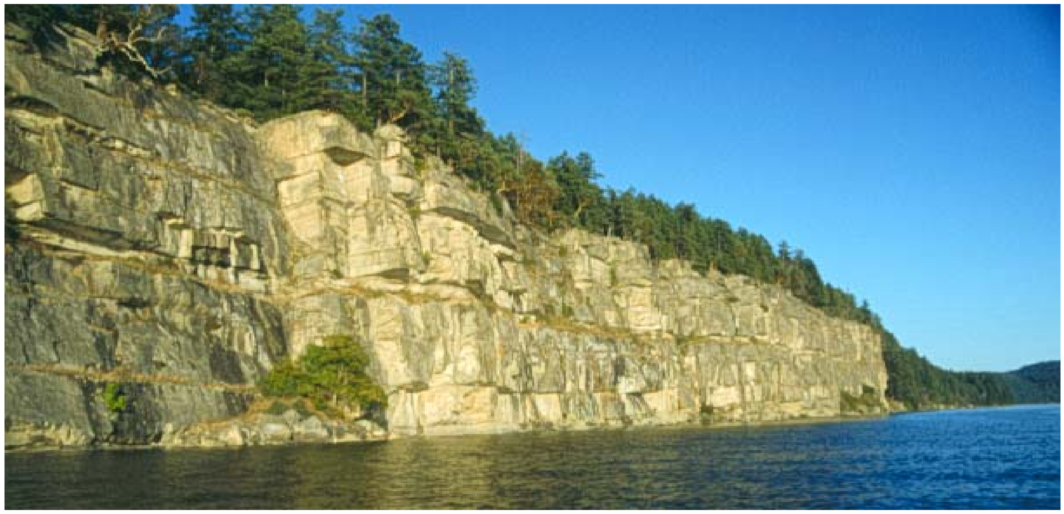

Figure 2-7: Sandstone exposure showing widely spaced bedding perpendicular joints (fractures).

Figure 2-8: Mudstone unit showing dense fracturing.

Figure 2-9: The Harris Fault on Saturna Island is highly weathered and creates a topographic depression.

Most of the soils on the islands were originally transported and deposited by glaciers, rivers, lakes and the sea during the last glaciation, some 15,000 to 25,000 years ago. Only a few of the soils have developed on recent fluvial materials, shorelines, organic deposits, and on colluvial and glacial till deposits of the sloping topography (van Vliet *et al*., 1987; 1991; Mathews *et al*., 1970). Low-lying coastal areas are covered by glaciomarine drift, beach materials, till and/or glaciofluvial/fluvial sand and gravel. Higher elevations (i.e., about 600-900 m above sea level) within the region are covered by till or colluviated till, glaciofluvial sand and gravel, and more recent colluvium (Blyth and Ruther, 1993). The thick mantle of till deposits during the last glaciation has been eroded from the upland areas, exposing the underlying bedrock, with only some small pockets remaining on protected side slopes of the ridges. Deeper till deposits, occurring in the lowland areas of the islands, are often covered by shallow, coarse- and fine-textured marine deposits. Fine- to moderately fine–textured deposits are found in depression areas and basins (van Vliet *et al*., 1987; 1991). General sediment thickness varies from very thin (i.e., few centimeters) on topographically high areas along the slope of the hills to several meters thick in some of the low-lying areas and valleys.

2.4 HYDROGEOLOGY AND RECHARGE

Surface water drainage on the islands is limited, and consists of small creeks and several small ephemeral streams. Commonly found in the area, however, are swamps located at both low and high elevations (Allen *et al.*, 2001). Reduced precipitation during the summer months, coupled with high temperature conditions, often leads to drying up of the surface water bodies, making groundwater storage the most common source of sustainable potable water supply for the inhabitants on the islands; although groundwater storage is also affected by low summer precipitation and high groundwater extraction rates.

The most highly productive aquifers of the islands are associated with the fractured areas near fault zones, and at the contacts between the mudstone and sandstone formations (van Vliet *et al*., 1987; 1991; Mackie, 2002). This is due to the very low primary porosity/permeability of the Nanaimo group of rocks. Water availability on each of the islands is, therefore, very much dependent on the presence of fractures in the bedrock formations, their size, abundance, orientation, and the type of fracture infilling.

The unconsolidated surficial materials do not constitute any major aquifers in the area, but in few locations with several meters of sediment depositions, shallow dug wells yield potable water for supply to family units.

Foweraker (1974) reported that all recharge to the groundwater system comes from precipitation that falls during late fall and winter months. He proposed that the rate at which precipitation recharges the aquifer depends on the nature (consolidated or unconsolidated, particle size distribution, and mineralogical content) and thickness of surficial deposits, vegetation cover, and the presence of preferential flow paths. Foweraker (1974) suggested that the thickness and nature of surficial materials (soils) tend to be the major controlling factor on precipitation infiltrating and percolating into the subsurface, because the bedrock formation in the area is mainly fractured. However, Mackie (2002) suggested that the bedrock is variably fractured with the interbedded sandstone and mudstone zones offering the greatest permeability, due to the higher intensity of bedding perpendicular to joints, compared to massive sandstone. Furthermore, Mackie (2002) also suggested that discrete fractures and fault zones would be primary sites for infiltration given their high intensity of fracturing. The vegetation of the islands has been disturbed extensively by logging and fire (Eis and Craigadallie, 1980); hence it has less influence on the infiltration and subsequent recharge to the aquifer. High topographic areas are thought to act as recharge zones, with the lowland coastal areas serving as discharge zones. Coincidently, most of the drilled wells in the area are situated along the low-lying coastal areas mainly because of development preference.

CHAPTER 3. CLIMATE CHANGE MODELING

3.1 CLIMATE MODELS

Climate models are tools for studying local, regional or global climate behaviour and its variability over changing conditions on the Earth. They come in different forms, ranging from simple models of the energy-balance type to comprehensive three-dimensional general circulation models or global climate models (GCMs). Simple climate models are useful in studying climate sensitivity of a particular process over a wide range of parameters (an example is in the preliminary analysis of climate sensitivity to various emission scenarios) or when used as components of integrated assessment models, like the analyses of the potential costs of emission reductions or impacts of climate change (Mearns *et al*., 2001).

GCMs are the most sophisticated tools available for accurate simulation of the current global climate and future climate scenario projections. Their formulation usually takes into account the behavior and interaction of flow systems in the biosphere, hydrosphere, cryosphere, atmosphere and geosphere in the climate system. GCMs are cartesian point models and are run at different horizontal and vertical resolutions for use in different parts of the world; the resolution of any particular model depends on the technical details used in its formulation and the model's intended application (Wikipedia, 2005). Available models in use in various regions of world include:

1. CCSR/NIES AGCM + CCSR OGCM Models by the Center for Climate System Research & National Institute for Environmental Studies;
2. CGCM1 and CGCM2 by the Canadian Center for Climate Modelling and Analysis (CCCma);
3. CSIRO-Mk2 by the Commonwealth Scientific and Industrial Research Organisation;

4. HADCM3 by the Hadley Center for Climate Prediction and Research in UK;
5. GFDL Model by the Geophysical Fluid Dynamics Laboratory of the National Oceanic and Atmospheric Administration in United States;
6. ECHAM4/OPYC Coupled Model by the Max Planck Institute für Meteorologie in Germany.

In this thesis, current and future climates for the Gulf Islands are simulated using the first version of the Coupled Global Climate Model (CGCM1) predictor variables. The choice of CGCM1 is based on its wide recognition as one of the leading performers in climate simulation (Hengeveld, 2000), and its successful use in similar research in southern British Columbia (e.g., Allen *et al*., 2004b).

3.2 THE 1ST COUPLED GLOBAL CLIMATE MODEL

Details of CGCM1 are fully described by Flato *et al.* (2000) and Hengeveld (2000). The model is made up of four main key components, namely:

1. an atmospheric general circulation model with 10 vertical levels and a horizontal resolution of approximately 3.7° of latitude and longitude (i.e., about 400 km);
2. an ocean general circulation model with 29 vertical layers, horizontal resolution of about 200 km, and capable of reproducing large-scale features of the ocean circulation as well as important water properties, such as temperature and salinity;
3. a thermodynamic sea ice model that allows ice to grow and melt in response to heat exchanges with the ocean and the atmosphere; and
4. a simple land surface model, which calculates runoff and soil moisture on the basis of the balance between precipitation, surface evaporation, and the water holding capacity of the soil.

A description of four ensembles of transient climate change simulations performed with the model is presented in Boer *et al*. (2000a). Three of these simulations used an effective greenhouse forcing change (i.e., greenhouse gas plus aerosol, GHG+A), corresponding to that observed from 1850 to 1990, and a forcing change, corresponding to an increase of CO_2 at a compounded rate of 1% until year 2001. The fourth considered the effect of greenhouse forcing only (GHG). The four forcing scenarios for the simulations were similar to the standard scenario (IS92a forcing scenario) set up by the Intergovernmental Panel on Climate Change (IPPC) for global climate studies, which allowed the results to be compared to others around. The IS92a scenario forecasts an increase in greenhouse gas emissions over the next century, based on estimated changes in energy demand, population growth, and other factors.

Boer *et al*. (2000a) reported that the simulation with GHG overestimated the amount of global temperature change by 0.8°C higher than observed since 1900. A comparison of all the GHG+A simulated (using both greenhouse gases and aerosols) and the observed global annual surface temperature anomaly from 1900 to 1990 showed an overall agreement in trend, and found the magnitude of the stochastic inter-annual variability to be the same (Hengeveld, 2000; Jones, 1994). In both the GHG+A and observed, the mean global temperature increase for the 20th century is roughly 0.6°C, although the model results underestimate the average global temperatures in the middle of the century. Global precipitation patterns also appear to be reproduced realistically, although they were more difficult to evaluate than temperature and pressure.

Projected changes in CGCM1 global surface temperature compared with observed trends, IPCC estimates from an experiment conducted in 1995, and other available models are presented in Figure 3-1. The projections shows significant warming from 2000 to 2100 by all the models, with temperature increases for this century generally above the IPCC range of 1-3.5°C (Figure 3-1). The CGCM1 simulated estimates remain close to the upper limit of the IPCC estimates until about 2060, like the other models. However, the projections of the various models begin to diverge, with the CGCM1 showing more warming by 2100 than either the IPCC estimate or the other two models whose experiments extend that far.

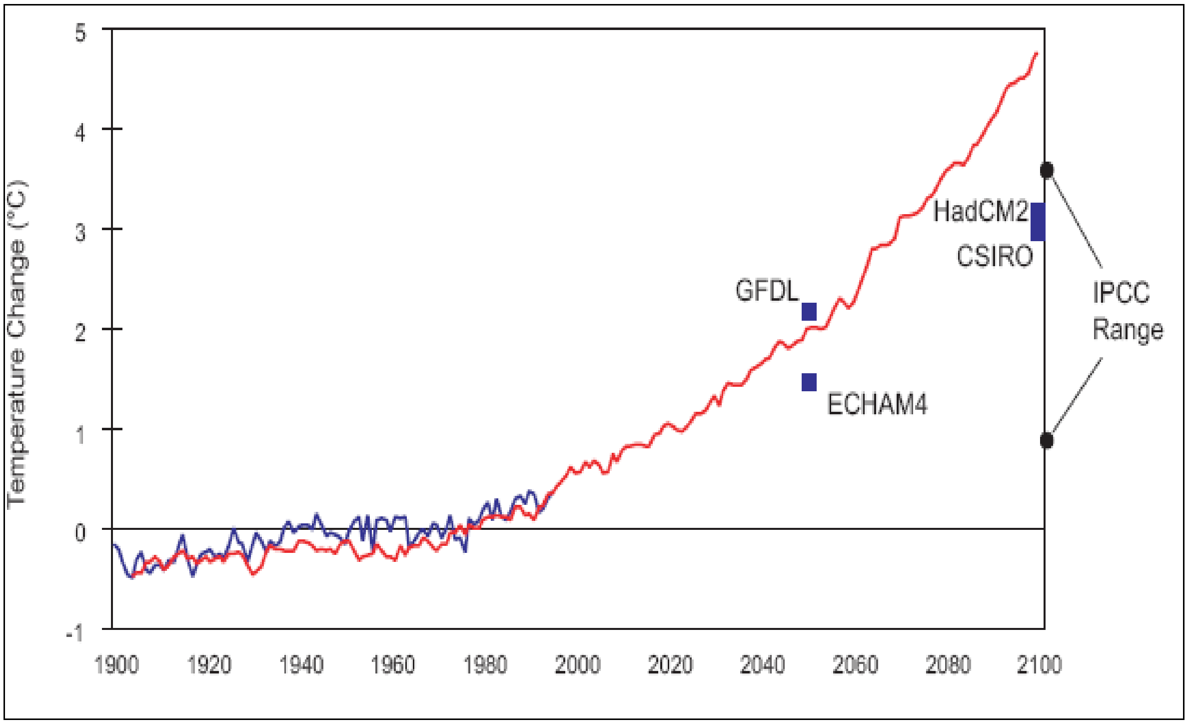

Figure 3-1: Projected changes in global surface temperature from CGCM1 (red line), IPCC (black dots), and other modeling experiments (blue squares). (Source: Boer *et al*. (2000); IPCC Data Distribution Center)

The ability of the CGCM1 to, particularly, reproduce present-day mean climate and its historical characteristics with respectable realism, and its overall good performance in comparison with the other models is an indication that it can be used to project credible future climates intended for the purpose of this research (i.e., up to the 2080s). However, like all GCMs, the usefulness of the model for climate studies in a small local area, like the Gulf Islands, is limited due to its coarse spatial resolution and inability to resolve small scale effects, such as clouds and topography, which affect local climatic conditions. To bridge the resolution gaps for GCMs to produce realistic local climate projections, downscaling techniques are usually applied to the GCM output.

3.3 DOWNSCALING TECHNIQUES

Downscaling techniques are used for post-processing GCM data as a means of addressing the disparity between the coarse spatial scales of GCMs and observations from local meteorological stations. The technique is mainly grouped into two main types: a) dynamical climate modeling, and b) statistical downscaling.

3.3.1. DYNAMICAL CLIMATE MODELING

This technique involves nesting a higher resolution Regional Climate Model (RCM) within a coarser resolution GCM. RCMs use the GCM to define time-varying atmospheric boundary conditions around a finite domain from which the physical dynamics of the atmosphere are modeled using horizontal grid spacing of about 20 – 50 km or less (Wilby and Dawson, 2004). They are used in a wide range of climate applications; from paleoclimate to anthropogenic climate change studies, and are reported to be consistent in response to different physically-based external forcings, and with the GCM (Hostetler *et al*., 1994; Wilby and Dawson, 2004). The main limitation of RCMs is that they are computationally demanding (much like the GCMs) and, therefore, place constraints on the feasible domain size, the duration of simulations, and the number of experiments that can be performed.

In Canada, a Canadian Regional Climate Model (CRCM) has been developed through the collaboration of a modeling team at the University of Quebec in Montreal and the Canadian Climate Centre (CCCma) team in Victoria. The CRCM has been used to simulate current and future climate for western Canada at spatial resolution fine enough to correctly represent local climatic processes (Laprise *et a*l., 1998; Caya and Laprise, 1999).

The model data are available to registered members over the internet as monthly summaries and as climatology. However, the lack of readily-available daily data from the model runs is seen as its main limitation for use in this study. To properly evaluate precipitation variability and change over the future, daily precipitation are required. More so, the climate series constructed from the CRCM are not consistent with those from GCMs, as their time periods are of shorter duration and do not correspond to that recommended by IPCC. Furthermore, previous work on climate change impacts on groundwater recharge (Allen *et al*., 2004b) used GCM rather than RCM output, and it was desired to remain consistent with the CGCM1 model used in that study.

3.3.2. STATISTICAL DOWNSCALING

Statistical downscaling techniques combine existing and past empirical knowledge to address the disparity between coarse spatial scales of GCMs and point meteorological observations. This methodology uses a statistically-based model to determine a relationship between regional or local climate variable(s) (known as predictands) and large-scale climate variables (referred to as predictors). The derived relationship between the predictors and predictands are applied on similar predictors from GCM simulations in the statistical model to estimate the corresponding local or regional climate characteristics. Available statistical downscaling models in use can be grouped as:

a) Synoptic weather typing, which involves grouping local meteorological data in relation to prevailing patterns of atmospheric circulation, and constructing future climate scenarios either by re-sampling from observed data distributions, or by generating synthetic sequences of weather patterns using Monte Carlo techniques and re-sampling from observed data.
b) Stochastic weather generation, which involves modifying parameters of conventional weather generators scaled in direct proportion to corresponding parameters in GCMs to generate local climate data.
c) Regression-based models, which use different mathematical transfer functions and a statistical fitting procedure to derive empirical relationships between local predictands and regional scale predictors.

> Individual downscaling schemes differ according to the choice of predictor variables of statistical fitting procedures (Wilby and Dawson, 2004).

The statistical downscaling models are computationally inexpensive, easily applied to output from different GCMs, and can be used to provide local information needed most often in many climate change impact applications. In addition, they offer a framework for testing the ability of physical models to simulate the empirically-found links between large-scale and small-scale climate (Osborn *et al*., 1999; von Storch *et al*., 1993; Noguer, 1994). However, the model's basic assumption (i.e., that the statistical relationships developed for present day climate also hold under different forcing conditions of future climates) is not verifiable, and requires high quality data for model calibration.

3.4 LOCAL CLIMATE DOWNSCALING USING SDSM

Due to the coarse resolution of the CGCM1, the Statistical Downscaling Model (SDSM), fully described in Wilby and Dawson (2004), was used to derive current and future local climates for the study area from CGCM1. SDSM is a software that enables the construction of climate change scenarios for individual sites at daily time scales, using a grid resolution GCM output. The version 3.1 of SDSM, used in this study, generally reduces the task of downscaling daily climate from a global model into seven discrete processes, namely: quality control and data transformation; predictor variable(s) screening; model calibration; weather generation; statistical analyses; graphing model output; and scenario generation.

The procedure for SDSM analysis always starts with the preparation of coincident predictor and predictand data sets. The predictor data set is obtained from the GCM output in the grid corresponding to the local study area, whereas the predictand is a long series of observed daily weather information (e.g., temperature, precipitation, solar radiation, sunshine hours, etc.) at the meteorological station representing the local area. The predictand data used in this study is the observed daily precipitation and temperature data from Victoria International Airport meteorological station. Both the predictor and predictand data are supplied by the user for SDSM analysis.

SDSM uses the information to develop a set of parameters, relating the predictors to the predictand, for deriving local current and future weather data, based on the output of the GCM time periods. The SDSM has been reported to have some problems in downscaling daily precipitation amounts at individual stations. This is due to the generally low predictability of daily precipitation amounts at local scales by regional forcing factors. This unexplained behavior is currently modeled stochastically (within SDSM itself) by artificially inflating the variance of the downscaled precipitation series to fit with daily observations. Ongoing research is attempting to address this problem (Wilby and Dawson, 2004). Regardless of this deficiency, Wilby and Dawson (2004) report that the model is the most viable downscaling tool in the public domain.

3.4.1. METHODOLOGY FOR SDSM

Five sets of data, summarized in Table 3-1, were downloaded from the Canadian Institute for Climate Studies (CICS) website for the nearest grid location to the study area (Y = 12 Latitude: 46.3886°N and X=15 Longitude: 123.75°W). The calibration data contains predictor variables for observed daily data derived from the National Centre for Environmental Prediction (NCEP) Re-analysis (Kalnay *et al.*, 1996) for the period 1961-2000. Most climate modeling experiments in North America use this NCEP dataset for calibrating downscaling models (CICS, 2005). The other four datasets contain predictor variables for current and future CGCM1 scenario experiments using greenhouse gas and sulphate aerosol (GHG+A1), and these were used in generating corresponding current and future climates of the study area. The NCEP dataset includes relative humidity, whereas CGCM1 datasets do not, so specific humidity was used when calibrating the model.

Table 3-1: Predictor variables for SDSM calibration and CGCM1 time periods (CICS, 2005).

Dataset	**Description**
Calibration	Observed daily data derived from the NCEP Re-analysis data set (National Centre for Environmental Prediction (Kalnay *et al*., 1996) for the period 1961-2000.
CGCM1_Current	Daily output from the first greenhouse gas + sulphate aerosol experiment undertaken with the CGCM1 global climate model (Boer *et al*., 2000) for the period 1961-2000.
CGCM1_2020s	Daily output from the CGCM1 GHG+A1 experiment for the period 2010-2039.
CGCM1_2050s	Daily output from the CGCM1 GHG+A1 experiment for the period 2040-2069.
CGCM1_2080s	Daily output from the CGCM1 GHG+A1 experiment for the period 2070-2099.

The daily weather data from the Victoria International Airport meteorological station was also reformatted to the SDSM requirements. Once all input data files are ready, the SDSM analyses could be performed as detailed below.

Quality Control and Data Transformations

In the quality control process, input file formats are verified, the total number of values in a file are counted, and the number of values "ok" are displayed. The difference between the total and "ok" values in a file is the missing data. The user then must trace all dates with missing values from the input file and pad them with -999 before moving to the stage of the analysis. The 31 missing values encountered during the analysis of the observed data all occurred at the same times; between 1990 to 1993 for both temperature and precipitation.

The default model settings specified by Wilby *et al*. (2002) were used in all the quality control checks, except for the observed daily precipitation, where a 4^{th} root model transformation and variance inflation were applied. The precipitation values are transformed by 4^{th} root to normalize the distribution and make it less skewed to low precipitation values. Since observed daily solar radiation data were not available for the study area meteorological stations, it was not possible to downscale from SDSM. Daily solar radiation data were extracted directly from CGCM1 published output results on Environment Canada website (2005) in a grid location corresponding to the study area since this was not possible to downscale.

A summary of the quality control results and modified model settings are presented in Table 3-2.

Table 3-2: Quality Control Results and Modified Model Settings

	Precipitation	**Temperature**
Number of Values	14610	14610
Missing Values	31	31
Bias Correction	1	1
Variance Inflation	14	12
Transformation	4^{th} root	–
Event Threshold	0	–

Selection of Predictor Variables

Selecting the appropriate predictor variables is viewed as the most challenging aspect of the entire downscaling procedure, because the choice of predictors largely determines the character of the downscaled climate. The predictor variables are meteorological variables generated from CGCM1 model runs for the selected grid square. The process is carried out by using the predictand (i.e., either the observed precipitation or temperature) to screen all the 26 predictor variables for SDSM use, as provided by CICS. Monthly regressions of the predictors with the predictand variable are run, a correlation matrix and explained variance produced, and the predictor variables that are the most correlated with the predictand (and are statistically significant, low p-value, $p < 0.05$) are selected. The model was run using an unconditional process for the temperature, and a conditional process for precipitation where amounts depend on wet-day occurrence.

The selected best predictors for precipitation and temperature from the variable screening analyses, and the rest of predictors from the CGCM1 experiments, are presented in Table 3-3. The associated monthly partial correlation coefficients (denoted by 'r'), and p-values of predictor variables for the precipitation and temperature of the study area are shown in Tables 3-4 and 3-5, respectively.

The results of the variable screening analyses show that the variables mslp, p8_v, p850 and s500 are more suitable in predicting the precipitation. The variables happen to be more useful in their seasonal predictions as compared to the monthly predictions, as evidenced by the higher seasonal r-values and corresponding low p-values. This is an indication that the local seasonal precipitation trend is more similar to the CGCM1 predictions than the monthly trend. The specific humidity at a 500 hPa height is observed to be a useful predictor variable, followed by 850 hPa geopotential height, and this may be due to the effect of the mountains/hills in the study area reported to have a strong influence on precipitation; hence these variables would take into account the topography of the area during the downscaling.

Unlike precipitation, the local temperature is observed to be modeled very well from the CGCM1 by the variables temp, p_u, p500, p850, and s850 in both the monthly and seasonal process. This means both the seasonal and monthly local trend of temperature is similar to the regional CGCM1 prediction, which is likely due to the fact that the model is linked to temperature directly. The variables mostly produced high correlation values, with p-values less than 0.05, implying that the predictor-predictand relationship is not by chance. A negative correlation coefficient for a predictor variable indicates that it has an inverse relationship with the predictand.

Model Calibration

The model calibration process uses a specified predictand and predictors to construct downscaled models, based on multiple linear regression equations. The selected predictor variables, from the variable screening process, and their corresponding predictand, are used in this process to produce a parameter file for the predictand. The monthly model type is used in calibrating for both temperature and precipitation predictor variables, using the unconditional and conditional model processes, respectively. A conditional process for precipitation is used as its local amount depends on wet-/dry-day occurrence, which, in turn, depends on regional-scale predictors, such as humidity and atmospheric pressure (Wilby *et a*l., 2002). The parameter files generated were used in creating NCEP-based synthetic weather data for the study area. Analyses of the model calibration results in comparison with the observed meteorological data are presented in Section 3-5. For precipitation, the statistics performed in SDSM are mean, median, max, sum, variance, dry and wet spells length, and % wet days. Minimum precipitation is always zero, so it was not analyzed. For temperature the statistics are mean, median, min, max, variance and sum.

Generation of Climate Period Data

Four climate periods, namely: current climate, 2020's climate, 2050's climate, and 2080's climate, were generated based on the CGCM1 predictor datasets in Table 3-1. In each climate period generation process, the corresponding predictor dataset from CGCM1 was specified within SDSM (note that SDSM automatically selects the correct predictors using the parameter file).

Daily data sets were generated for each time period. All results were analyzed in SDSM by creating monthly statistics, listed in the previous section, for each generated time period data, and comparing to the observed.

Data Analysis

The data analysis screen in SDSM provides a means for performing statistical tests on both the generated climate sets and the observed station data. The model default statistics, namely, monthly/seasonal/annual means, maxima, minima, sums and variances, were performed on the observed and generated precipitation and temperature data. In addition, % wet and mean dry-/wet-spell lengths statistics were also performed for the daily precipitation series.

The outputs of these statistical analyses, shown in Appendix A, were imported to MS Excel for computation of calibration and model errors, as well as to generate graphical comparisons. Although a graphical comparison of the outputs can also be performed in the SDSM, it is limited to two sets of data at a time.

Table 3-3: Downscaling predictor variable from CGCM1

Variable Code	Description	Precipitation	Temperature
temp	Mean Temperture		√
mslp	Mean sea level pressure	√	
p500	500 hPa geopotential height		√
p850	850 hPa geopotential height	√	√
rhum	Near surface relative humidity		
shum	Near surface specific humidity		
s500	Specific humidity at 500 hPa height	√	
s850	Specific humidity at 8500 hPa height		√
p_f	Surface airflow strength		
p_u	Surface zonal velocity		√
p_v	Surface meridional velocity		
p_z	Surface vorticity		
p_th	Surface wind direction		
p_zh	Surface divergence		
p5_f	500 hPa airflow strength		
p5_u	500 hPa zonal velocity		
p5_v	500 hPa meridional velocity		
p5_z	500 hPa vorticity		
p5th	500 hPa wind direction		
p5zh	500 hPa divergence		
p8_u	850 hPa zonal velocity		
p8_f	850 hPa airflow strength		
p8_v	850 hPa meridional velocity	√	
p8_z	850 hPa vorticity		
p8th	850 hPa wind direction		
p8zh	850 hPa divergence		

Table 3-4: Partial correlation values for precipitation predictor variables.

			Winter			Spring			Summer			Autumn		
			Dec	Jan	Feb	Mar	Apr	May	Jun	Jul	Aug	Sep	Oct	Nov
mslp	monthly	**r**	-0.04	0.30	-0.05	-0.05	-0.04	-0.02	-0.04	-0.04	-0.04	-0.02	-0.07	-0.06
		p	0.10	0.06	0.14	0.16	0.27	0.43	0.23	0.25	0.23	0.46	0.04	0.07
	seasonal	**r**		-0.05			-0.04			-0.04			-0.05	
		p		0.01			0.02			0.04			0.01	
p8_v	monthly	**r**	0.14	0.13	0.09	0.11	0.08	0.08	0.05	0.01	-0.01	0.08	0.13	0.11
		p	0.00	0.00	0.00	0.00	0.02	0.00	0.15	0.52	0.55	0.01	0.00	0.00
	seasonal	**r**		0.12			0.10			0.02			0.12	
		p		0.00			0.00			0.36			0.00	
p850	monthly	**r**	-0.04	-0.08	-0.06	-0.06	-0.03	-0.01	-0.02	-0.01	-0.04	-0.02	-0.07	-0.07
		p	0.22	0.02	0.06	0.05	0.29	0.54	-0.42	0.51	0.22	0.46	0.02	0.03
	seasonal	**r**		-0.06			-0.06			-0.02			-0.07	
		p		0.00			0.00			0.22			0.00	
s500	monthly	**r**	0.22	0.13	0.12	0.14	0.05	0.06	0.08	0.06	0.04	0.04	0.07	0.13
		p	0.00	0.00	0.00	0.00	0.10	0.08	0.02	0.07	0.26	0.19	0.03	0.00
	seasonal	**r**		0.16			0.08			0.06			0.07	
		p		0.49			0.00			0.00			0.00	

Table 3-5: Partial correlation for temperature predictor variables

			Winter			Spring			Summer			Autumn		
			Dec	Jan	Feb	Mar	Apr	May	Jun	Jul	Aug	Sep	Oct	Nov
p_u	monthly	**r**	-0.20	0.13	0.05	-0.10	-0.22	-0.28	-0.21	-0.29	-0.33	-0.25	-0.13	-0.03
		p	0.00	0.00	0.15	0.00	0.00	0.00	0.00	0.00	0.00	0.00	0.00	0.31
	seasonal	**r**		0.07			-0.10			-0.26			-0.13	
		p		0.00			0.00			0.00			0.00	
p500	monthly	**r**	0.15	0.17	0.26	0.34	0.47	0.60	0.51	0.37	0.36	0.51	0.29	0.21
		p	0.00	0.00	0.43	0.00	0.00	0.00	0.00	0.00	0.13	0.00	0.00	0.00
	seasonal	**r**		0.17			0.42			0.45			0.36	
		p		0.00			0.00			0.00			0.00	
p850	monthly	**r**	0.22	-0.14	-0.19	-0.18	-0.25	-0.34	-0.20	-0.08	-0.02	-0.25	-0.22	-0.18
		p	0.00	0.00	0.00	0.00	0.00	0.11	0.00	0.01	0.49	0.00	0.00	0.00
	seasonal	**r**		-0.13			-0.18			-0.09			-0.20	
		p		0.00			0.00			0.20			0.00	
s850	monthly	**r**	0.25	0.29	0.28	0.22	0.26	0.23	0.12	0.10	0.21	0.36	0.22	0.40
		p	0.00	0.00	0.00	0.00	0.00	0.00	0.00	0.00	0.00	0.10	0.00	0.00
	seasonal	**r**		0.27			0.27			0.20			0.31	
		p		0.00			0.00			0.00			0.00	
temp	monthly	**r**	0.25	0.41	0.44	0.44	0.28	0.19	0.14	0.08	0.05	0.03	0.41	0.36
		p	0.00	0.00	0.00	0.00	0.00	0.00	0.00	0.01	0.16	0.29	0.00	0.00
	seasonal	**r**		0.45			0.39			0.11			0.45	
		p		0.00			0.00			0.00			0.00	

3.5 RESULTS OF SDSM DOWNSCALING

This section summarizes and presents graphically the results of the SDSM calibration and weather time series generation. The graphs were derived from the statistical analysis output from SDSM using either the monthly or seasonal statistics (plotted on the x-axis) and the statistically-generated variable (e.g., mean monthly temperature, mean monthly precipitation, downscaling bias, % wet days, etc. plotted on the y-axis). In addition, standard deviation was used in analyzing the variability of both the observed and generated future precipitations. The variability obtained indicates how an observed or generated dataset is spread out of its mean. The SDSM statistical analyses generated a daily dataset variance, which was converted to standard deviation by the relation: standard deviation = square root of variance. A uniform color code is employed for the observed and downscaled statistical variable for easy identification and inter-comparison.

3.5.1. PRECIPITATION

Calibration

Analyses of the calibration results for mean monthly precipitation shows both the downscaled (NCEP) and the current predicted (CGCM1) data to over-estimate the observed precipitation from March to May, and slightly under-estimate observed precipitation from December to February. Generally, reasonable estimations are obtained from June to November (Figure 3-2). The average monthly calibration (NCEP) and CGCM1 bias (i.e., average % error for all months) of approximately 12% and 13%, respectively, to the observed seems reasonably good. However, individual monthly percentage errors for some of the months, like May and April, are quite high.

Seasonally, the model poorly predicts winter and spring precipitations, with significant high negative (-19.57% and -5.02% for CGCM1 and NCEP, respectively) and positive (50.36% and 47.48% for CGCM1 and NCEP, respectively) errors in these seasons, respectively (Figure 3-3). This may be due to the fundamental limitations of the model in predicting observed precipitation as reported by Wilby *et al.* (2002). On the other hand, the average seasonal calibration (NCEP) and CGCM1 biases of approximately 12% and 11%, respectively, to the observed are seems good.

The downscaled (NCEP) and CGCM1-current monthly standard deviations (Figure 3-4) were not well simulated by the SDSM. The variability of the NCEP and CGCM1-current values are almost the same for most months. However, the monthly standard deviation for April and May are very poor (about 40% bias for April, 60% bias for May).

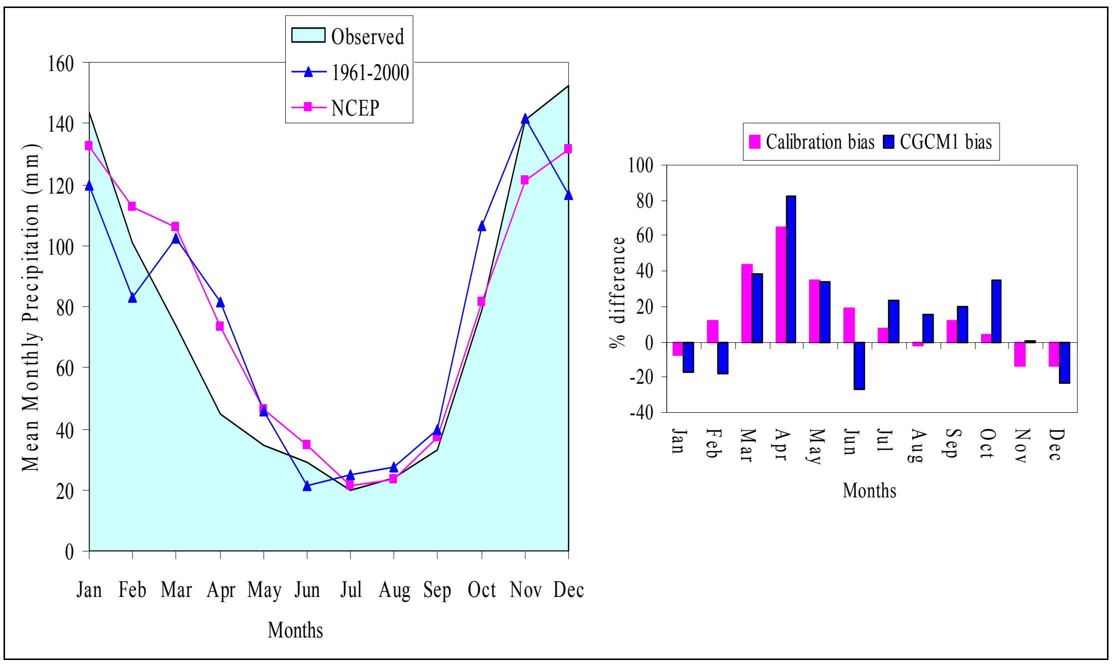

Figure 3-2: Comparing SDSM downscaled monthly averages for precipitation (both downscaled NCEP and CGCM1 current) to the observed climate.

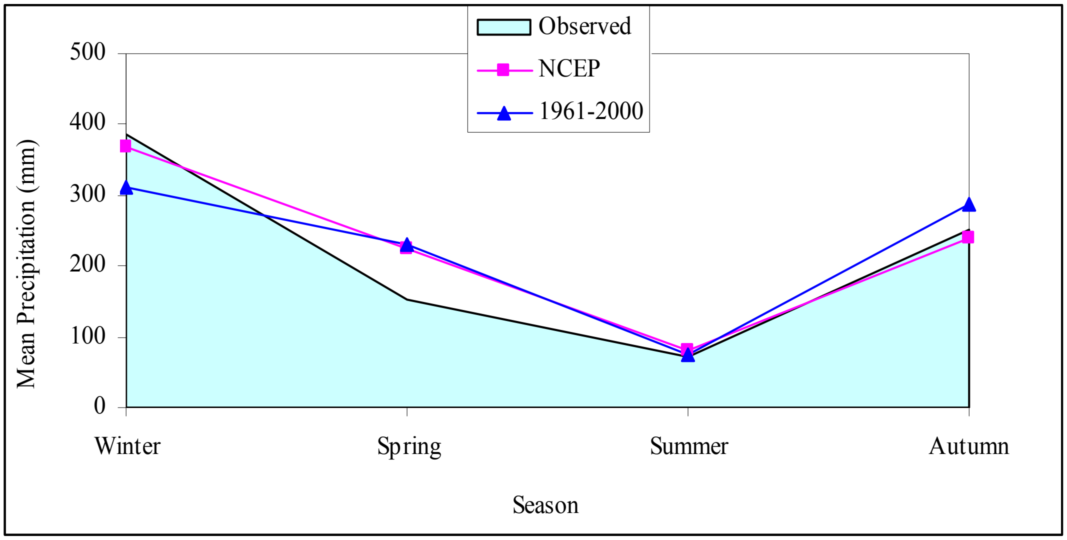

Figure 3-3: Comparing SDSM downscaled seasonal precipitation (both downscaled NCEP and CGCM1 current) to the observed climate.

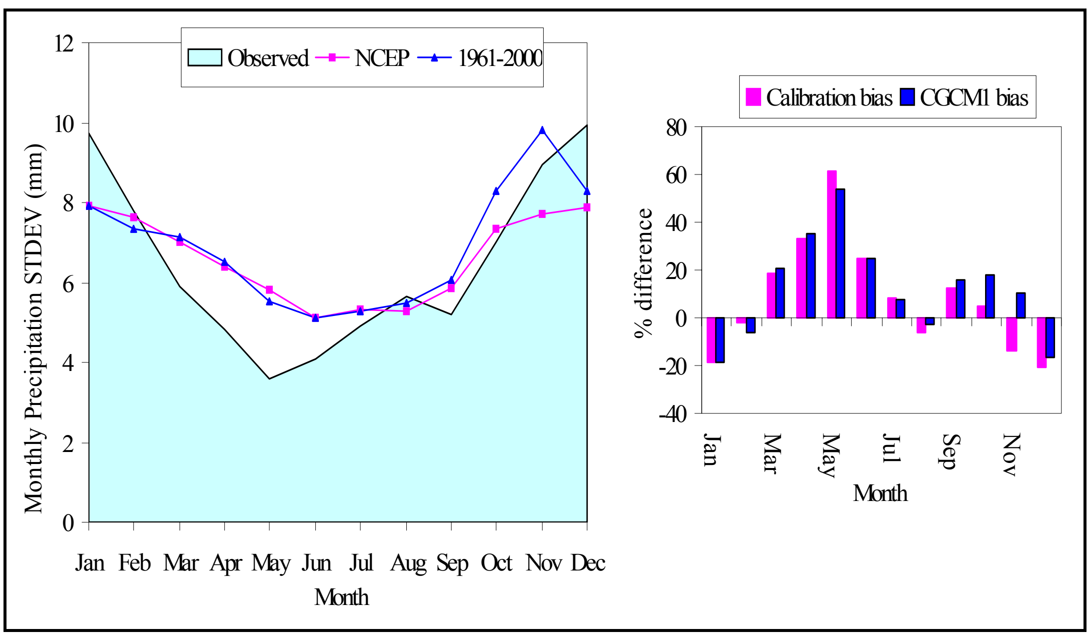

Figure 3-4: Comparing the standard deviation for SDSM downscaled seasonal precipitation (both downscaled NCEP and CGCM1 current) to the observed climate.

Future Precipitation

The mean annual precipitation downscaling with SDSM is predicted to increase by 52%, 65% and 88% relative to the observed for 2020's, 2050's and 2080's, respectively. Also, a progressive increase in precipitation for all months is predicted for all future time periods relative to current, Figure 3-5. On average, current mean monthly precipitation is predicted to increase by 47%, 56% and 69% for the 2020s, 2050s and 2080s future periods, respectively. However, monthly changes are more variable; increments in the future are significantly below the monthly average from March to July, and about twice the average between August and February. Likewise, relative changes in seasonal future precipitation, increases progressively for all seasons (Figure 3-6). The future spring precipitation is predicted to increase in 2080s by 20%, relative to current precipitation. A comparison of monthly and seasonal future precipitation standard deviations of the CGCM1 time periods and the observed are shown Figure 3-7. The variability for all the future time periods follows a similar pattern, increasing progressively for each month and in all the seasons.

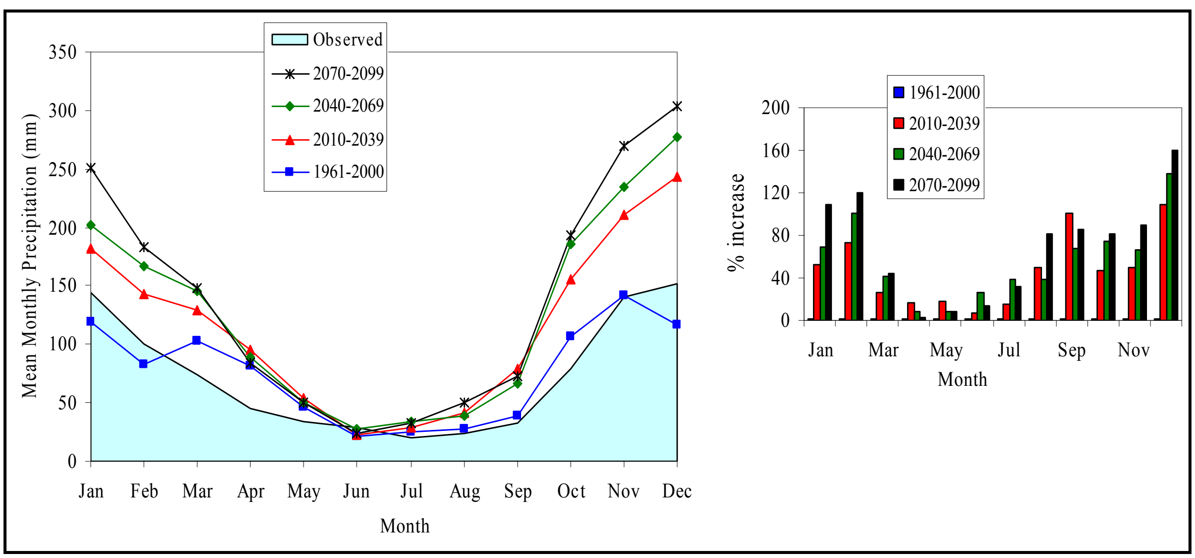

Figure 3-5: Comparing downscaled current and future monthly precipitation to observed climate for different time periods. (Expressed as percentage increase also).

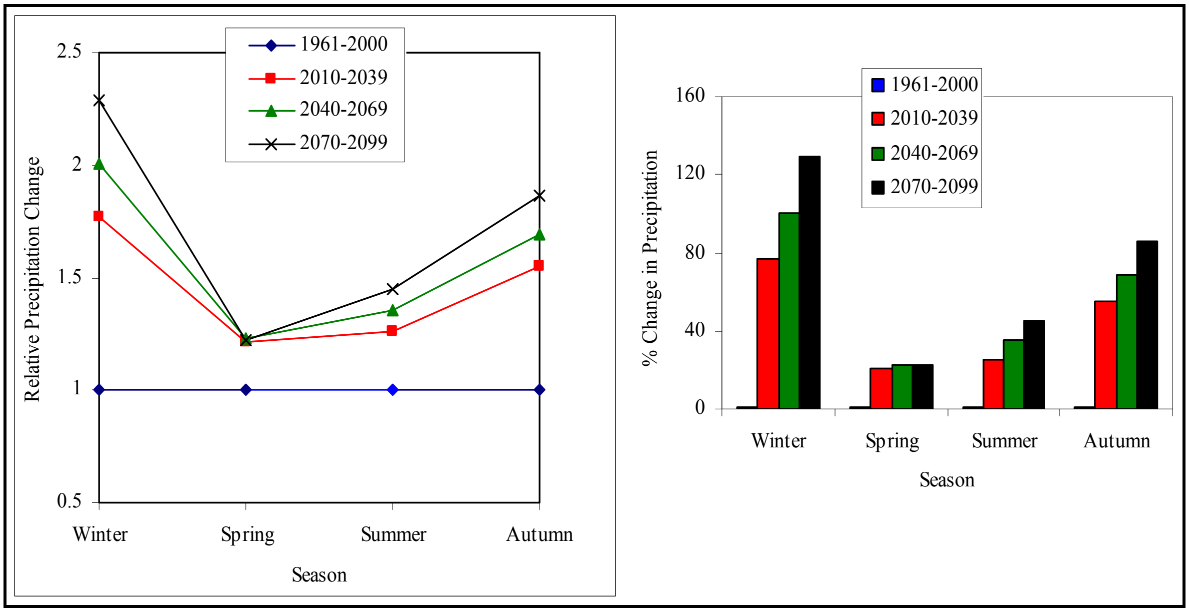

Figure 3-6: Comparing downscaled current and future seasonal precipitation to observed climate for different time periods (Expressed in terms of both relative changes and percentage increase).

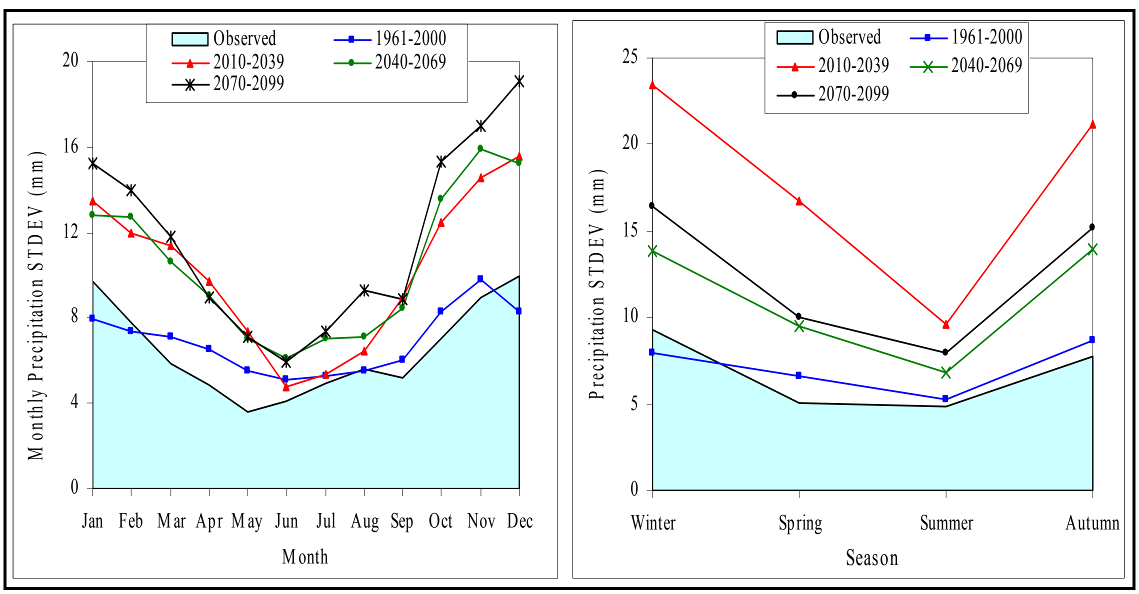

Figure 3-7: Comparing the standard deviation for downscaled monthly and seasonal precipitation to the observed climate.

% Wet Days

Monthly % wet days are indication of how often it rains in a month, and is an indirect measure of precipitation frequency and duration. SDSM downscaling calibration results are shown in Figure 3-8. The model generally downscales the observed monthly wet days (%) very well, with average monthly calibration and CGCM1 biases of -3% and -2%, respectively. The model's prediction of % wet days in the month of June is quite poor (i.e., 42% bias), although its calibration to absolute values gave was quite good (i.e., -13% bias). Downscaling seasonal wet days (%), Figure 3-9, shows summer and winter predictions to be underestimated, whereas both autumn and spring estimations are slightly overestimated. There is a progressive increase in % wet days for the months of autumn and winter into the future (Figure 3-10), whereas the spring and summer months have virtually no increase.

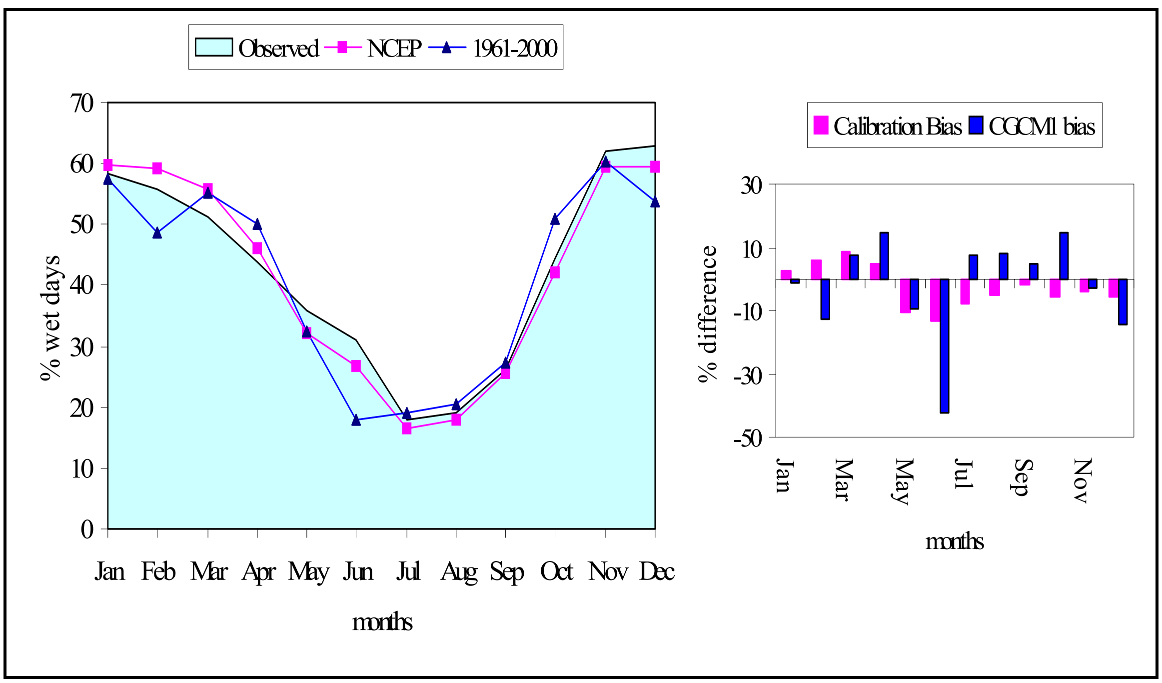

Figure 3-8: Performance of SDSM in downscaling monthly % wet days

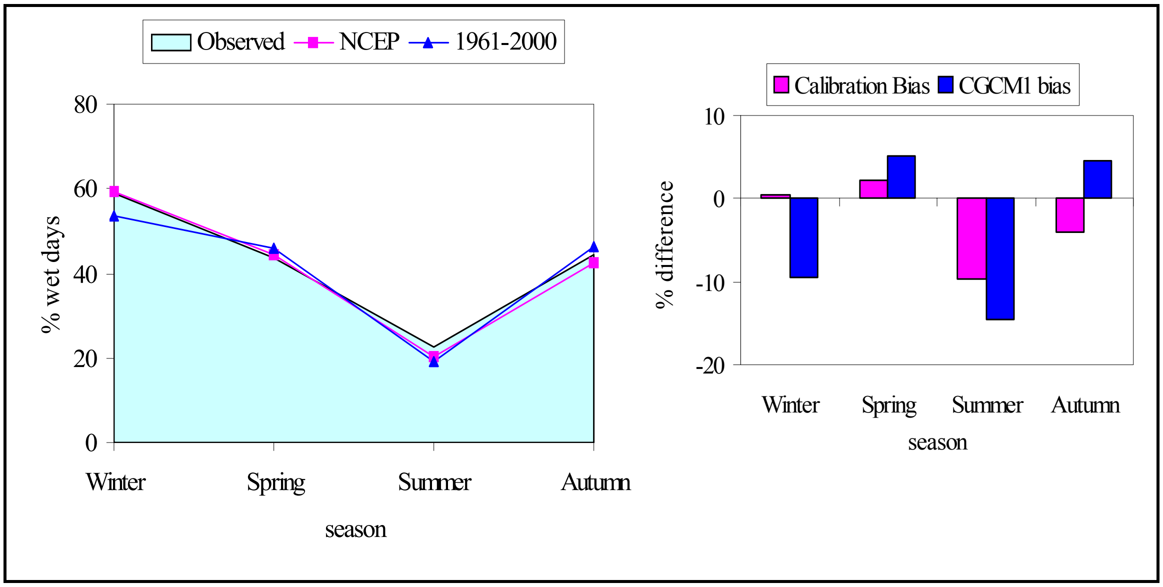

Figure 3-9: SDSM performance for downscaling seasonal % wet days.

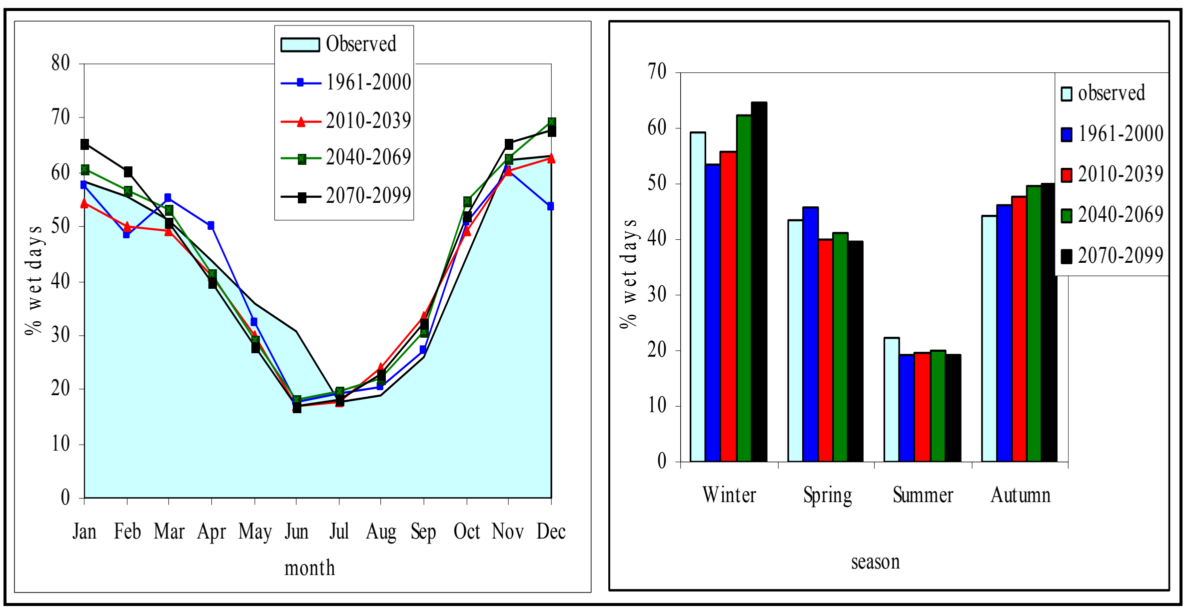

Figure 3-10: Comparing mean monthly and seasonal % wet days of the observed to both the current and future CGCM1 generated time periods.

Wet Spell Length

SDSM downscaling calibration results of wet spell lengths are shown in Figure 3-11. The wet spell length refers to the number of consecutive days with non-zero or, at least higher than zero, precipitation. SDSM underestimates fairly consistently throughout the year the monthly wet spell length for both the downscaled (NCEP) and current CGCM1 time period relative to observed. The percent difference from current CGCM1 and observed exceeds -30% for February and June. The average monthly difference is approximately 13% and 20% lower for NCEP and CGCM1, respectively, in comparison to the observed.

A comparison of the monthly and seasonal dry spell lengths for observed and CGCM1 time periods is shown in Figure 3-12. Monthly wet spell length between April and August are generally of the same magnitude for current and future time periods. From September through March, the wet spell length increased by approximately one half day from the current to the 2050's future period, respectively.

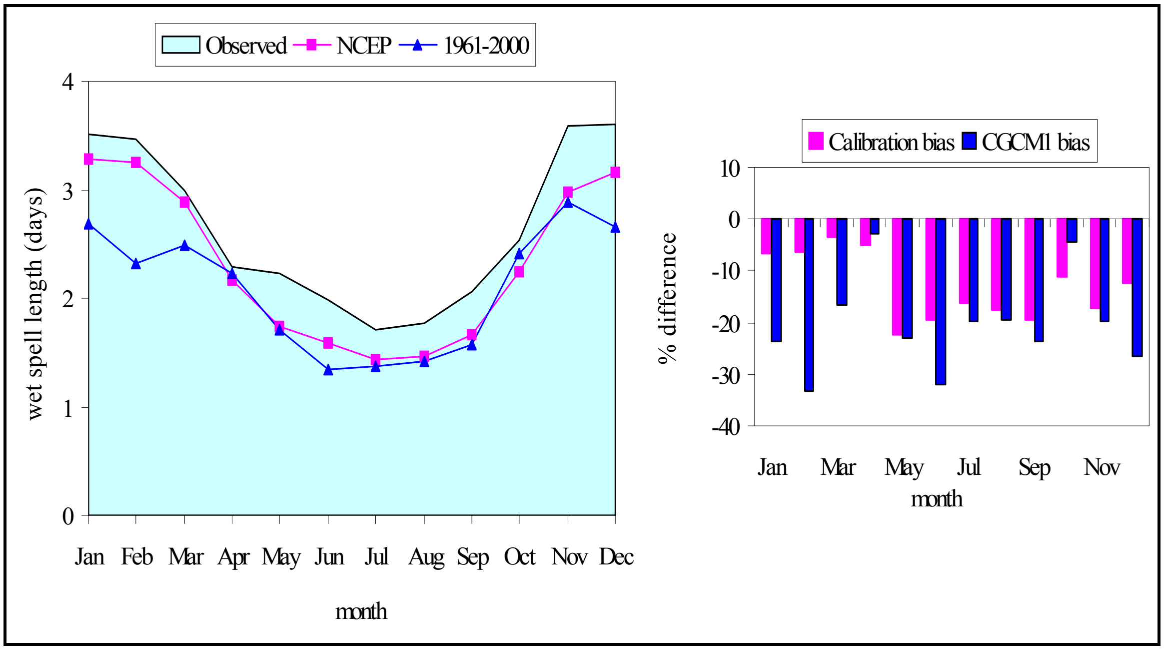

Figure 3-11: Performance of SDSM in downscaling monthly wet spell length.

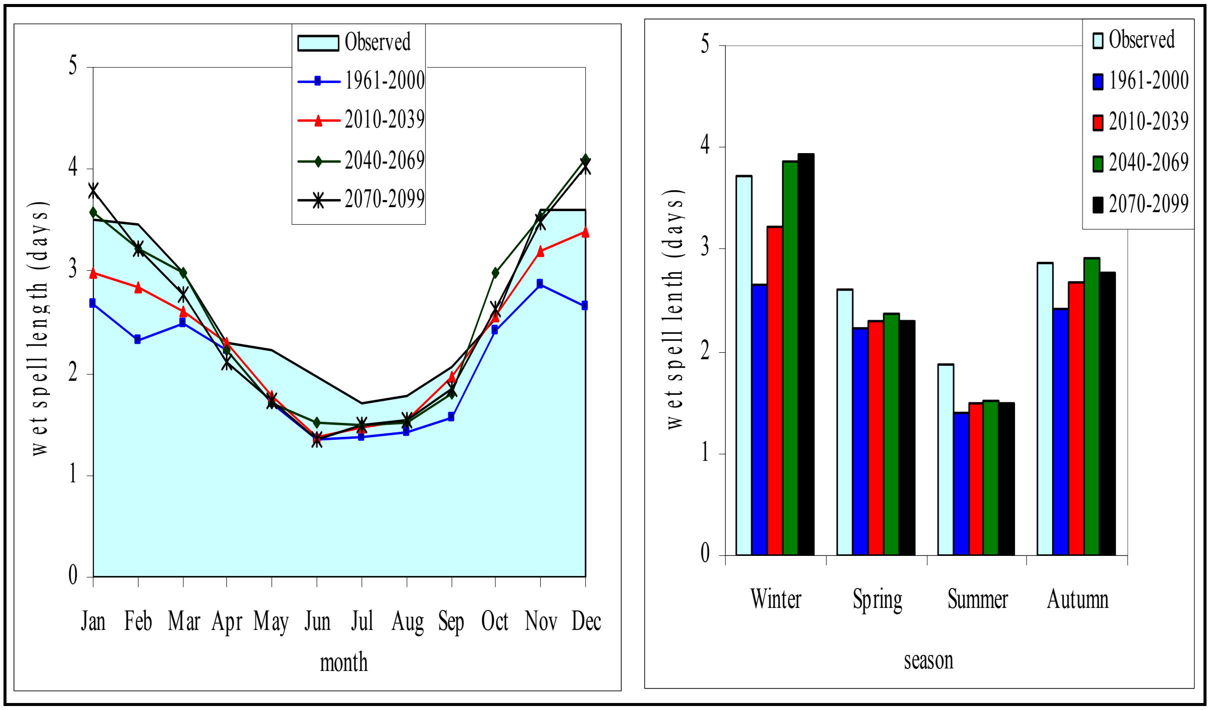

Figure 3-12: Comparing mean monthly and seasonal wet spell length of the observed to both the current and future CGCM1 generated time periods.

Dry Spell Length

Dry spell length indicates the number of consecutive days without precipitation The monthly downscaled (NCEP) and current modeled dry spell lengths are lower, having less than 30% bias for all months, in comparison to the observed values (Figure 3-13), except for June where it is overestimated to be approximately 30%.

A comparison of the monthly and seasonal dry spell lengths for observed and CGCM1 time periods is shown in Figure 3-14. The simulated future dry spell lengths are, on average, roughly the same for both current and future time periods, except in the spring months where the simulated future dry spells are slightly higher than current (about a day difference).

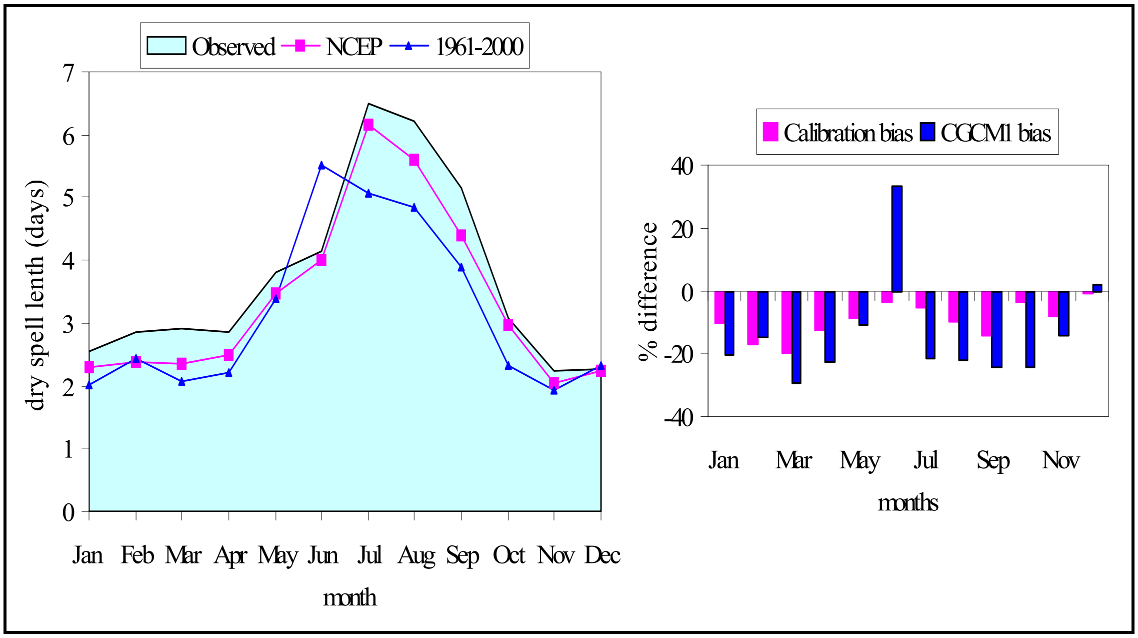

Figure 3-13: Performance of SDSM in downscaling monthly dry spell length.

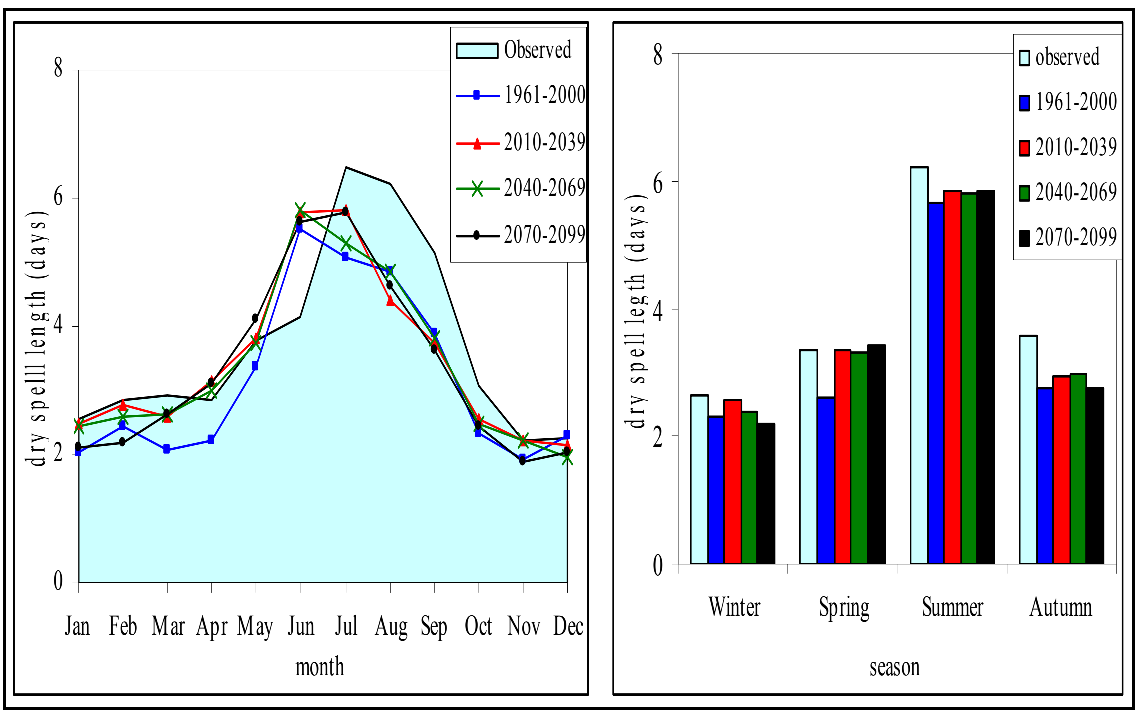

Figure 3-14: Comparing mean monthly and seasonal dry spell lengths of the observed to both the current and future CGCM1 time periods generated.

3.5.2. TEMPERATURE

The performance of SDSM in downscaling monthly mean temperatures, as shown in Figure 3-15, is much better than for monthly precipitation, with the error more randomly distributed. The average calibration bias (with NCEP) is about 0.2%, whereas bias with the CGCM1-current predicted time period is about 2%. SDSM predicts both the monthly and seasonal temperatures to increase progressively in the future (Figures 3-16 and 3-17, respectively). The mean monthly temperature is predicted to rise by 1.14^{o}C in 2020's, 2.05^{o}C in the next 30 years, and up to 3.5^{o}C by the end of the century. Summer temperature increases progressively by 0.5°C in each of the future periods, whereas the increment for the other seasons varies between 0.5°C - 1.0°C.

Standard deviation of downscaled mean monthly temperature is shown in Figure 3-18. SDSM downscaled NCEP variability very well, where the simulated current temperature variability was underestimated by 9% on the average, but by 15% (average) for the summer months.

The standard deviations of the monthly predicted CGCM1 future time periods are all estimated to be lower than the observed (Figure 3-19), except in April, when is the same. There is virtually no monthly change in variability over the future. Future seasonal variability of summer and winter temperature is the same for all the time periods and with the observed.

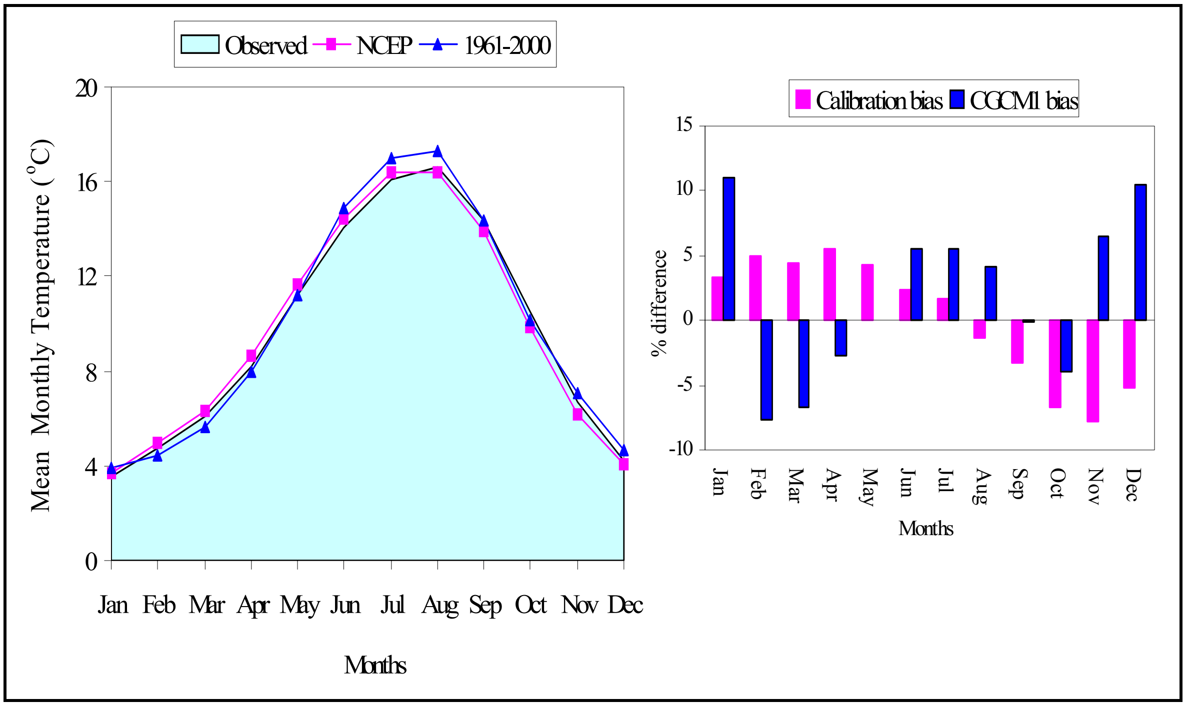

Figure 3-15: SDSM performance for downscaling mean monthly temperature.

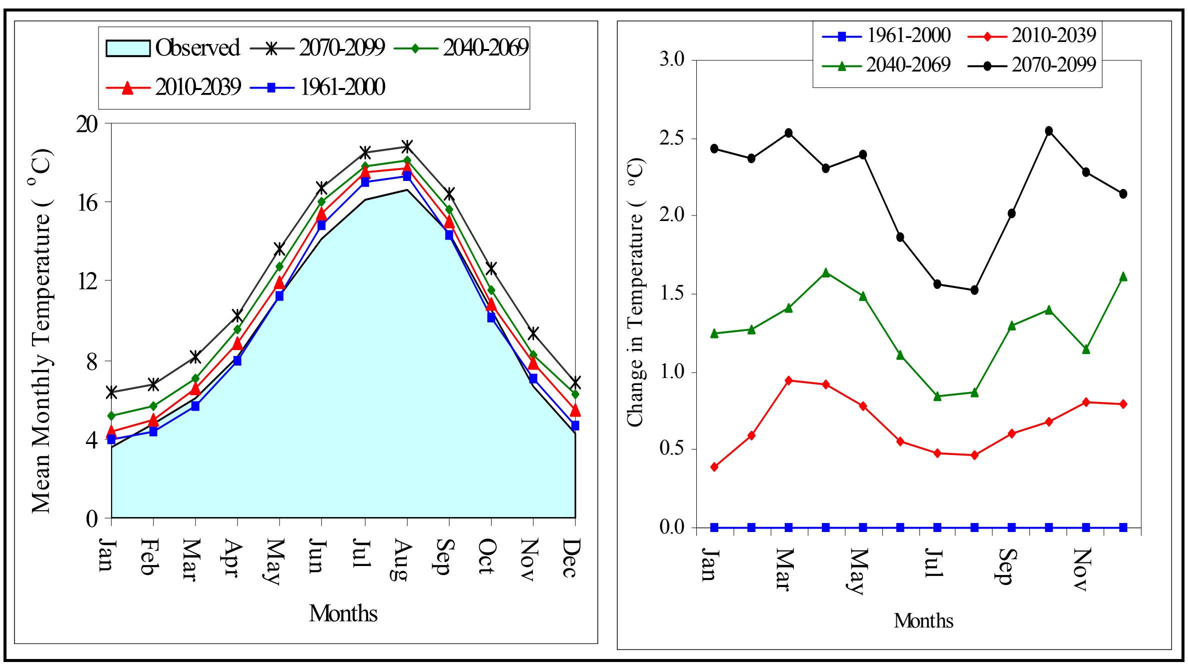

Figure 3-16: Comparing the mean monthly temperature and the change in temperature relative to observed for the various CGCM1 time periods.

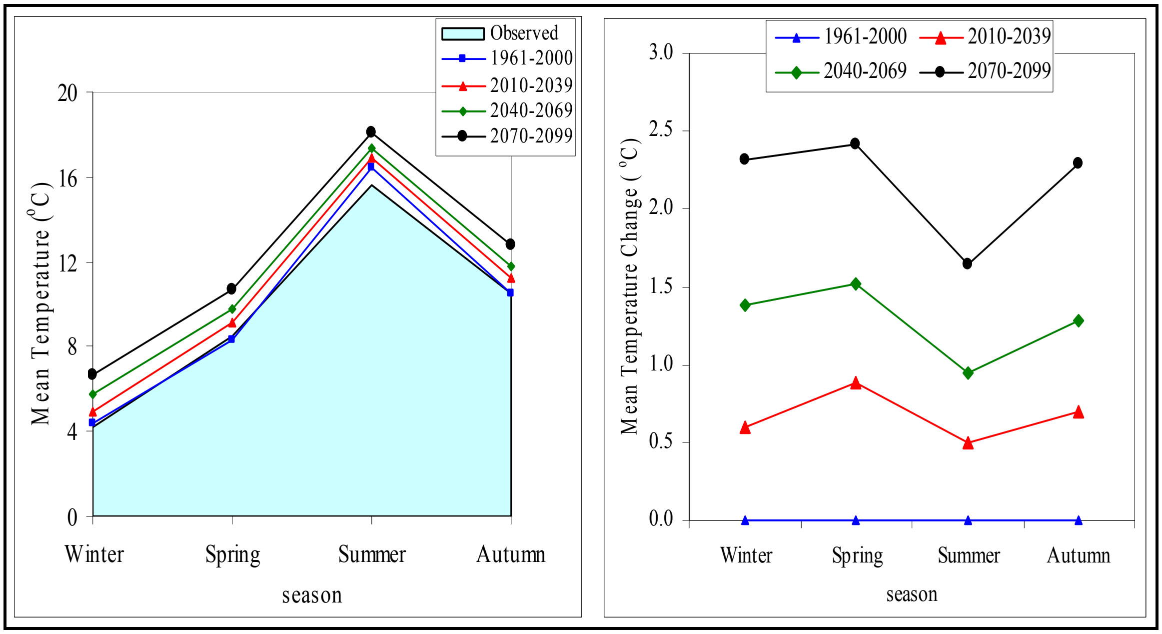

Figure 3-17: Comparing the mean seasonal temperature and the change in temperature relative to observed for the various CGCM1 time periods.

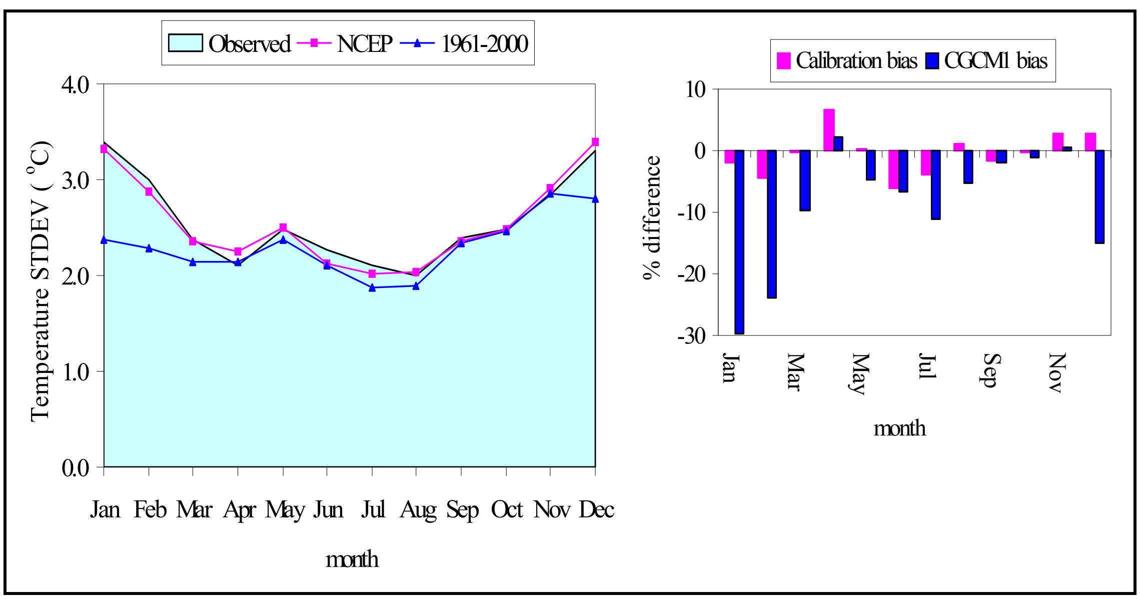

Figure 3-18: SDSM performance for downscaling monthly temperature standard deviation.

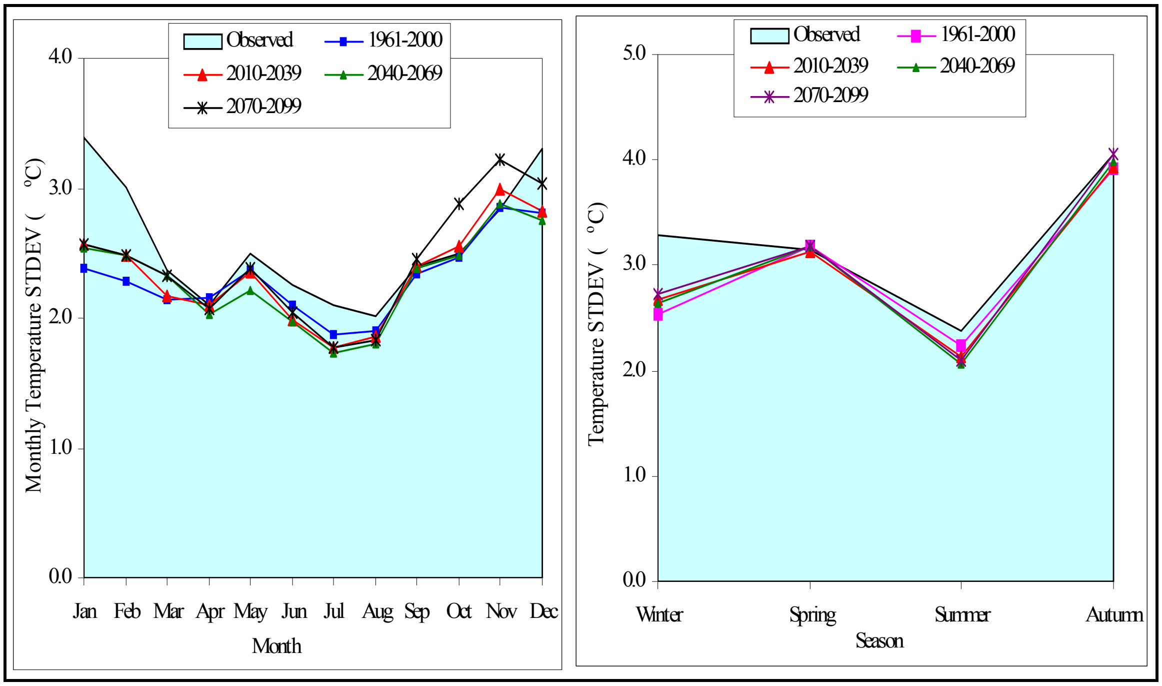

Figure 3-19: Comparing monthly and seasonal temperature standard deviations for observed and generated CGCM1 time periods.

3.6 DISCUSSION

Whereas SDSM downscaling of monthly temperature is well calibrated against observed temperature, downscaling of precipitation -monthly, dry and wet spell lengths- is not as well calibrated. The parameters for downscaling are the same as that used for estimating the future precipitations, therefore, the same degree of errors are to be expected in the predicted future precipitation amounts. This has to be taken into consideration whenever using the predicted future values in any studies (e.g., the recharge estimations for this thesis) in comparison to current conditions.

To overcome the discrepancy between downscaled and observed precipitation, a stochastic weather generator, LARS-WG, will be used to simulate current climate and future climate time series based on the observed climate and the shifts in temperature and precipitation derived from SDSM. These stochastic weather series will be use for the recharge simulations. A schematic diagram for the entire process of generating weather input for the recharge simulations of this thesis is shown in Figure 3-19. The details of the process are provided in the following chapter.

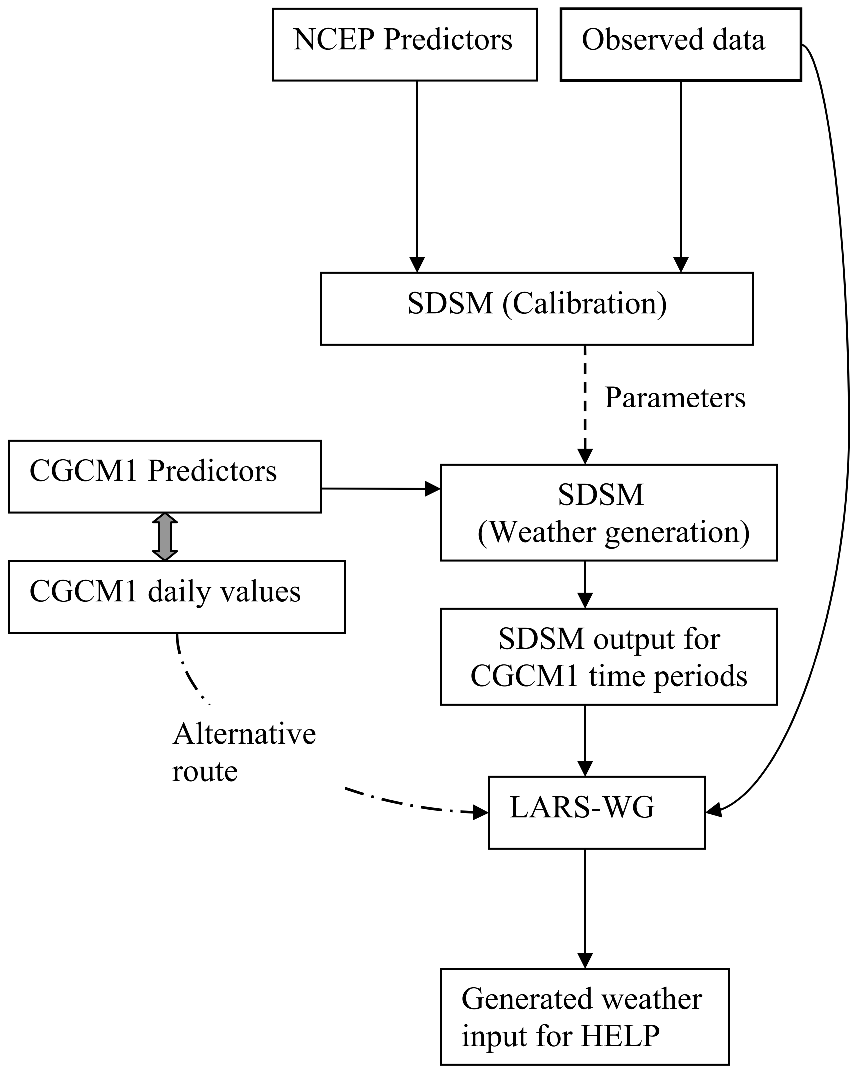

Figure 3-20: Weather input generation process for the recharge estimation.

CHAPTER 4. RECHARGE MODELING WITH HELP

4.1 INTRODUCTION

Groundwater recharge to the aquifers in the study area is modeled using the Visual HELP (Hydrologic Evaluation of Landfill Performance) model, which is part of the WHI UnSat Suite software (Waterloo Hydrogeologic Inc., 2003). HELP is a quasi-two-dimensional, deterministic, water-routing model used for predicting landfill hydrologic processes, testing the effectiveness of landfill designs, and assessment of groundwater recharge rates. A detailed description of the model is presented in Schroeder *et al*. (1994).

The model uses numerical solution techniques that account for the effects of surface storage, snowmelt, runoff, infiltration, evapotranspiration, vegetative growth, soil moisture storage, lateral surface drainage, and unsaturated vertical drainage (or leakage through soil), as well as landfill-related effects, such as leachate recirculation, geomembranes, or composite liners. The general required input data for running the model are categorized as:

1. Weather data, comprising precipitation, solar radiation, temperature, and parameters of evapotranspiration;
2. Soil and/or aquifer media properties made up of porosity, field capacity, wilting point, slope, and hydraulic conductivity; and
3. Engineering design data, where applicable, consisting of liners, leachate and runoff collection system, and surface slope.

Since recharge to any groundwater system mainly depends on local climate and the properties of the aquifer, only the first two categories of input data are needed for HELP model runs for the purpose of recharge modeling. Hence, these are described in detail in the following sections.

4.2 WEATHER DATA GENERATION

The HELP model requires daily values of precipitation, temperature, solar radiation, and a constant evapotranspiration parameter set for estimating recharge (also described as leakage or percolation through the bottom layer in a profile in the HELP model), runoff, evapotranspiration, etc. These data can be imported into HELP from a weather data file for a particular meteorological station or generated synthetically using the built-in Richardson's Weather Generator (WGEN).

The WGEN weather generator was developed by the Agricultural Research Services of the United States Department of Agriculture (USDA), and is primarily based on the procedure described by Richardson (1981). WGEN generates daily values of precipitation, maximum temperature, minimum temperature, and solar radiation for an n-year period at a given location (Richardson and Wright, 1984) using monthly precipitation and temperature means, and evapotranspiration parameters for the location. Since the occurrence of rain on a given day has a major influence on temperature and solar radiation for the day, the model generates precipitation for a given day independent of the other variables. Maximum temperature, minimum temperature, and solar radiation are then generated according to whether a wet (defined as a day with 0.01 inch or more precipitation) or dry day was previously generated. The model is designed to preserve the dependence in time, the correlation between variables, and the seasonal characteristics in actual weather data for a given location.

Although WGEN is part of the UnSat Suite HELP model, it was not used in generating the weather data for recharge modeling due to its known inadequacy in modeling wet and dry periods, as reported by Wilks and Wilby (1990) and other similar recharge modeling work carried out at Grand Forks of BC (Allen *et al*., 2004b). However, it was used to produce the required weather input files, after which, the data in the files were substituted with weather data of the same format generated using LARS-WG, which is known to overcome the shortcomings of WGEN and better simulates the observed climate (Semenov *et al*., 1998; Allen *et* *al.*, 2004b). This is done in order to maintain the naming convention and location of the files as has been created by the WGEN weather generator.

Daily weather data for study area were generated with WGEN by using the monthly normals of precipitation and temperature, and the evapotranspiration parameters (see Appendix B) of the representative weather station at Victoria Airport. The generated weather files, which were later replaced with LARS-WG data for the HELP recharge modeling are as follows:

1. _weather1.dat - Daily Precipitation,
2. _weather2.dat - Mean Daily Temperature,
3. _weather3.dat - Daily Solar Radiation, and
4. _weather4.dat - Evapotranspiration Parameters (not replaced).

4.3 WEATHER GENERATION WITH LARS-WG

4.3.1. BRIEF DESCRIPTION OF LARS-WG

The most recent version (ver. 3.1) of the Long Ashton Research Station Weather Generator (LARS-WG), which can be used for simulating weather data at a single site (Racsko *et al*., 1991; Semenov *et al*., 1998; Semenov & Brooks, 1999) under both current and future conditions, was used in generating daily precipitation, temperature and solar radiation inputs for the HELP modeling. LARS-WG is a stochastic weather generator based on the series weather generator, which utilizes semi-empirical distributions for the lengths of wet and dry series, precipitation and solar radiation, described in Racsko *et al*. (1991).

LARS-WG simulates precipitation occurrence as alternate wet and dry series, where a wet day is defined to be a day with precipitation greater than zero. The length of each series is chosen randomly from the wet or dry semi-empirical distribution for the month in which the series starts. In determining the distributions, observed series are also allocated to the month in which they start. For a wet day, the precipitation value is generated from the semi-empirical precipitation distribution for the particular month, independent of the length of the wet series or the amount of precipitation on previous days. Daily minimum and maximum temperatures are considered as stochastic processes, with daily means and daily standard deviations conditioned on the wet or dry status of the day. Solar radiation distribution, which varies significantly on wet and dry days, is modeled independently of temperature using separate semi-empirical distributions that describe wet and dry days differently. If solar radiation data are unavailable, then sunshine hours, which are automatically converted to solar radiation using the approach described in Rietveld (1978), may be used (Semenov and Barrow, 2002).

4.3.2. OUTLINE OF THE LARS-WG PROCESS

The process of generating synthetic weather data in LARS-WG is divided into three distinct steps, namely; model calibration, model validation, and generation of synthetic weather data. A detailed description of the procedure to be followed in generating weather data with LARS-WG is given in the users manual (Semenov and Barrow, 2002).

Model Calibration

Model calibration process in LARS-WG is carried out using the 'Site Analysis' function on the main menu to determine the statistical characteristics of the observed weather data. The function analyses the observed data to produce information in two separate output files –statistics and parameter files. For this research, observed weather data from Victoria Airport meteorological station, comprising daily precipitation, minimum temperature, maximum temperature and sunshine hours (used in place of solar radiation due to it non-availability) were used in the site analysis process. The daily data for the years 1961-1990 were extracted from the historic weather records from the station data and reformatted into the required input format of the site analysis function in LARS-WG. Sample of inputs used in the site analysis process, and the two output files produced are presented in Appendix B.

Model Validation

Model validation was carried using the Qtest function in the model to determine how well the model simulates the observed climate data. The function generates synthetic data from parameters of the observed data in one step, and then carries out a statistical comparison on the probability distributions of the both the synthetic and observed data using the Chi-square goodness-of-fit test (χ^2), and the means and standard deviations using t- and F-tests, respectively. In order to ensure that the simulated data probability distributions are close to the true long-term observed distributions for the site in question, a large number of years of simulated weather data should be generated (Semenov and Barrow, 2002). Thus 30 years of synthetic data, in conformity with the duration of the observed and CGCM1 time periods, was generated for the model validation.

The statistical tests (χ^2, t- and F- tests) carried out in Qtest look for differences between the simulated climate and the 'true' climate. Each of the tests considers a particular weather statistic, and compares the values from the observed and simulated data. The tests calculate a p-value, which is used to accept or reject the hypotheses that the two sets of data could have come from the same distribution (i.e., when there is no difference between the observed and simulated climate for that variable). A very low p-value, and a corresponding high χ^2 value means the simulated climate is unlikely to be the same as the observed climate; hence must be rejected. Although a p-value of 0.05 is the common significance level used in most statistics, the authors (Semenov and Barrow, 2002) of the model suggests a p-value of 0.01 be used as the acceptable significance limit of the model results. Significant differences between the observed and simulated data may arise from the model smoothing the observed data, errors in the observed data, random variation in the observed data, and unusual climate phenomenon at a climate station making a particular year's climate very different. Further explanations of these possible differences are discussed in the manual (Semenov and Barrow, 2002). Table 4-1 shows the statistical analyses results of the model's performance in simulating the observed station data.

Table 4-1: Statistical analyses of LARS-WG performance in simulating the observed data using the Qtest function. df is degrees of freedom.

Wet/Dry Precipitation Series					
Months	**WET/Dry**	**df**	**χ^2**	**p-value**	**Comment**
Dec - Feb	Wet	9	2.82	0.971	very good fit
	Dry	9	5.62	0.777	very good fit
Mar - May	Wet	9	2.23	0.987	very good fit
	Dry	9	1.51	0.997	very good fit
Jun - Jul	Wet	6	3.17	0.788	very good fit
	Dry	8	2.03	0.98	very good fit
Sep - Nov	Wet	9	3.61	0.935	very good fit
	Dry	7	1.83	0.969	very good fit
Extreme Weather Spells					
Months	**FROST/HOT**	**df**	**χ^2**	**p-value**	**Comment**
Dec - Feb	FROST	9	40.95	0	no fit
	HOT	0	0	1	perfect fit
Mar - May	FROST	5	2.51	0.775	very good fit
	HOT	0	0	1	perfect fit
Jun - Jul	FROST	0	0	1	perfect fit
	HOT	2	1.28	0.528	good fit
Sep - Nov	FROST	5	10.2	0.07	moderate fit
	HOT	1	0	1	perfect fit
Precipitation Distribution					
Months		**df**	**χ^2**	**p-value**	**Comment**
January		8	1.07	0.998	very good fit
February		9	1.77	0.995	very good fit
March		8	2.49	0.962	very good fit
April		7	1.39	0.986	very good fit
May		9	1.87	0.993	very good fit
June		12	6.56	0.885	very good fit
July		5	0.90	0.97	very good fit
August		7	1.62	0.978	very good fit
September		7	1.00	0.995	very good fit
October		8	2.48	0.963	very good fit
November		9	2.76	0.973	very good fit
December		13	25.70	0.019	poor fit

Synthetic Weather Generation

Once the performance of the model calibrations have been verified, synthetic weather data for different time periods can be simulated using the 'Generator' function of the software. This function has the capability of simulating synthetic data of the same characteristics as the observed, or generating weather data corresponding to a scenario of climate change. For the purpose of this research, the generator function was used to produce synthetic weather corresponding to the downscaled SDSM output representing the CGCM1 time periods 1961-1990, 2010-2039, 2040-2069 and 2070-2099. The generated weather data were then used as input for the HELP recharge estimations. Outlined below are the steps followed in generating the LARS-WG synthetic data:

1) Extract daily Precipitation and Temperature from the each SDSM output for each time period. Daily solar radiation data were extracted directly from CGCM1 published output results on Environment Canada website (2005) in a grid location corresponding to the study area since this was not possible to downscale.
2) Format data for each time period as required for input in Site Analysis
3) Undertake Site Analysis for each time period.
4) Perform a Qtest for each time period.
5) Calculate relative change in precipitation (m.rain), relative change in wet and dry spell length (wet and dry, respectively), absolute change in temperature, relative change in mean temperature standard deviation (sd) and mean change in solar radiation (rad) between the base (1961-1990) and future time periods.
6) Create Scenario files, shown in Table 4-2, for generation of the synthetic weather data.

Table 4-2: Climate Scenario files used in generating synthetic weather for the different time periods.

[NAME]
SDSMbase_1961-1990

[DATA]	m.rain	wet	dry	tem	sd	rad
Jan	1.00	1.00	1.00	0.00	1.00	0.00
Feb	1.00	1.00	1.00	0.00	1.00	0.00
Mar	1.00	1.00	1.00	0.00	1.00	0.00
Apr	1.00	1.00	1.00	0.00	1.00	0.00
May	1.00	1.00	1.00	0.00	1.00	0.00
Jun	1.00	1.00	1.00	0.00	1.00	0.00
Jul	1.00	1.00	1.00	0.00	1.00	0.00
Aug	1.00	1.00	1.00	0.00	1.00	0.00
Sep	1.00	1.00	1.00	0.00	1.00	0.00
Oct	1.00	1.00	1.00	0.00	1.00	0.00
Nov	1.00	1.00	1.00	0.00	1.00	0.00
Dec	1.00	1.00	1.00	0.00	1.00	0.00

[END]

[NAME]
SDSMScene_2010-2039

[DATA]	m.rain	wet	dry	tem	sd	rad
Jan	1.53	1.19	1.25	1.27	1.00	0.10
Feb	1.87	1.25	1.11	1.44	1.06	0.10
Mar	1.24	0.99	1.24	0.29	1.02	0.40
Apr	1.19	0.96	1.56	1.25	0.95	0.90
May	1.16	1.04	1.12	1.00	1.20	1.10
Jun	1.09	0.89	0.96	1.12	1.07	0.10
Jul	1.08	1.21	1.14	1.36	1.01	0.20
Aug	1.29	1.39	1.07	1.15	1.02	-0.70
Sep	1.98	1.45	1.07	0.72	1.01	-0.70
Oct	1.42	0.82	1.13	1.20	1.00	-0.20
Nov	1.44	1.29	1.05	1.29	0.99	0.00
Dec	2.21	1.11	0.85	1.62	0.92	-0.40

[END]

[NAME]
SDSMScene_2040-2069

[DATA]	m.rain	wet	dry	tem	sd	rad
Jan	1.71	1.53	1.10	1.99	1.04	-0.10
Feb	2.16	1.79	1.09	2.43	1.02	-0.20
Mar	1.42	1.20	1.21	1.49	1.00	0.30
Apr	1.04	0.87	1.68	1.92	1.04	0.70
May	0.96	0.94	1.14	1.66	1.06	0.20
Jun	1.63	1.19	1.13	1.75	1.14	0.20
Jul	1.28	1.19	1.05	2.47	0.97	-0.30
Aug	1.59	1.23	1.03	2.45	1.01	-0.40
Sep	1.53	1.28	1.09	1.70	1.01	-0.50
Oct	1.66	1.11	1.15	2.54	1.04	-0.60
Nov	1.62	1.49	1.09	1.89	1.08	-0.30
Dec	2.41	1.53	0.67	2.32	0.91	-0.60

[END]

[NAME]
SDSMScene_2070-2099

[DATA]	m.rain	wet	dry	tem	sd	rad
Jan	2.28	1.41	0.94	3.24	1.11	-0.10
Feb	2.43	1.43	0.74	2.88	1.05	-0.40
Mar	1.42	1.12	1.27	2.52	1.03	0.10
Apr	1.06	0.84	1.49	2.86	1.02	0.60
May	1.03	0.98	1.35	3.25	1.21	-0.20
Jun	1.58	0.98	1.04	3.44	1.06	-0.70
Jul	1.30	1.20	1.12	3.59	1.03	-1.10
Aug	2.03	1.13	0.91	3.96	1.10	-1.50
Sep	1.89	1.61	0.99	3.11	1.06	-1.60
Oct	1.99	1.01	1.10	4.13	1.14	-0.70
Nov	1.71	1.43	0.88	4.39	1.04	-0.50
Dec	2.79	1.66	0.75	4.49	1.06	-0.50

[END]

4.3.2. RESULTS OF LARS-WG

This section discusses the results of model's simulation performance and the generation of synthetic weather data for the various time periods. The weather variables -precipitation and temperature- generated by LARS-WG are compared with the observed weather, data generated with WGEN and directly from SDSM output.

Precipitation

LARS-WG gave very good χ^2 and p-values (see Table 4-1) for both the precipitation and wet/dry series, indicating a very good fit of the model simulation results to the observed. Similarly, the simulated mean monthly precipitation values match very well to the observed, but with an average monthly bias of about 1.5% (Figure 4-1). The LARS-WG generated precipitation better represents the observed than that generated with SDSM (Figure 4-2). More so, the precipitation values obtained from LARS-WG using direct daily CGCM1 output are of the same pattern (Figure 4-2).

On the other hand, the variability (defined by standard deviation values) of LARS-WG simulated monthly precipitation is higher than the observed, especially from October to March (Figure 4-3). However, the same variability pattern is observed (i.e., greater variability in January, decreasing progressively up to July, and then increasing steadily again to December and January).

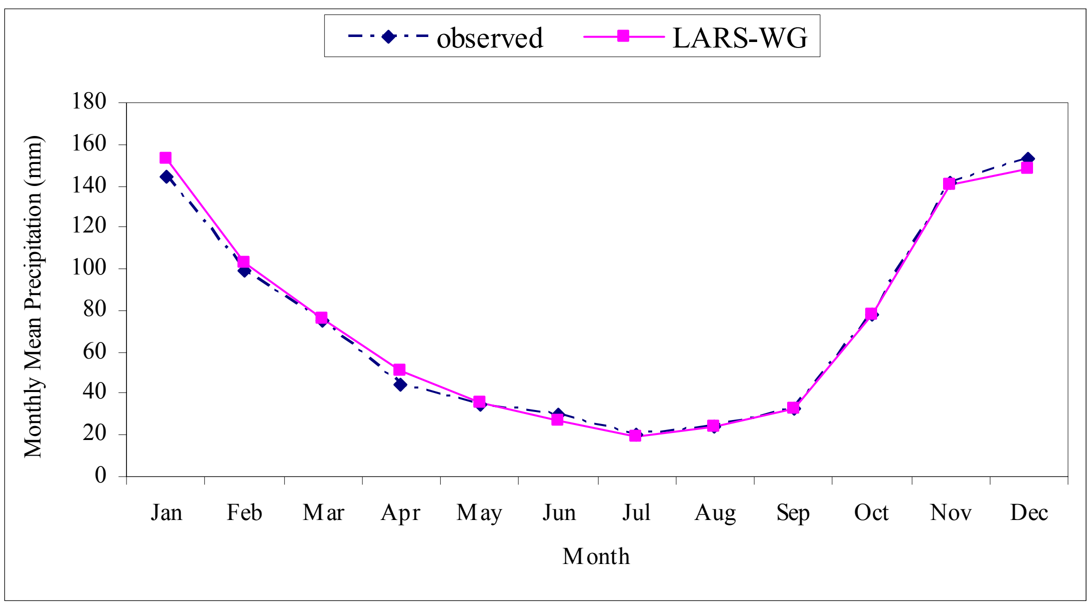

Figure 4-1: Comparing the observed mean monthly precipitation at Gulf Islands, BC, to the LARS-WG simulated values.

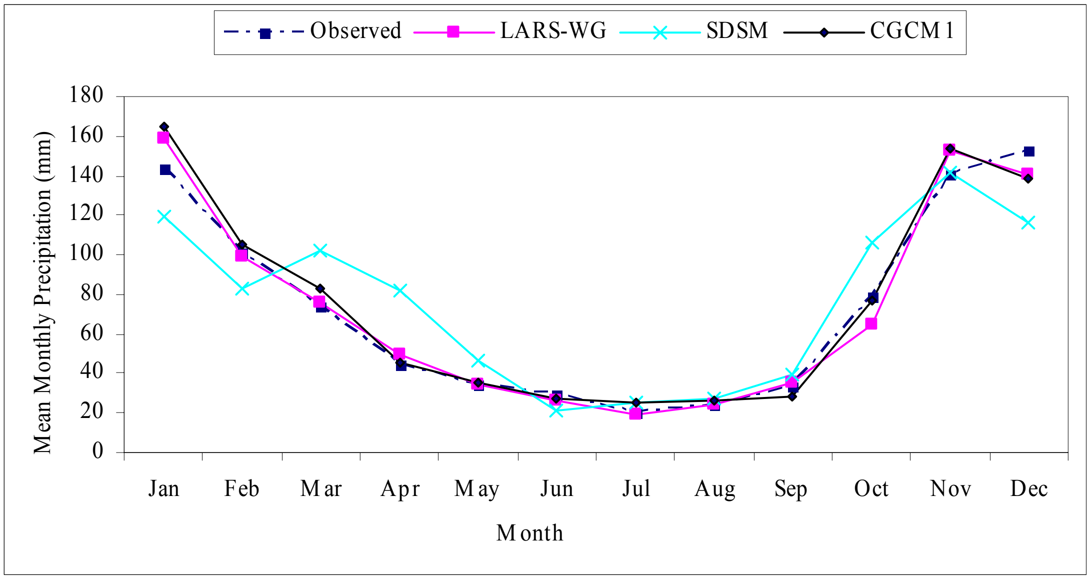

Figure 4-2: Comparing mean monthly precipitation generated using LARS-WG from SDSM output and LARS-WG from direct CGCM1 daily data, and WGEN generated with the observed.

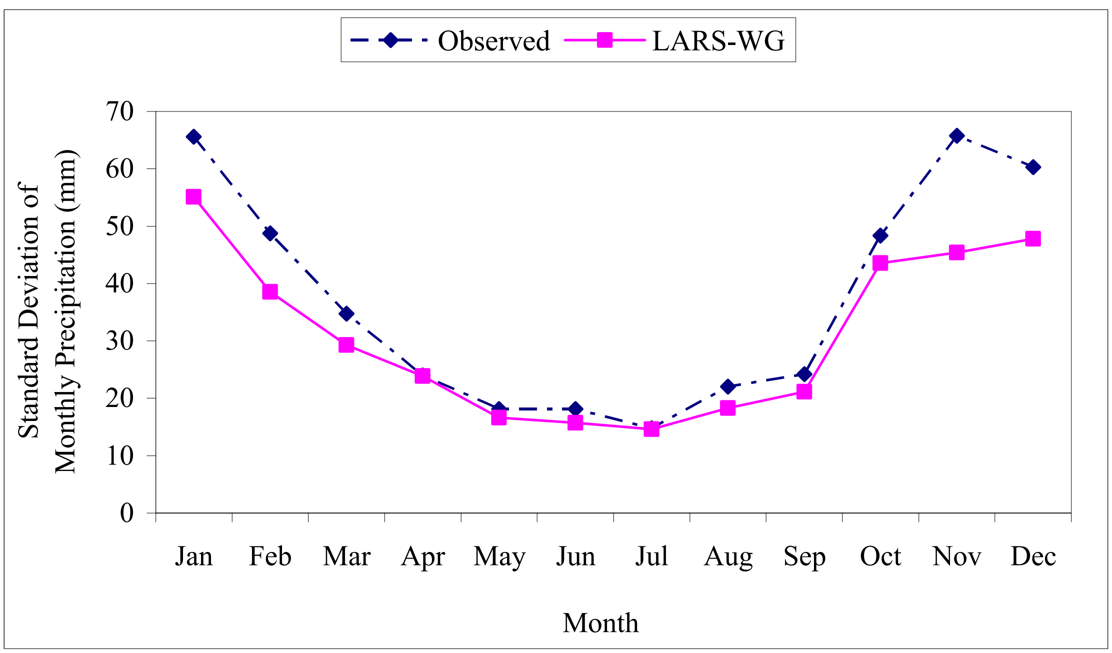

Figure 4-3: Comparing LARS-WG simulated monthly precipitation standard deviation with the observed standard deviation.

Temperature

The LARS-WG simulated monthly and daily maximum/minimum temperature values match very well with the observed values of the study area for all months (Figure 4-4), although the statistical test result, in Table 4-2, showed no fit for December to February during frost conditions. Likewise, the LARS-WG simulates the observed temperature better than both the SDSM and direct CGCM1 output (Figure 4-5). Figure 4-6 shows the calculated standard deviation of the daily minimum and maximum of the LARS-WG simulated temperature compared to the observed. The variability pattern of the simulated temperature is very similar to the observed, with a difference of up to 0.4°C lower in some months.

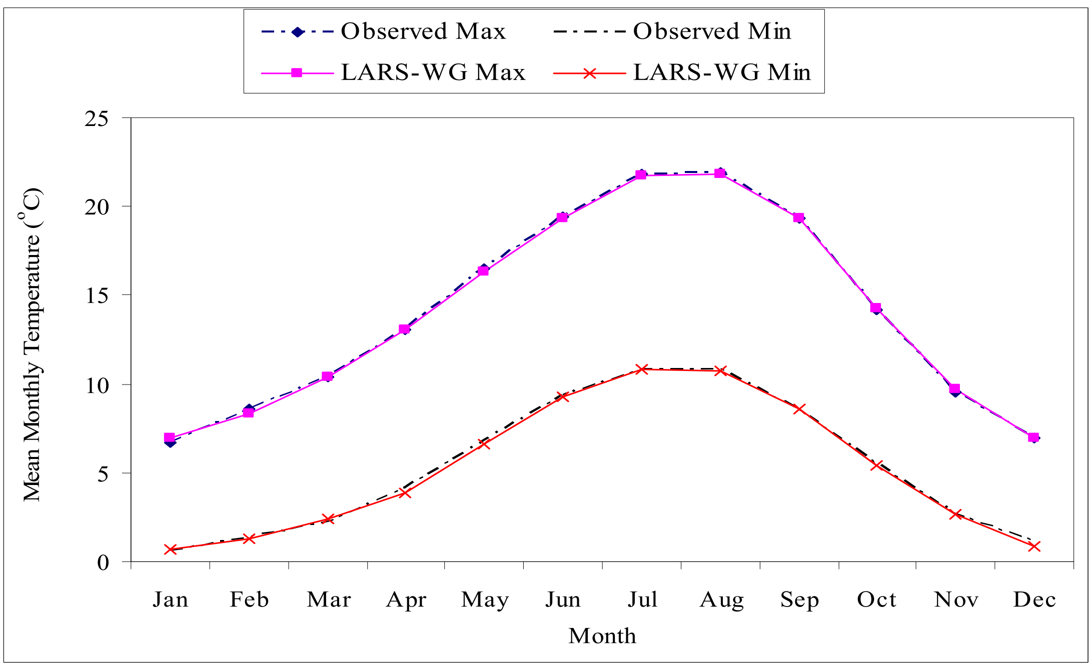

Figure 4-4: Performance of LARS-WG in simulating monthly maximum and minimum temperature of Gulf Islands.

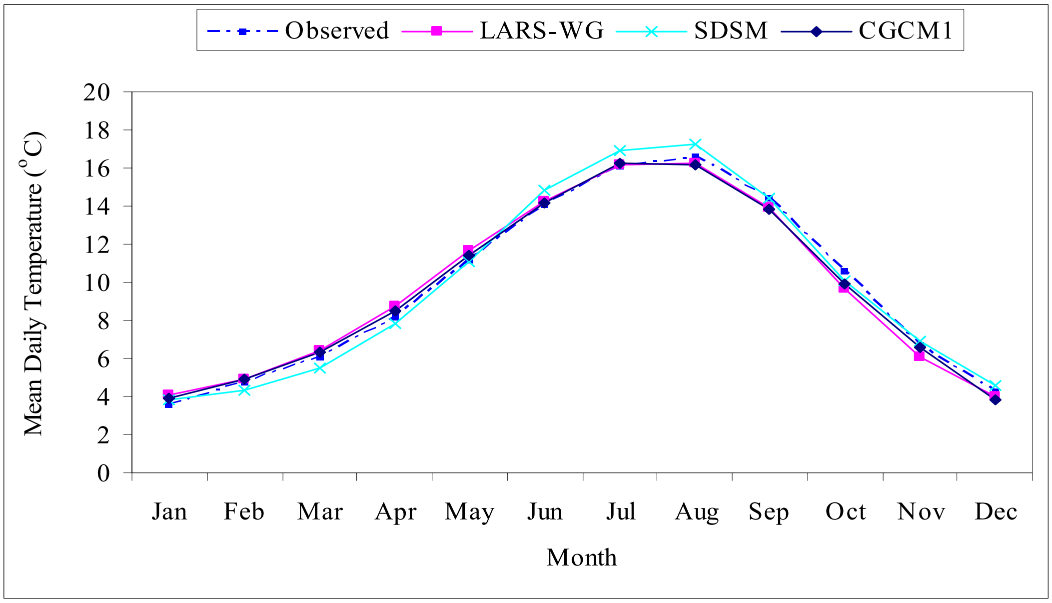

Figure 4-5: Comparing mean monthly temperature generated using LARS-WG from SDSM output with direct CGCM1 daily data, SDSM output and the observed values.

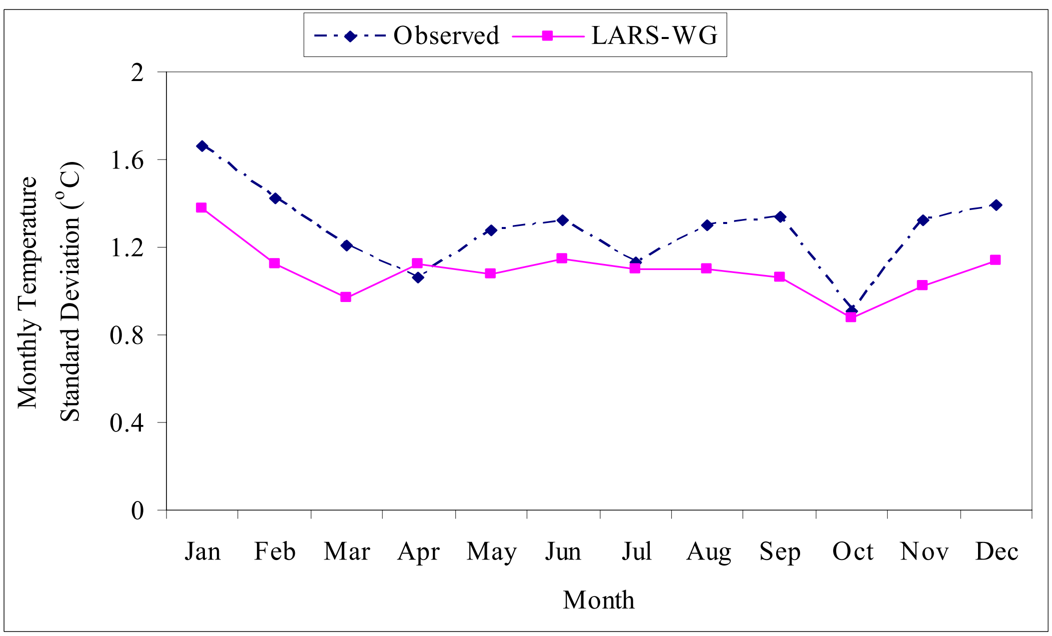

Figure 4-6: Comparing the LARS-WG simulated mean temperature standard deviation with the observed.

Solar Radiation

Like the temperature, solar radiation was well reproduced by the LARS-WG simulations. The mean monthly solar radiation of the LARS-WG generated output is between 0.4 – 1.2 MJ/m^2 lower than the observed (Figure 4-7). The observed values, here, are the observed sun hours, converted solar radiation by LARS-WG. Variability in the simulated daily solar radiation is widely distributed as compared to the narrow range of variability for the observed values (Figure 4-8).

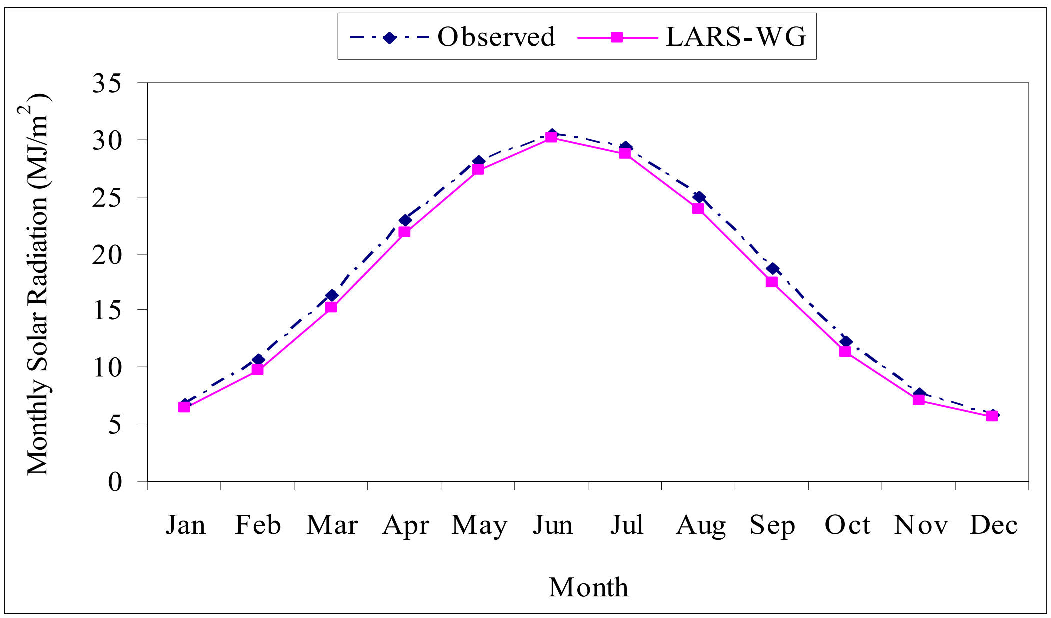

Figure 4-7: LARS-WG performance in simulating the calculated observed daily solar radiation of Gulf Islands.

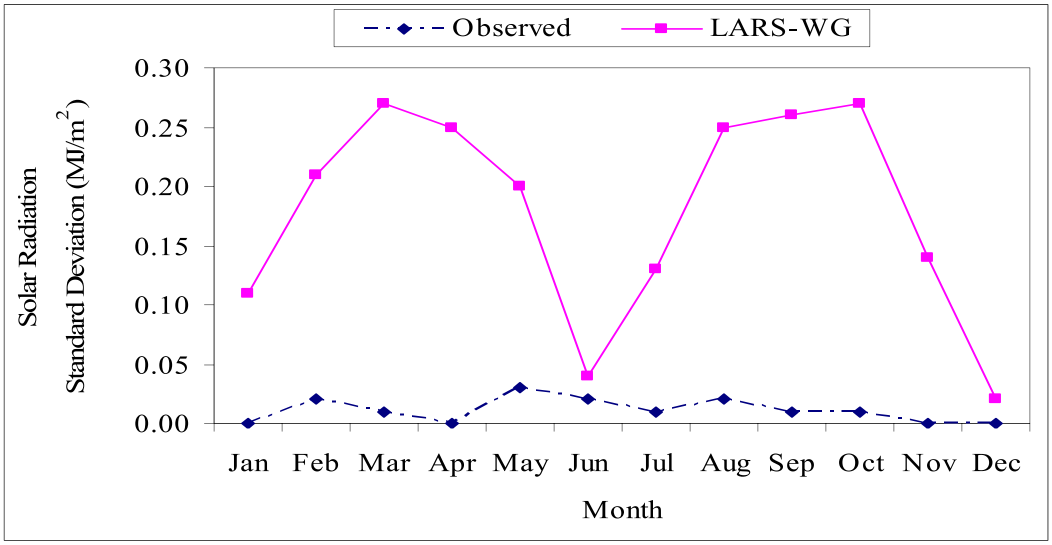

Figure 4-8: Comparing LARS-WG simulated standard deviation in daily solar radiation with the calculated observed values.

4.4 DESCRIPTION OF VERTICAL PROFILE INPUTS

A vertical percolation column in HELP represents all the soil layers and bedrock above the groundwater table in an aquifer. The model estimates recharge based on the specified properties of the geologic media (hydraulic conductivity, field capacity, wilting point, and porosity), the thickness of the individual layers within the column, and the slope and drainage of these layers (where necessary). Within UnSat Suite there is a user interface for HELP, hence Visual HELP, which facilitates column design and project management with a pre-existing database of soils and their properties, as well as a material designer for specifying new materials.

The main inputs used for the HELP recharge modeling are the aquifer hydraulic properties, which are, in this particular region, strongly related to fracturing, the soil thickness and properties, and the depth to water table. These variables vary from one location to the other. Ultimately, the combinations of these parameters determine the rate at which recharge reaches the groundwater system of an aquifer.

Since the HELP model predicts recharge at point locations in an aquifer, many different vertical percolation profiles, representative of the average stratigraphy at particular locations, were developed. Each profile is characterized by the soil type (including the surface slope, where applicable), the depth to water table and the aquifer media geology. A profile differs from the others by, at least, one of these parameters.

The data for construction of the vertical percolation profiles was derived from two sources:

a) The Province of British Columbia maintains a water well database (WELLS), in which information obtained by a driller at the time of well construction is stored. Such information includes, for example, well depth, water depth at the end of drilling, construction method, an estimate of well yield, and a lithology log. Lithology data for the Gulf Islands had been previously extracted and standardized[1] (Allen, personal communication, 2006) for use in vulnerability mapping for the Gulf Islands.
b) Simon Fraser University, in collaboration with the Geological Survey of Canada developed a set of intrinsic vulnerability maps for the Gulf Islands, following a modified DRASTIC method (DRASTIC Fm). GIS datasets consisted of either raster or polygon coverages for each of the DRASTIC input parameters. D - depth to water table, R – estimated recharge[2], A - aquifer media, S – soil media, T – topography, I – Impact of Vadose zone (estimated vertical permeability), and C – conductivity of the aquifer media.

[1] The standardization program created at Simon Fraser University was used to standardize the lithologies. Standardization is based on a set of rules that allow dominant material types to be identified based on first appearance of the term or by other qualifiers (e.g., silty sand means "sand" is the dominant material type with "silt" as the secondary material). Grain size and colour, as well as fracturing are descriptors.
[2] Recharge for the DRASTIC vulnerability maps was estimated using HELP, but only in a very simplistic fashion.

An additional parameter, Fm – Fractured media, based on fracture lineaments, was also available.

4.4.1. SURFICIAL SEDIMENT (SOIL) TYPE

The vertical soil profile overlying the aquifer, its thickness and properties - porosity, field capacity and hydraulic conductivity - are needed for HELP recharge modeling. This information determines how fast recharge water, which is precipitation in the case of this study, is transported to the groundwater system. Information on the different soils on the Gulf Islands was obtained both from GIS soils maps and the provincial WELLS database. The soils map provided the distribution of the surficial sediments on each island, while the database provided information on the average soil depth for each class of soil considered.

Four main soil classes, namely; clay (Clay), topsoil (TS) (loamy sand overburden), glacial till (GT), and gravelly sand (GS) were identified as the predominant surficial materials reported on the well logs. The original soil names, their description and assigned soil classes are presented in Table B-3 of Appendix B. The distribution of these surficial materials on the islands is shown on Map 4-1. The average thickness of these formations above the water table, estimated from Mayne Island only and assumed to be the same for all the islands, and their properties are summarized in Table 4-3. The properties of the soils -saturated hydraulic conductivity (Ksat), porosity, field capacity and wilting point- represent average values estimated from the literature (Fetter, 2001; Domenico and Schwartz, 1998) and the materials database of the HELP model.

Table 4-3: Summarized properties of soils used in HELP recharge modeling.

Soil Class	Thickness (m)	Ksat (cm/s)	Porosity (Vol/Vol)	Field Capacity	Wilting Point (Vol/Vol)
Top Soil (TS)	1.43	1.00×10^{-3}	0.45	1.3×10^{-1}	5.80×10^{-2}
Clay (Clay)	3.96	2.00×10^{-7}	0.47	2.84×10^{-1}	1.35×10^{-1}
Glacial Till (GT)	3.03	1.00×10^{-4}	0.35	1.05×10^{-1}	4.70×10^{-2}
Gravelly Sand (GS)	0.73	1.00×10^{-2}	0.42	4.50×10^{-2}	1.80×10^{-2}

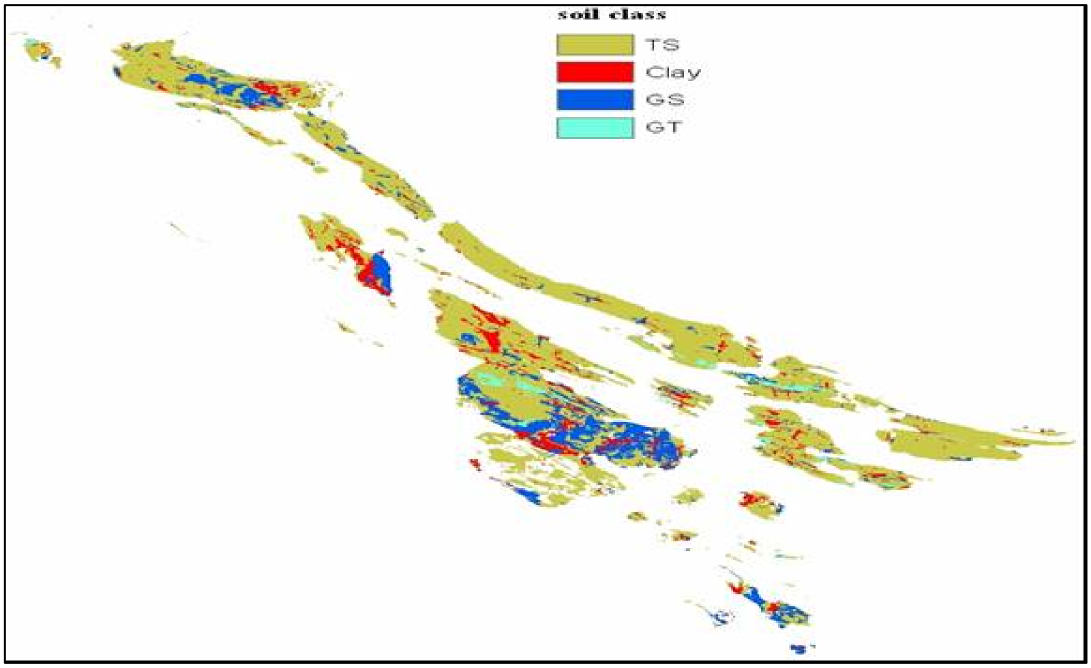

Map 4-1: Predominant surficial material (soil) types on Gulf Islands.

4.4.2. AQUIFER MEDIA

Bedrock maps (Mustard, 1994) had been reclassified during the DRASTIC Fm mapping project to correspond to each of mudstone-dominant and sandstone-dominant lithologies. Superimposed on these are the fault zones, which cross-cut all formations.

On-going research on the Gulf Islands (Surette, in prep) resulted in a classification of the aquifer media of Gulf Islands into three groups, namely; less fractured sandstone (LFSS), fractured interbedded mudstone and sandstone (IBMS-SS), and fault zones (FZ), based on the lithology and structural setting. The study uses the concept of hydrostructural domains (Mackie, 2002), applied to a dataset comprising about 9000 fractures measured at 157 stations on the islands to model the vertical hydraulic conductivities of the different aquifer media with the aid of FracMan XP for MODFLOW and GMS. The model estimated vertical hydraulic conductivities of the three formations are shown in Table 4-4.

Table 4-4: Vertical hydraulic conductivities of the fractured aquifer media.

Aquifer Unit	**Hydraulic Conductivity (m/s)**
LFSS – Less Fractured Sandstone	5.71×10^{-8}
IBMS-SS – Interbedded Mudstones and Sandstones	1.09×10^{-7}
FZ –Fault Zones	9.48×10^{-8}

Using the geologic maps as a base, the three classes of aquifer media were assigned. Map 4-2 shows the different aquifer media geology classes on the islands.

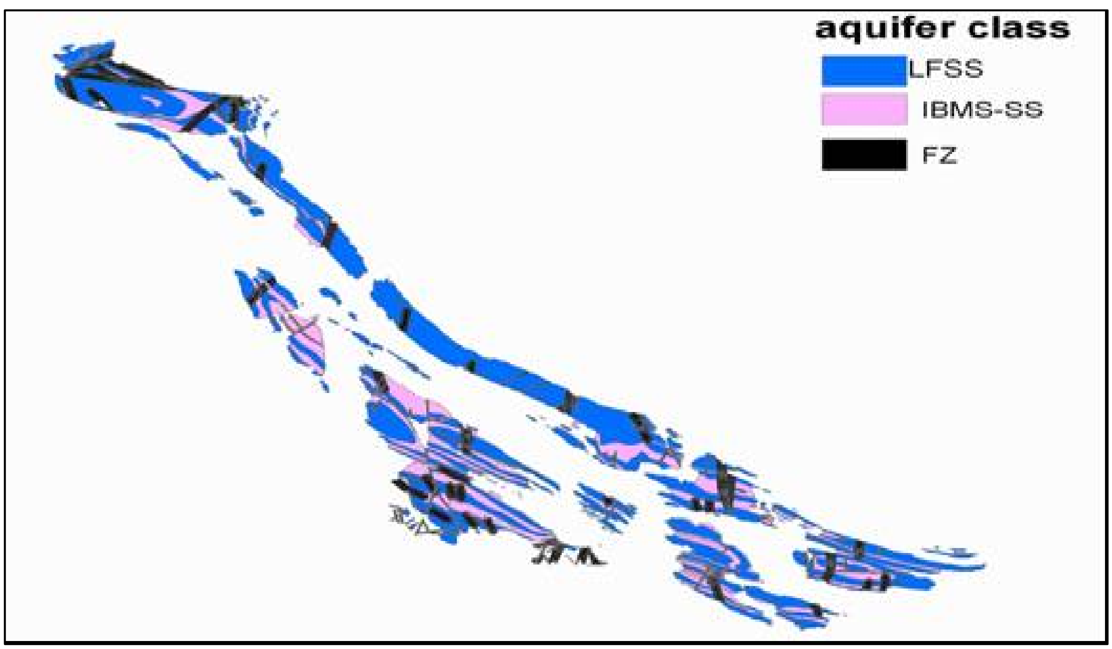

Map 4-2: Re-classified Gulf Islands aquifer media types

4.4.3. DEPTH TO WATER TABLE

The depth to water table is the distance from the ground surface to the water level in the aquifer. It is needed in determining the thickness of the sediment columns that are to be used in the recharge modeling. Depth to water table was estimated directly from the static water levels documented for the well logs of Mayne Island, and assumed to be representative, of the study area. The static water level is a one-time measure of the depth of water in a well, immediately taken after drilling, and is assumed to be representative of the groundwater level in the aquifer. Out of 504 wells drilled on the island (i.e., Mayne Island), only 166 had measured values of static water levels. Descriptive statistical analyses of these values were used to categorize the water depth, based on the minimum, maximum and the quartile breaks Table 4-5. The mid point of each range of water depth was then used as representative thickness of the sediment columns in the HELP recharge estimations of the Gulf Islands. Map 4-3 shows the distribution of the representative water depths on the islands.

Table 4-5: Statistical analyses results of static water levels in the well logs and the representative water depths using in creating HELP columns for recharge modeling.

Description	Results	Water Depth Range (m)	HELP Column (m)
Count	166.00		
Mean	7.65		
Minimum	0.30	0.30 – 2.74	1.52
1st Quartile	2.74	2.75 – 5.33	4.04
Median	5.33	5.34 - 9.14	7.24
3rd Quartile	9.14	9.15 - 39.62	24.40
Maximum	39.62		
STDEV	7.56		

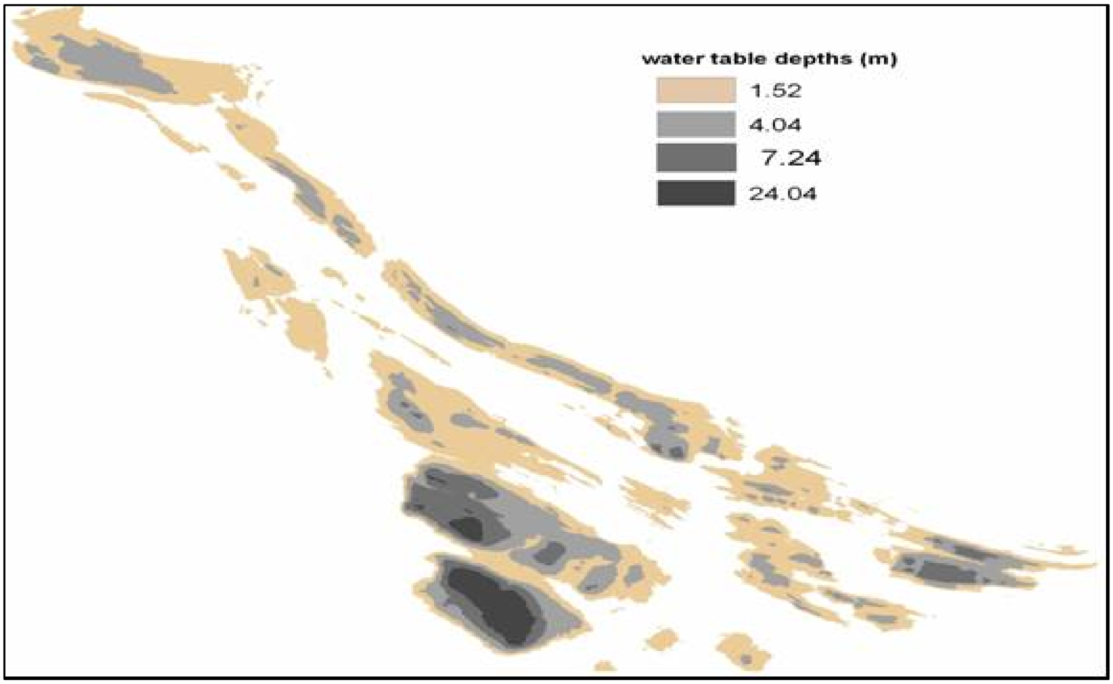

Map 4-3: Distribution of representative water depths on the islands.

4.5 SENSITIVITY ANALYSIS

Prior to running the HELP model for recharge estimations, a sensitivity analysis was perform to evaluate the effects of all the model input parameters, except the main vertical profile input (see section 4.4 above), on recharge. Each of the parameters -Leaf Area Index (LAI), Evaporative Zone Depth (EZD), Drainage Slope (S), Slope Length (SL), HELP Column Area (A) and Runoff Curve Number (CN)- were varied and the mean annual water balance at the end of the recharge simulations were compared to determine its influence. The analysis was performed with the same climate data on a 4 m thick vertical column profile with less fractured sandstone aquifer media and a combination of all the different soil types.

The results of the analysis, presented in Table B-4 of Appendix B, shows EZD has great influence on recharge, LAI and CN have moderate influence, S has low influence, while SL and A has no influence on the recharge. Hence, appropriate values of the sensitive parameters, Table 4-6 and Figure B-1 (see Appendix B) were used for the recharge modeling of the Gulf Islands. The estimated S and CN values were obtained from Gulf Islands digital elevation map and U.S. L-THIA (2005), respectively. The vegetation cover on the islands are typically treed, hence LAI of 100 cm was used to represent a typical root depth, while the percentage of the surface area from which runoff is possible was assumed to be 100 %.

Table 4-6: Estimated curve number and drainage slopes for the soil classes of Gulf Islands.

Soil Class	Curve Number (CN)	Drainage Slope (S in %)
TS	70	47
Clay	77	7
GT	55	268
GS	50	35

4.6 STEPS FOR HELP RECHARGE MODELING

A total of 48 vertical percolation columns were created for the study area, based on a combination of the three aquifer media types, four different soil formations, and the four depths to water table (i.e., $3 \times 4 \times 4 = 48$). However, only 44 of them were used in HELP recharge estimations since 4 of the combinations were, practically, a repetition of already created combinations due to the greater thicknesses of clay and glacial till soils than the first representative water depth. The spatial distribution of the combinations is shown in Map 4-4. Each sediment column is made up of two layers, with the soil layer overlying the aquifer media (Figure 4-9). In order to differentiate the appearance of the two layers in the sediment profiles for easy identification, a vertical percolation layer and horizontal drainage layer were used for the soil and aquifer media designs, respectively. It should be noted that the model performance is not affected in any way when a vertical percolation or lateral drainage layer is used in the column designs, since lateral inflow into the vadose zone is not considered in this particular study, i.e., vertical flow only is considered. With the exception of the topsoil, all the soil and aquifer media types were created in the HELP material database for designing the sediment columns.

The HELP recharge modeling procedure involved creating the vertical percolation columns representative of aquifer recharge zone conditions, running the weather generator to obtain the weather inputs (here the LARS-WG output were substituted), and then running the model for recharge through the columns. The user must specify the initial water content for all the layers within a column or allow the model to compute it, by default, before running the recharge simulations. The latter approach was used in this study, whereby the model assigns realistic values of initial moisture storage for the layers in the column, simulates one year of hydrology, and then uses the moisture storage obtained as initial values of the layers in the recharge modeling process.

The HELP model was then used to compute daily, monthly and annual recharge for all the columns using the same 30 year daily weather dataset generated for each CGCM1 time period from LARS-WG.

The recharge results are exported to MS Excel for analysis and then to ArcGIS where raster calculations are performed to compute spatially distributed recharge for all the CGCM1 time periods. Finally, Gulf Islands is classified into recharge zones using the recharge values linked to the aquifer media map, soil classification map and water table depth map for the climate change impact assessments.

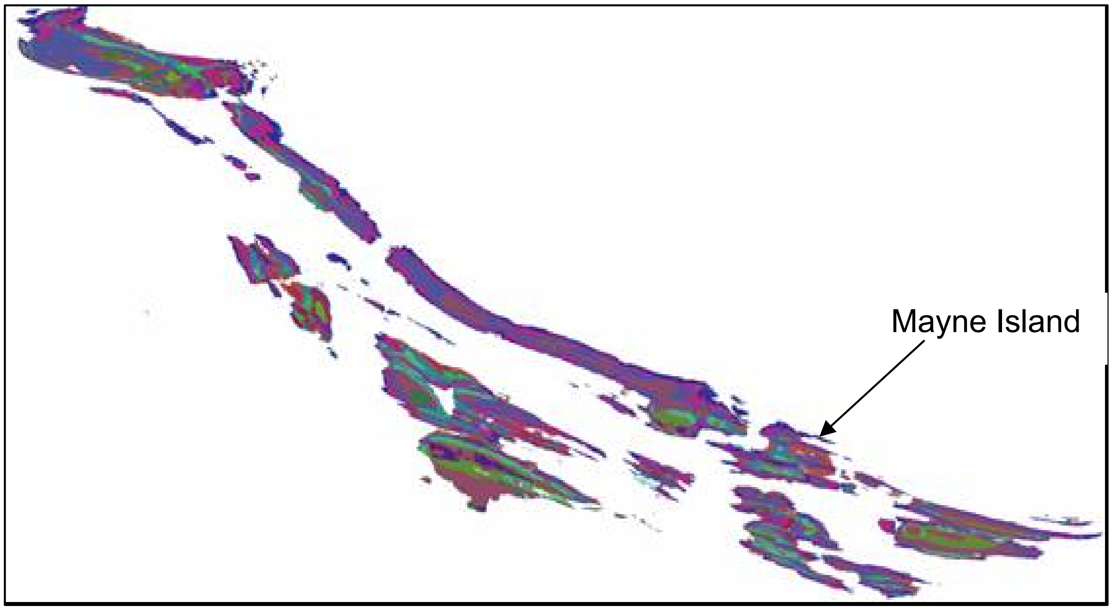

Map 4-4: Spatial distribution of Gulf Island recharge zones.

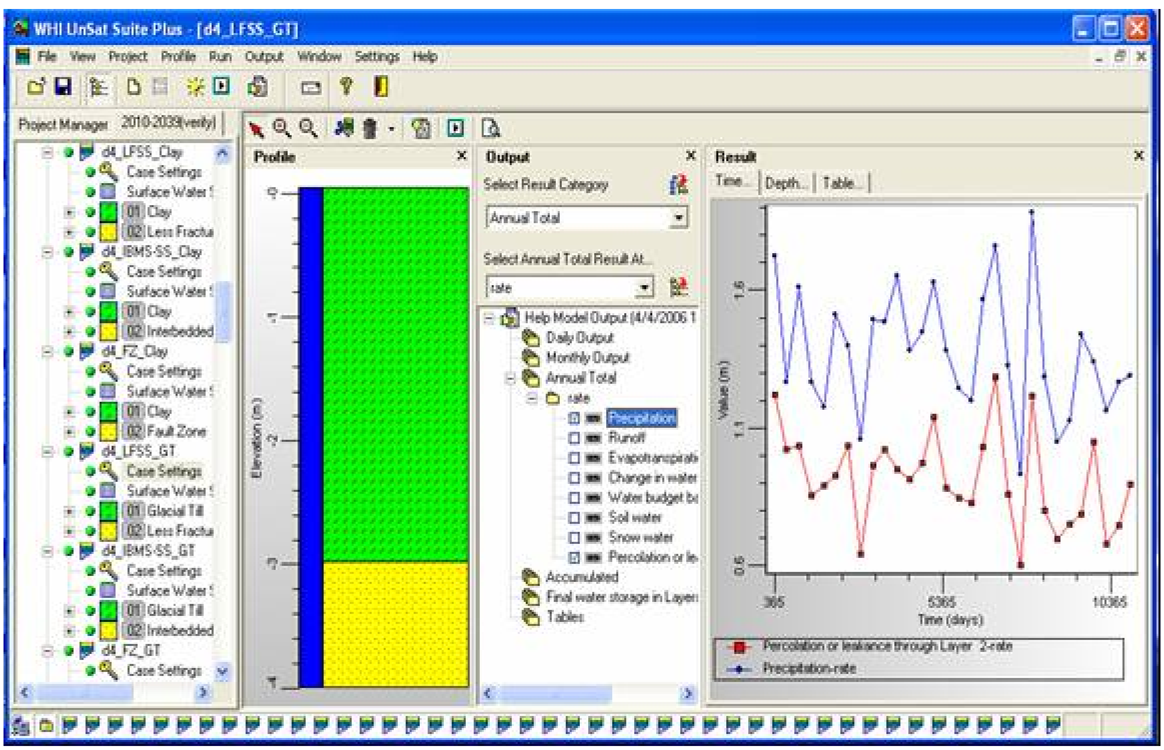

Figure 4-9: HELP model interface displaying vertical profile and results of recharge estimations.

CHAPTER 5. RECHARGE MODELING RESULTS

HELP recharge modeling of the Gulf Islands aquifers using the four different CGCM1 time period climates are presented and discussed in this section. A summary of the modeled values, expressed as mean monthly recharge (i.e., average monthly recharge over a 30 years time period) and mean annual water balance for each representative HELP column are presented in Appendix C. The summarized values were linked to the recharge zones for the current and future CGCM1 time periods. Predicted changes in both the mean monthly and annual recharge were converted to percentage differences: (future – current) / current, and also linked to the recharge zones for spatial mapping.

For clarity and easy understanding, only the spatially distributed recharge maps of Mayne Island (see Map 4-4) will be shown in the discussion of the results.

5.1 CURRENT RECHARGE

The current spatially distributed mean annual recharge to the Gulf Islands aquifer, Map 5-1, ranges between 184 to 578 mm/yr, representing between 20% to 60% of the mean annual precipitation. Mean annual recharge for all recharge zones combined is approximately 45% of mean annual precipitation (Table 5-1).

Figures 5-1 and 5-2 show the mean monthly precipitation and recharge to the Gulf Islands aquifers (i.e., the mean recharge estimates from all the representative HELP columns) for the different climate time periods. Mean monthly recharge to the aquifer, Map 5-2, varies between 14 to 41 mm/month (i.e., the average of value for the monthly means). Lower recharge (i.e., below the monthly mean) occurs in July through to October, with the latter receiving the lowest. Higher recharge occurs in December to March while November, April and May receive moderate recharge. The monthly recharge pattern is a reflection of the temporal distribution of precipitation (see Figure 5-1), which happens to be only source of recharge to aquifer.

Mean annual precipitation (i.e., the SDSM and LARS-WG combined output used in running the model) (Table 5-1) is predicted to increase by about 61%, 72% and 82% in 2010-2039, 2040-2069 and 2070-2099, respectively, from the current. The mean annual recharge is consequently observed to progressively increase from the current time period into the future, as precipitation increases. Details on each time period are provided in the following sections.

5.2 2010-2039 RECHARGE

The CGCM1 2010-2039 climate time period predicts between 16 to 94% increase in mean annual recharge (Map 5-3a). Predicted mean monthly recharge to the aquifer, shown in Map 5-4a, increases between 17 to 77 mm/month. Similarly, low recharge values occur in July through to October with the lowest occurring in September. High recharge occurs in December to February, while November and March though to June receive moderate recharge.

5.3 2040-2069 RECHARGE

The 2040-2069 climate time period predicts an increase of 31 to 111 % in mean annual recharge (Map 5-3b). Predicted mean monthly recharge to the aquifer, shown in Map 5-4b, increases between 20 to 84 mm/month. Lower recharge values occur in July to October, with September receiving the lowest recharge. Higher recharge values are received in November to March, while April to June receives moderate recharge.

5.4 2070-2090 RECHARGE

The 2070-2090 climate time period predicts an increase of 27 to 130 % in mean annual recharge (Map 5-3c). The predicted mean monthly recharge, shown in Map 5-4c, varies between 18 to 91 mm/month. Maximum recharge is occurs in December, whereas the minimum is received in October. Lower recharge values occur in July to October, higher values in November through to April while moderate recharge occur in May and June.

Table 5-1: Mean annual water balance from HELP simulations for the different time periods. (**Note**: Ppt = Precipitations; Colored values represent % increase in mean annual precipitation).

Parameters (mm)	**Current**	**% Ppt**	**2020's**	**% Ppt**	**2050's**	**% Ppt**	**2070's**	**% Ppt**
PRECIPITATION	880.48		1413.97	60.59	1517.24	72.32	1599.06	81.61
RUNOFF	47.38	5.38	158.05	11.18	163.57	10.78	187.27	11.71
EVAPOTRANSP.	435.24	49.43	522.05	36.92	556.48	36.68	548.87	34.32
RECHARGE	394.81	44.84	730.30	51.65	796.22	52.48	861.78	53.89
STORAGE	3.05	0.35	3.57	0.25	0.97	0.06	1.14	0.07

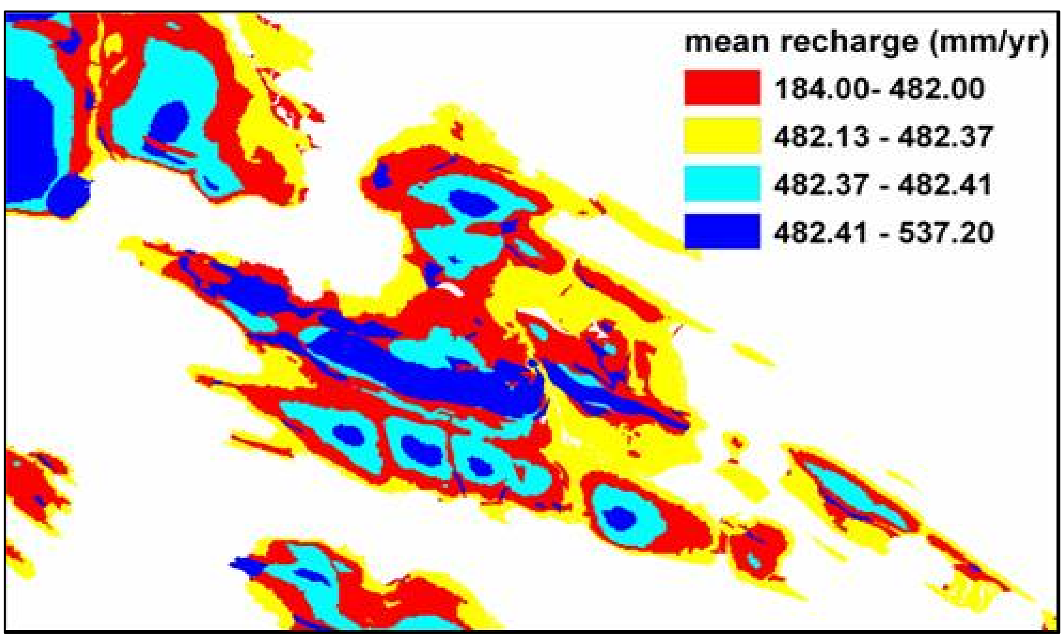

Map 5-1: Mean annual recharge to the aquifer estimated in HELP for the current CGCM1 time period. Quartile ranges shown.

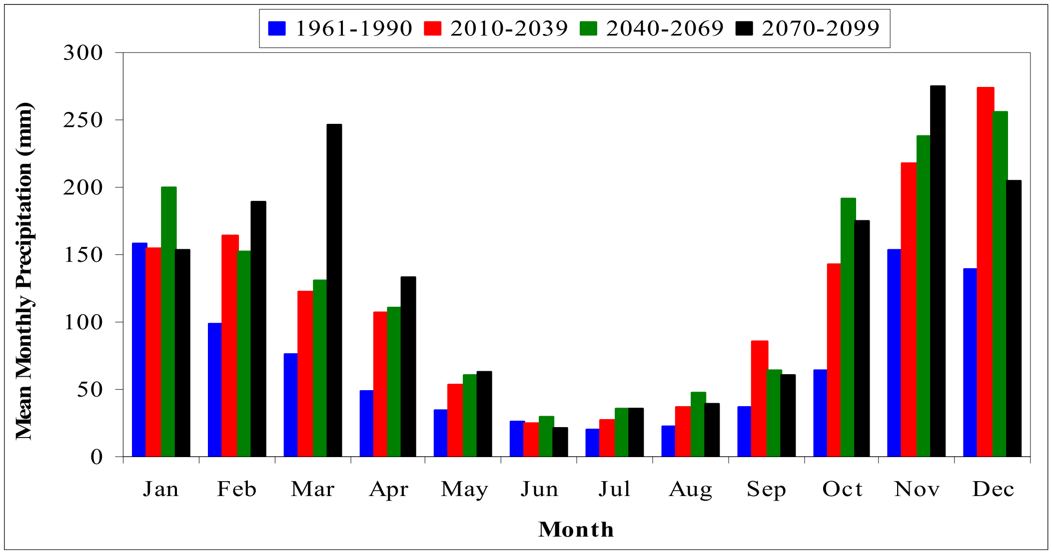

Figure 5-1: LARS-WG generated mean monthly precipitation used in the HELP recharge modeling.

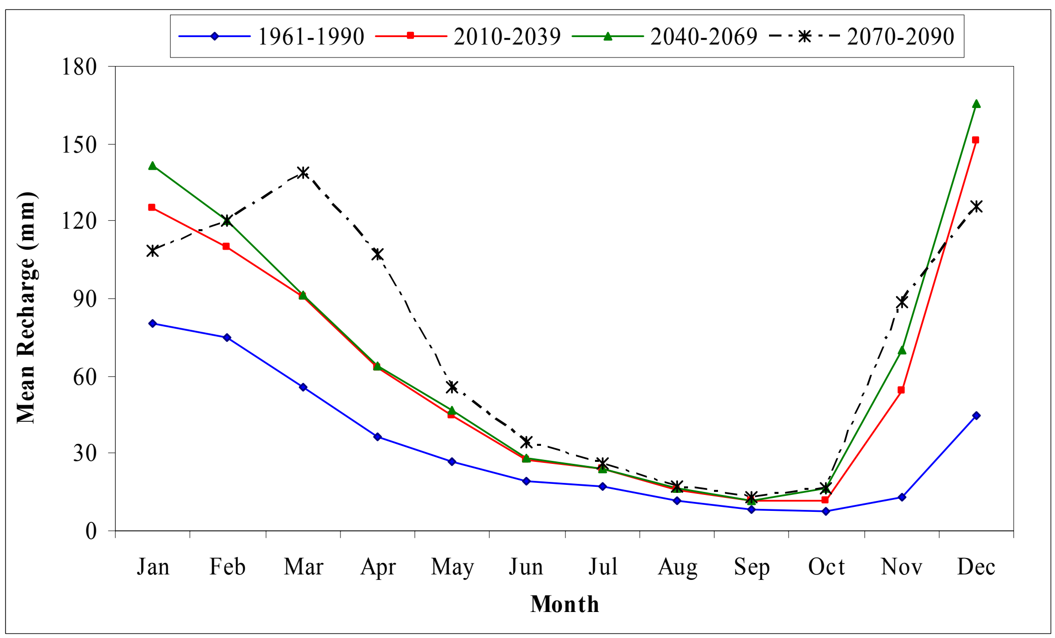

Figure 5-2: HELP monthly recharge estimates of the Gulf Islands aquifers for current and future CGCM1 time periods.

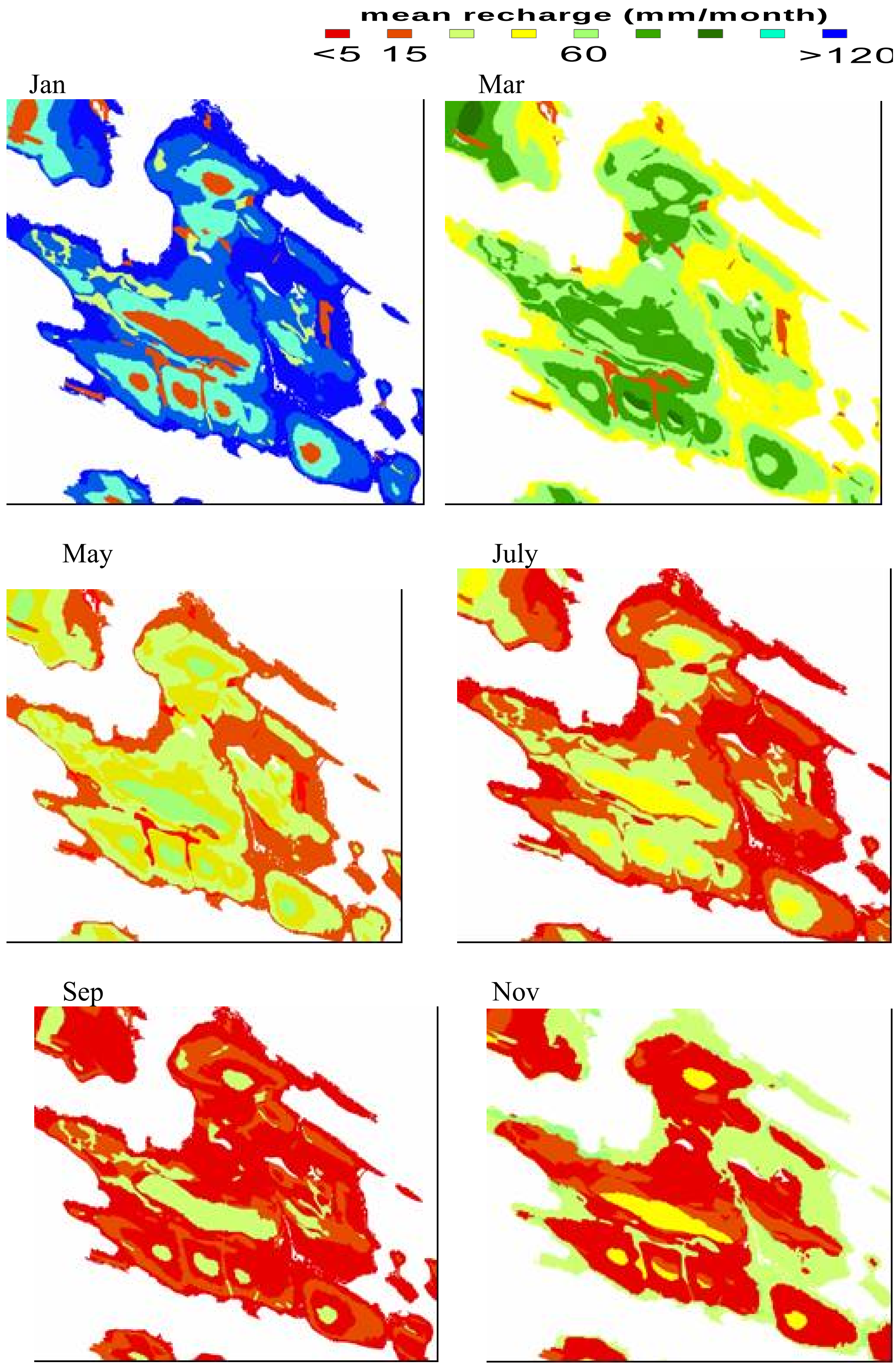

Map 5-2: Mean monthly recharge to the Gulf Islands aquifer for current CGCM1 time period

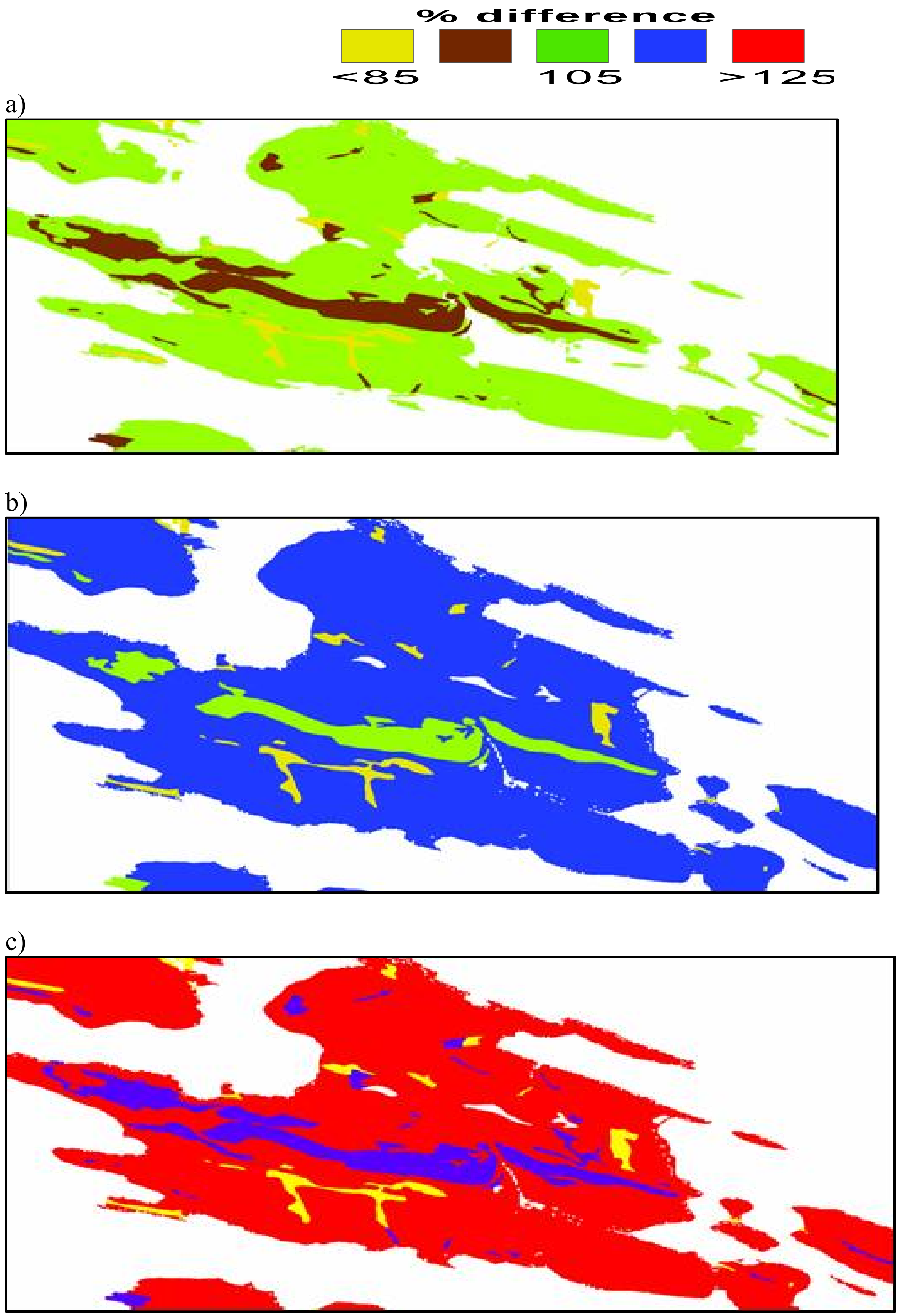

Map 5-3: Mean annual recharge to the Gulf Islands for future CGCM1 time periods: (a) percent change for 2010-2039 time period, (b) percent change for 2040-2069 time period, and (c) percent change for 2070-2099 time period.

a)

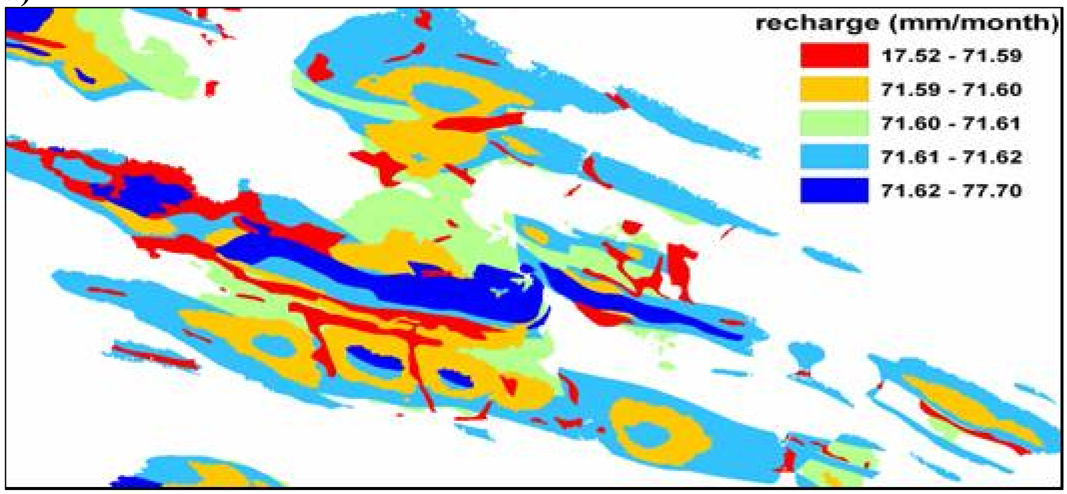

b)

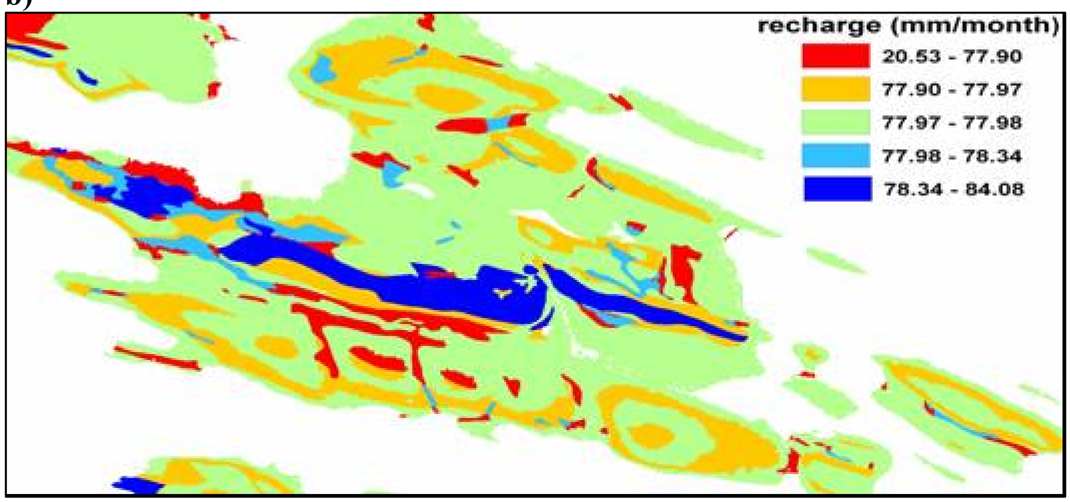

c)

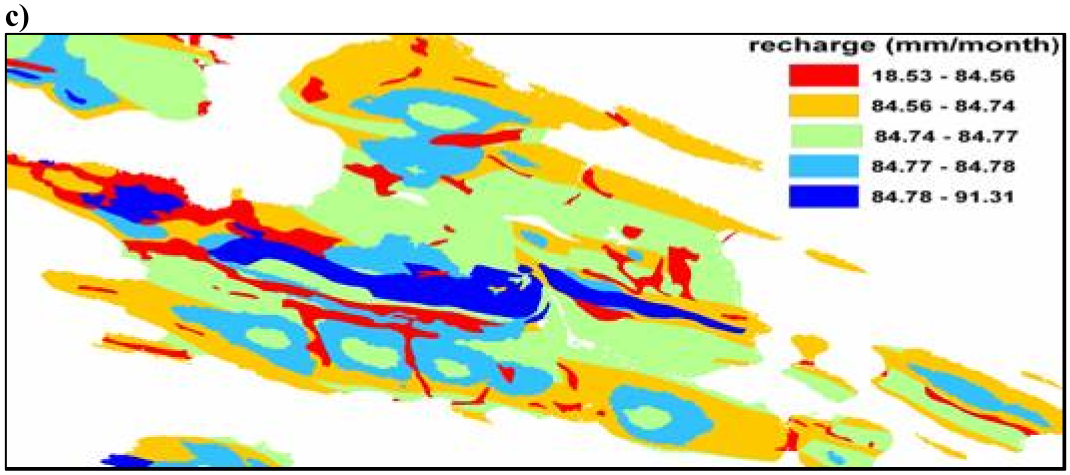

Map 5-4: Average monthly recharge to the Gulf Islands aquifer for the future CGCM1 time periods: a) 2020's, b)2050's and c) 2080's.

CHAPTER 6. CONCLUSIONS

The following conclusions are made from the analyses performed in this research:

1. The climate of Gulf Islands can be adequately represented by that of Victoria Airport in any studies that require long term historic data, such as recharge estimation. Average monthly temperature on the islands, in comparison to Victoria, is higher by about 5% whereas precipitation is up to about 10 % lower.

2. Climate change data predictions for the Gulf Islands for the next 100 years were downscaled from CGCM1 using SDSM. Current predicted temperature was well calibrated to observed, but calibration of precipitation was relatively poor. Errors in individual monthly precipitation ranged from -19 to 50%. Hence, all the SDSM outputs were run through the stochastic weather generator, LARS-WG, to reduce the downscaling errors. SDSM output through LARS-WG produced a very good fit to both the observed precipitation and temperature, with about 1.5% and less than 0.4% errors, respectively. The SDSM downscaled results predict that annual precipitation on the Gulf Islands will increase progressively by 52%, 65% and 82% in the 2020's, 2050's and 2080's, respectively. Mean monthly temperature is also predicted to increase progressively from the present by 1.14ºC in the 2020's, 2.05ºC in the next 30 years, and up to about 3.5ºC by end of the century.

3. Using HELP and ArcGIS, spatially distributed mean annual and monthly recharge to the Gulf Islands was estimated to be in the range of 184 to 537 mm/year (or an average of 14 to 41 mm/month), although mean monthly recharge varies considerably throughout the year with some months (August, September and October) receiving less than 1 mm at certain locations. More than half of the precipitation from December to June contributes to recharge, while less than 40 % of precipitation from July to

November is received as recharge. Highest recharge on the islands is in December, whereas the lowest often occurs in between July and October.

4. The upper range of the recharge estimates is higher than previous estimates based on well hydrograph analysis (which themselves are uncertain due to uncertainties in the storage properties of the aquifer). Typically those analyses yielded less than 200 mm/year. Thus, there remains some uncertainty in the absolute values of present day recharge on the Gulf Islands. It is speculated that perhaps the HELP software under-predicts runoff, despite attempts to ensure that the factors influencing runoff (curve number and slope) were duly considered in the simulations. Notwithstanding these uncertainties, the shifts in climate anticipated for the region can be used to gauge future relative changes in recharge.

5. Recharge is predicted to increase progressively from current to future CGCM1 time periods as precipitation amounts increases, since it is the only source for the recharging the aquifer on the islands. The amount of precipitation received as annual recharge increases from the current (44 %), by 7%, 8% and 9% in the 2020's, 2050's and 2080's, respectively.

REFERENCES

Allen, D.M. Personal Communication, 2006. Department of Earth Sciences, Simon Fraser University, Burnaby, BC, Canada.

Allen, D.M., Mackie, D.C. and Wei, M. 2004a. Groundwater and Climate Change: A Sensitivity Analysis for the Grand Forks Aquifer, Southern British Columbia, Canada. Hydrogeology Journal, 12(3):270-290.

Allen D.M., Scibek, J., Whitfield, P. and Wei, M. 2004b. Climate Change and Groundwater: A Modelling Approach for Identifying Impacts and Resource Sustainability in the Central Interior of British Columbia. Report prepared for Natural Resources Canada, Climate Change Action Fund, 404 pp., published as pdf file on government website: http://www.adaptation.nrcan.gc.ca/.

Allen, D.M.; Matuso, G.; Suchy, M.; Abbey, D.G. 2001. A Multidisciplinary Approach to Studying the Nature and Occurrence of Saline Groundwater in the Gulf Islands, British Columbia, Canada. In: Proceedings of the First International Conference on Saltwater Intrusion and Coastal Aquifers - Monitoring, Modeling, and Management, Essaouira, Morocco.

Allison, G. B. 1988. A Review of some of the Physical, Chemical and Isotopic Techniques available for Estimating Groundwater Recharge, In: Estimation of Natural Groundwater Recharge, edited by I. Simmers, D. Reidel Publishing, Dordrecht, Netherlands, p49-72.

Bear, J. and Cheng, H. D. 1999. Seawater Intrusion in Coastal Aquifers – Concepts, Methods and Practices. Kluwer Academic Publisher, Dordrecht, Boston, London, 625 pp.

Boer, G.J., Flato, G.M. and Ramsden, D. 2000. A Transient Climate Change Simulation with Historical and Projected Greenhouse Gas and Aerosol Forcing: Projected Climate for the 21st Century. Climate Dynamics, 16, p427-450.

Boer, G.J., Flato, G.M., Reader, M.C., and Ramsden, D. 2000a. A Transient Climate Change Simulation with Historical and Projected Greenhouse Gas and Aerosol Forcing: Experimental Design and Comparison with the Instrumental Record for the 20th Century." Climate Dynamics, 16, p405-425.

Blyth, H.E.; Ruther, N.W. 1993. Quartenary Geology of Southern Vancouver Island and Gulf Islands (92B/5, 6, 11, 12, 13 and 14). Geological Fieldwork 1992, Paper 1993-1.

British Columbia Government Statistics. 2004. Local Health Area 64 - Statistical Profile of Gulf Islands, http://www.bcstats.gov.bc.ca/data/sep/lha/lha_64.pdf.

Caya, D. and Laprise, R. 1999. A Semi-Implicit Semi-Lagrangian Regional Climate Model: the Canadian RCM. Monthly Weather Review 127, p341-362.

Claussen, M., L.A. Mysak, A.J.Weaver, M. Crucifix,T. Fichefet, M.-F.Loutre, S.L.Weber, J. Alcamo,V.A. Alexeev, A. Berger, R. Calov, A. Ganopolski, H. Goosse, G. Lohmann, F. Lunkeit, I.I. Mokhov,V. Petoukhov, P. Stone and Z.Wang, 2002. Earth System Models of Intermediate Complexity: Closing the Gap in the Spectrum of Climate System Models. Climate Dynamics, 18:579-586.

CICS, Canadian Institute for Climate Studies. 2005. Canadian Climate Change Scenarios, www.cics.uvic.ca/scenarios/

Cook, P.G. and Robinson, N.I. 2002. Estimating Groundwater Recharge in Fractured Rock from Environmental 3H and 36Cl, Clare Valley, South Australia, Water Resources Research, vol. 38, Issue 8, p1-11.

Domenico, P.A.; Schwartz, W.S. 1998. Physical and Chemical Hydrogeology, 2nd edition. John Wiley and Sons Inc., New York. 506 pp.

Eis, S.; Craigdallie, D. 1980. Gulf Islands of British Columbia: A Landscape Analysis. Canadian Forest Service, Pacific Forest Research Centre, Inf. Rep. No. BC-X-216, Victoria, B.C. 39 pp

Environment Canada. 2005. Daily and Monthly Weather Records. http://climate.weatheroffice.ec.gc.ca/climateData.

Flato, G.M., Boer, G.J., Lee, W.G., McFarlane, N.A., Ramsden, D., Reader, M.C., and Weaver, A.J. 2000. The Canadian Centre for Climate Modelling and Analysis Global Coupled Model and its Climate. Climate Dynamics, 16, p451-467.

Foweraker, J.C. 1974. Groundwater Investigations on Mayne Island, Report No.1: Evaluation, Development, and Management of the Groundwater Resource on Mayne Island. Groundwater Division, Water Investigation Branch, B.C. Department of Lands, Forests and Water Resources. Victoria, B.C. 54 pp.

Freeze, C.W. 2001. Applied Hydrogeology, 4th edition. Prentice Hall Inc., New Jersey. 598 pp.

Global Change Strategies International Inc. and Environment Canada. 2000. Vulnerability and Adaptation to Climate Change. Environment Canada.

Hengeveld, H.G. 2000. A Discussion of Recent Simulations with CGCM. Climate Change Digest, Environment Canada, Special Edition, CCD 00-01, 32 pp.

Holland, S.S. 1976. Landforms of British Columbia: A Physiographic Outline. B.C. Department of Mines and Petroleum Resources Bull. 48, Victoria, B.C. 138 pp.

Hostetler, S. W., Giorgi, F., Bates, G. T., and Bartlein, P. J. 1994. Lake-Atmosphere Feedbacks Associated with Paleolakes Bonneville and Lahontan, Science 263, p665–668.

Jones, P.D. 1994. Hemispheric Surface Air Temperature Variations: A Reanalysis and an Update to 1993. J. Climate, 7, p1794-1802.

Kalnay, E., Kanamitsu, M., Kistler, R. 1996. The NCEP/NCAR 40-year Reanalysis Project. Bulletin of the American Meteorological Society, 77, p437-471.

Laprise, R., Caya, D., Giguere, M., Bergeron, G., Cote, H., Blanchet, J.-P., Boer, G.J. and McFarlane, N.A. 1998. Climate and Climate Change in Western Canada as Simulated by the Canadian Regional Climate Model. Atmosphere-Ocean 36, p119-167.

Mackie, D.C. 2002. An Integrated Structural and Hydrogeologic Investigation of the Fracture System in the Upper Nanaimo Group, Southern Gulf Islands, British Columbia. MSc. Thesis Report Submitted to Earth Sciences Department of Simon Fraser University, Canada. 358 pp.

Mathews, W.H.; Fyles, J.G.; Nasmith, H.W. 1970. Postglacial Crustal Movement in Northwestern British Columbia and Adjacent Washington State. Canadian Journal of Earth Sciences, vol. 7, p690-702.

Mearns, L.O.; M. Hulme,T.R; Carter, R; Leemans, M. Lal and P. Whetton, 2001. Climate scenario development. In: J.T. Houghton; Y. Ding; D.J. Griggs, M. Noguer; P.J. van der Linden; X. Dai; K. Maskell and C.A. Johnson (eds.). Climate Change 2001: The Scientific Basis. Contribution of Working Group I to the Third Assessment Report of the Intergovernmental Panel on Climate Change. Cambridge University Press. p739-768.

McCarthy, J.J.; Canziani, F.O.; Leary, A. N.; Dokken, D. J.; White, K.S. 2001. Climate Change 2001: Contribution of Working Group II to the Third Assesment Report of the Intergovernmental Panel on Climate Change. Cambridge University Press, 1042 pp.

Muller, J.E. 1977. Evolution of Pacific Margin, Vancouver Island and Adjacent Regions. Canadian Journal of Earth Sciences, vol. 14, p2062-2085.

Muller, J.E.; Jeletzky, J.A. 1970. Geology of the Upper Cretaceous Nanaimo Group, Vancouver Island and Gulf Islands, Canada. Geological Survey of Canada Paper 69-25, 77 pp.

Mustard, P.S. 1994. The Upper Cretaceous Nanaimo Group, Georgia Basin: in Geology and Geological Hazards of the Vancouver Region, Southwestern British Columbia. Edited by J.W.H. Monger. Geological Survey of Canada, Bull. 481, p27-95.

Noguer, M. 1994. Using Statistical Techniques to Deduce Local Climate Distributions. An Application for Model Validation. Meteor. Apps. 1, p277–287.

Osborn, T.J., K.R. Briffa, S.F.B. Tett, P.D. Jones and R.M. Trigo, 1999. Evaluation of the North Atlantic Oscillation as Simulated by a Coupled Climate Model. Climate. Dynamics. 15, p685-702.

Racsko, P., Szeidl, L. and Semenov, M.A. 1991. A serial approach to local stochastic weather models. Ecological Modelling 57, p27-41.

Richardson C.W. 1981. Stochastic Simulation of Daily Precipitation, Temperature, and Solar Radiation. Water Resources Research, 17, p182-190.

Richardson C.W., and D.A. Wright (1984) "WGEN: A Model for Generating Daily Weather Variables." ARS-8, Washington DC, USDA Agricultural Research Service.

Rietveld, M.R. 1978. A New Method for Estimating for Regression Coefficients in the Formula Relating Solar Radiation to Sunshine. Agricultural and Forest Meteorology 19, p243-252.

Scanlon, B. R., Healy, Rick, and Cook, P. G. 2002b. Choosing Appropriate Techniques for Quantifying Groundwater Recharge. Hydrogeology Journal, 10, p18–39.

Schroeder, P.R., Dozier, T.S., Zappi, P.A., McEnroe, B.M., Sjostrom, J.W. and Peyton R.L. (1994). The Hydrologic Evaluation of Landfill Performance (HELP) Model: Engineering Documentation for Version 3. EPA/600/R-94/168b. Washington DC, USEPA.

Semenov, M.A., and Barrow, E.M. 2002. LARS-WG – A stochastic weather generator for use in Climate Impact Studies. Version 3.0 User Manual, 27 pp.

Semenov, M. A. and Brooks, R. J. 1999. Spatial Interpolation of LARS-WG Stochastic Weather Generator in Great Britain. Climate Research 11, p137-148.

Semenov, M.A., Brooks, R.J., Barrow, E.M. and Richardson, C.W. 1998. Comparison of the WGEN and LARS-WG Stochastic Weather Generators for Diverse Climates. Climate Research 10, p95-107.

Surrette, M. in prep. Quantifying Hetergeneity in Variably Fracture Rock Using a Hydrostructural Domain Approach. M.Sc. Thesis, Department of Earth Sciences, Simon Fraser University, Burnaby, BC.

U.S. L-THIA. 2005. SCS Curve Number Method. http://www.ecn.purdue.edu/runoff/lthianew/documnt/scs.htm

van Vliet, I. J.P.; Kenney, E.A.; Green, A.J. 1987. Soils of the Gulf Islands of British Columbia. Agriculture Canada, Research Branch, B.C. Soil Survey Report No. 43, vol. 1, 146 pp.

van Vliet, I. J.P.; Kenney, E.A.; Green, A.J. 1991. Soils of the Gulf Islands of British Columbia. Agriculture Canada, Research Branch, B.C. Soil Survey Report No. 43, vol. 5, 136 pp.

von Storch, H.; Zorita, E. and Cubasch, U. 1993. Downscaling of Global Climate Change Estimates to Regional Scale: An Application to Iberian Rainfall in Winter Time. J. Climate, 6, p1161–1171.

Whitfield, P.H. and Taylor E. 1998. Apparent Recent Changes in Hydrology and Climate of Coastal British Columbia. In: Y. Alila (Ed.), Mountains to Sea: Human Interactions with the Hydrologic Cycle. Proceedings of the 51st Canadian Water Resources Conference, 22-29.

Wilby, R. L. and Dawson, C. W. 2004. Using SDSSM Version 3.1 – A Decision Support Tool For Regional Climate Change Impacts. SDSM User Manual, UK, 67 pp.

Wikipedia: The Free Encyclopedia. 2005. Climate Models, http://en.wikipedia.org/wiki/Climate_models

Winter T.C. 1983. The interaction of lakes with variably saturated porous media. Water Resources Research, 19, 5, p1203-1218.

York J.P., M. Person, W.J. Gutowski, T.C. Winter. 2002. Putting Aquifers into Atmospheric Simulation Models: An Example from the Mill Creek Watershed, Northeastern Kansas. Advances in Water Resources, 25, p221-238.

APPENDIX A:

SDSM STATISTICAL OUTPUT RESULTS

A1: PRECIPITATION

Table A-1: Summary Statistics for the Observed

Month	Mean	Maximum	Minimum	Variance	Sum	Wet-days%	Dry-spell	Wet-spell
January	7.98	92.80	0.20	94.94	143.92	0.58	2.55	3.52
February	6.43	48.20	0.20	60.75	100.85	0.56	2.86	3.46
March	4.67	50.30	0.20	34.79	73.94	0.51	2.92	2.99
April	3.41	53.20	0.20	23.25	44.76	0.44	2.87	2.29
May	3.11	21.20	0.20	13.00	34.49	0.36	3.79	2.23
June	3.16	31.00	0.20	16.83	29.23	0.31	4.14	1.98
July	3.62	50.00	0.20	24.19	20.02	0.18	6.49	1.71
August	4.09	41.70	0.20	31.90	24.05	0.19	6.23	1.77
September	4.21	45.20	0.20	27.19	33.03	0.26	5.15	2.07
October	5.73	57.40	0.20	49.20	78.86	0.45	3.08	2.53
November	7.58	59.00	0.20	79.72	141.04	0.62	2.24	3.59
December	7.85	81.10	0.20	98.94	152.23	0.63	2.26	3.61
Winter	7.48	92.80	0.20	86.77	387.31	0.59	2.65	3.72
Spring	3.82	53.20	0.20	25.45	153.18	0.44	3.35	2.60
Summer	3.55	50.00	0.20	23.24	73.30	0.22	6.22	1.87
Autumn	6.29	59.00	0.20	60.75	252.93	0.44	3.59	2.86
Annual	5.69	92.80	0.20	58.22	876.40	0.42	3.92	2.87

Table A-2: Summary Statistics for CGCM1 Current

Month	Mean	Maximum	Minimum	Variance	Sum	Wet-days%	Dry-spell	Wet-spell
January	6.71	64.59	0.00	62.81	119.61	0.58	2.02	2.69
February	6.09	61.82	0.00	53.73	82.95	0.49	2.44	2.32
March	6.00	60.30	0.00	50.78	102.59	0.55	2.06	2.49
April	5.44	49.54	0.00	42.66	81.67	0.50	2.21	2.23
May	4.57	40.36	0.00	30.66	46.06	0.32	3.38	1.72
June	3.99	34.09	0.00	26.10	21.36	0.18	5.51	1.35
July	4.16	37.25	0.00	27.96	24.78	0.19	5.08	1.38
August	4.36	37.66	0.00	30.11	27.72	0.21	4.85	1.42
September	4.82	44.22	0.00	36.56	39.51	0.27	3.90	1.57
October	6.75	69.39	0.00	68.77	106.56	0.51	2.33	2.42
November	7.82	100.16	0.00	96.46	141.65	0.60	1.92	2.88
December	7.01	70.47	0.00	68.87	116.74	0.54	2.31	2.65
Winter	6.64	80.97	0.00	62.52	311.50	0.53	2.32	2.66
Spring	5.46	63.50	0.00	43.42	230.32	0.46	2.61	2.24
Summer	4.18	45.21	0.00	28.23	73.86	0.19	5.64	1.40
Autumn	6.83	103.72	0.00	75.60	287.72	0.46	2.77	2.41
Annual	6.07	110.24	0.00	57.60	911.19	0.41	3.23	2.25

Table A-3: Summary Statistics for NCEP Calibrated data

Month	Mean	Maximum	Minimum	Variance	Sum	Wet-days%	Dry-spell	Wet-spell
January	7.17	60.95	0.00	65.19	132.72	0.60	2.29	3.28
February	6.76	67.38	0.00	59.71	112.75	0.59	2.37	3.25
March	6.14	55.41	0.00	49.35	105.92	0.56	2.34	2.89
April	5.34	47.96	0.00	39.80	73.60	0.46	2.50	2.17
May	4.67	44.37	0.00	34.30	46.39	0.32	3.48	1.73
June	4.32	35.69	0.00	27.24	34.65	0.27	3.99	1.59
July	4.24	35.00	0.00	28.89	21.56	0.16	6.15	1.43
August	4.24	36.20	0.00	29.73	23.57	0.18	5.61	1.46
September	4.81	38.33	0.00	33.79	37.06	0.26	4.41	1.66
October	6.26	56.00	0.00	52.34	81.70	0.42	2.97	2.24
November	6.80	59.43	0.00	58.60	121.45	0.60	2.05	2.97
December	7.15	68.54	0.00	65.03	131.58	0.59	2.24	3.16
Winter	7.03	77.99	0.00	63.51	367.85	0.59	2.37	3.39
Spring	5.51	60.12	0.00	42.89	225.91	0.45	2.88	2.33
Summer	4.27	41.87	0.00	28.48	79.78	0.20	5.71	1.52
Autumn	6.22	64.11	0.00	52.10	240.21	0.42	3.25	2.41
Annual	6.08	80.97	0.00	51.57	922.95	0.42	3.50	2.49

Table A-4: Summary Statistics for CGCM1 2010-2039

Month	Mean	Maximum	Minimum	Variance	Sum	Wet-days%	Dry-spell	Wet-spell
January	10.81	125.89	0.00	201.95	182.15	0.54	2.49	2.98
February	10.26	92.98	0.01	164.12	143.55	0.50	2.78	2.85
March	8.46	90.51	0.00	110.23	129.55	0.49	2.61	2.61
April	7.71	85.46	0.00	104.32	94.75	0.41	3.15	2.30
May	5.85	56.78	0.01	58.84	54.35	0.30	3.83	1.78
June	4.52	31.99	0.01	29.22	22.81	0.17	5.76	1.38
July	5.16	46.56	0.01	43.69	28.40	0.18	5.81	1.47
August	5.58	46.94	0.01	46.61	41.64	0.24	4.41	1.55
September	7.93	125.31	0.01	144.04	79.50	0.33	3.73	1.97
October	10.19	119.20	0.01	175.80	156.09	0.49	2.57	2.55
November	11.66	131.56	0.00	219.21	211.29	0.60	2.21	3.21
December	12.54	127.10	0.01	243.99	243.19	0.63	2.16	3.39
Winter	11.32	147.78	0.00	208.69	550.54	0.56	2.58	3.22
Spring	7.55	106.42	0.00	96.53	278.65	0.40	3.36	2.29
Summer	5.15	55.88	0.00	41.13	92.85	0.20	5.84	1.49
Autumn	10.28	160.23	0.00	188.87	446.88	0.48	2.93	2.68
Annual	9.33	181.67	0.00	159.28	1387.28	0.41	3.65	2.50

Table A-5: Summary Statistics for CGCM1 2040-2069

Month	Mean	Maximum	Minimum	Variance	Sum	Wet-days%	Dry-spell	Wet-spell
January	10.69	102.72	0.00	162.98	201.42	0.61	2.43	3.57
February	10.53	103.86	0.01	162.60	166.88	0.57	2.57	3.22
March	8.80	81.04	0.01	112.58	144.95	0.53	2.64	2.97
April	7.12	66.83	0.00	81.94	88.62	0.42	3.00	2.22
May	5.46	55.38	0.00	49.83	49.56	0.29	3.74	1.71
June	4.92	38.31	0.01	37.58	27.00	0.18	5.81	1.52
July	5.59	47.81	0.01	49.92	34.42	0.20	5.28	1.48
August	5.66	46.51	0.01	50.77	38.60	0.22	4.85	1.52
September	7.15	56.51	0.01	71.31	66.05	0.31	3.82	1.81
October	10.88	114.90	0.01	184.91	185.21	0.55	2.50	3.00
November	12.46	137.83	0.01	252.10	234.62	0.63	2.23	3.53
December	12.88	119.51	0.01	232.22	276.99	0.69	1.95	4.09
Winter	11.48	131.03	0.00	190.66	624.47	0.62	2.38	3.86
Spring	7.45	86.64	0.00	89.46	283.13	0.41	3.31	2.36
Summer	5.41	57.09	0.00	46.72	100.03	0.20	5.82	1.53
Autumn	10.77	149.44	0.00	193.73	485.87	0.50	2.97	2.92
Annual	9.60	156.38	0.00	155.17	1514.33	0.43	3.63	2.75

Table A-6: Summary Statistics for CGCM1 2070-2099

Month	Mean	Maximum	Minimum	Variance	Sum	Wet-days%	Dry-spell	Wet-spell
January	12.33	124.44	0.01	232.80	250.31	0.65	2.13	3.78
February	10.81	123.29	0.01	195.22	182.73	0.60	2.20	3.22
March	9.37	98.35	0.00	139.81	148.23	0.51	2.62	2.76
April	7.06	66.92	0.01	79.92	84.08	0.40	3.10	2.10
May	5.73	49.04	0.00	50.91	49.79	0.28	4.12	1.74
June	4.74	40.04	0.01	35.03	24.22	0.17	5.63	1.36
July	5.80	47.38	0.01	54.10	32.56	0.18	5.76	1.49
August	7.07	66.02	0.01	85.84	50.37	0.23	4.63	1.55
September	7.52	62.70	0.01	78.67	73.09	0.32	3.63	1.85
October	12.02	132.21	0.01	234.90	193.18	0.52	2.46	2.64
November	13.74	142.99	0.01	289.16	269.30	0.65	1.90	3.49
December	14.44	188.51	0.01	362.72	303.89	0.68	2.04	4.03
Winter	12.65	195.88	0.00	271.12	713.16	0.65	2.18	3.94
Spring	7.75	102.23	0.00	101.37	282.09	0.40	3.43	2.29
Summer	6.00	70.80	0.00	62.57	107.15	0.19	5.84	1.48
Autumn	11.80	160.54	0.00	230.61	535.58	0.50	2.77	2.77
Annual	10.52	205.48	0.00	203.01	1661.75	0.43	3.55	2.69

A2: TEMPERATURE

Table A-7: Summary Statistics for Observed

Month	Mean	Maximum	Minimum	Variance
January	3.55	11.90	-10.90	11.46
February	4.77	11.70	-10.40	9.03
March	6.06	12.40	-3.20	5.62
April	8.18	15.60	2.80	4.42
May	11.20	20.80	0.00	6.20
June	14.09	22.60	6.70	5.10
July	16.10	25.90	9.90	4.41
August	16.58	24.60	10.90	4.03
September	14.39	22.70	5.00	5.72
October	10.54	18.40	1.70	6.20
November	6.66	14.50	-6.90	8.06
December	4.24	13.20	-13.10	10.91
Winter	4.17	13.20	-13.10	10.76
Spring	8.48	20.80	-3.20	9.92
Summer	15.61	25.90	6.70	5.65
Autumn	10.53	22.70	-6.90	16.51
Annual	9.73	25.90	-13.10	27.57

Table A-8: Summary Statistics for CGCM1 Current

Month	Mean	Maximum	Minimum	Variance
January	3.83	11.31	-3.30	5.69
February	4.32	11.57	-2.52	5.39
March	5.48	12.97	-0.77	4.56
April	7.84	15.76	1.29	4.63
May	11.06	18.70	4.15	5.54
June	14.82	21.47	8.06	4.52
July	16.91	23.03	10.75	3.52
August	17.25	23.86	11.19	3.73
September	14.39	21.59	6.79	5.38
October	10.07	17.11	2.53	5.83
November	6.94	16.25	-1.37	8.00
December	4.59	13.59	-3.44	7.95
Winter	4.25	13.59	-3.83	6.48
Spring	8.13	18.70	-0.77	10.19
Summer	16.34	23.97	8.06	5.06
Autumn	10.46	21.59	-1.37	15.60
Annual	9.82	23.97	-3.83	28.54

Table A-9: Summary Statistics for NCEP Calibration data

Month	Mean	Maximum	Minimum	Variance
January	3.67	12.26	-7.12	11.04
February	5.00	13.13	-8.42	8.24
March	6.33	13.85	-1.66	5.59
April	8.64	15.86	1.98	5.03
May	11.69	20.32	4.27	6.25
June	14.43	21.25	7.49	4.49
July	16.36	22.81	10.09	4.07
August	16.36	22.82	9.63	4.13
September	13.92	21.08	6.18	5.55
October	9.83	17.75	0.86	6.16
November	6.14	14.68	-4.98	8.51
December	4.03	13.34	-9.10	11.51
Winter	4.21	13.61	-9.56	10.64
Spring	8.89	20.32	-1.66	10.49
Summer	15.73	23.23	7.49	5.05
Autumn	9.96	21.08	-4.98	16.73
Annual	9.72	23.24	-9.56	27.51

Table A-10: Summary Statistics for CGCM1 2010-2039

Month	Mean	Maximum	Minimum	Variance
January	4.34	12.67	-3.07	6.56
February	4.99	12.40	-4.40	6.16
March	6.60	14.01	0.09	4.69
April	8.88	15.45	2.58	4.39
May	11.98	19.10	4.87	5.53
June	15.43	21.74	9.26	3.93
July	17.46	23.10	12.04	3.14
August	17.74	23.56	11.81	3.46
September	14.98	22.83	7.60	5.73
October	10.80	18.27	3.13	6.50
November	7.90	17.27	-0.98	8.96
December	5.49	14.36	-2.98	7.99
Winter	4.94	14.50	-4.48	7.16
Spring	9.16	19.10	0.09	9.80
Summer	16.89	23.64	9.26	4.56
Autumn	11.22	22.83	-0.98	15.42
Annual	10.58	23.72	-4.48	27.75

Table A-11: Summary Statistics for CGCM1 2040-2069

Month	Mean	Maximum	Minimum	Variance
January	5.19	13.25	-2.52	6.41
February	5.67	12.84	-2.74	6.19
March	7.07	13.88	-5.16	5.44
April	9.60	16.07	3.60	4.09
May	12.69	19.48	5.72	4.92
June	15.99	22.21	9.70	3.89
July	17.83	23.25	12.18	3.00
August	18.14	24.07	12.45	3.24
September	15.67	23.16	7.52	5.67
October	11.52	19.06	3.81	6.18
November	8.24	17.42	-0.63	8.27
December	6.30	14.80	-2.30	7.55
Winter	5.72	14.80	-3.28	6.95
Spring	9.79	19.48	-5.16	10.16
Summer	17.34	24.15	9.70	4.27
Autumn	11.81	23.16	-0.63	15.85
Annual	11.19	24.31	-5.20	26.78

Table A-12: Summary Statistics for CGCM1 2070-2099

Month	Mean	Maximum	Minimum	Variance
January	6.37	14.45	-1.61	6.60
February	6.77	14.81	-0.69	6.18
March	8.19	15.80	-0.49	5.42
April	10.26	17.48	3.63	4.31
May	13.60	21.36	6.00	5.65
June	16.74	23.47	9.93	4.15
July	18.55	24.23	12.91	3.13
August	18.80	24.41	13.11	3.34
September	16.40	24.32	8.82	6.03
October	12.67	22.14	4.20	8.31
November	9.37	19.30	0.08	10.36
December	6.83	16.48	-2.46	9.23
Winter	6.65	16.68	-2.55	7.42
Spring	10.69	21.36	-0.49	10.16
Summer	18.04	24.70	9.93	4.37
Autumn	12.81	24.41	0.08	16.39
Annual	12.08	24.98	-2.57	26.42

APPENDIX B:

WEATHER GENERATION

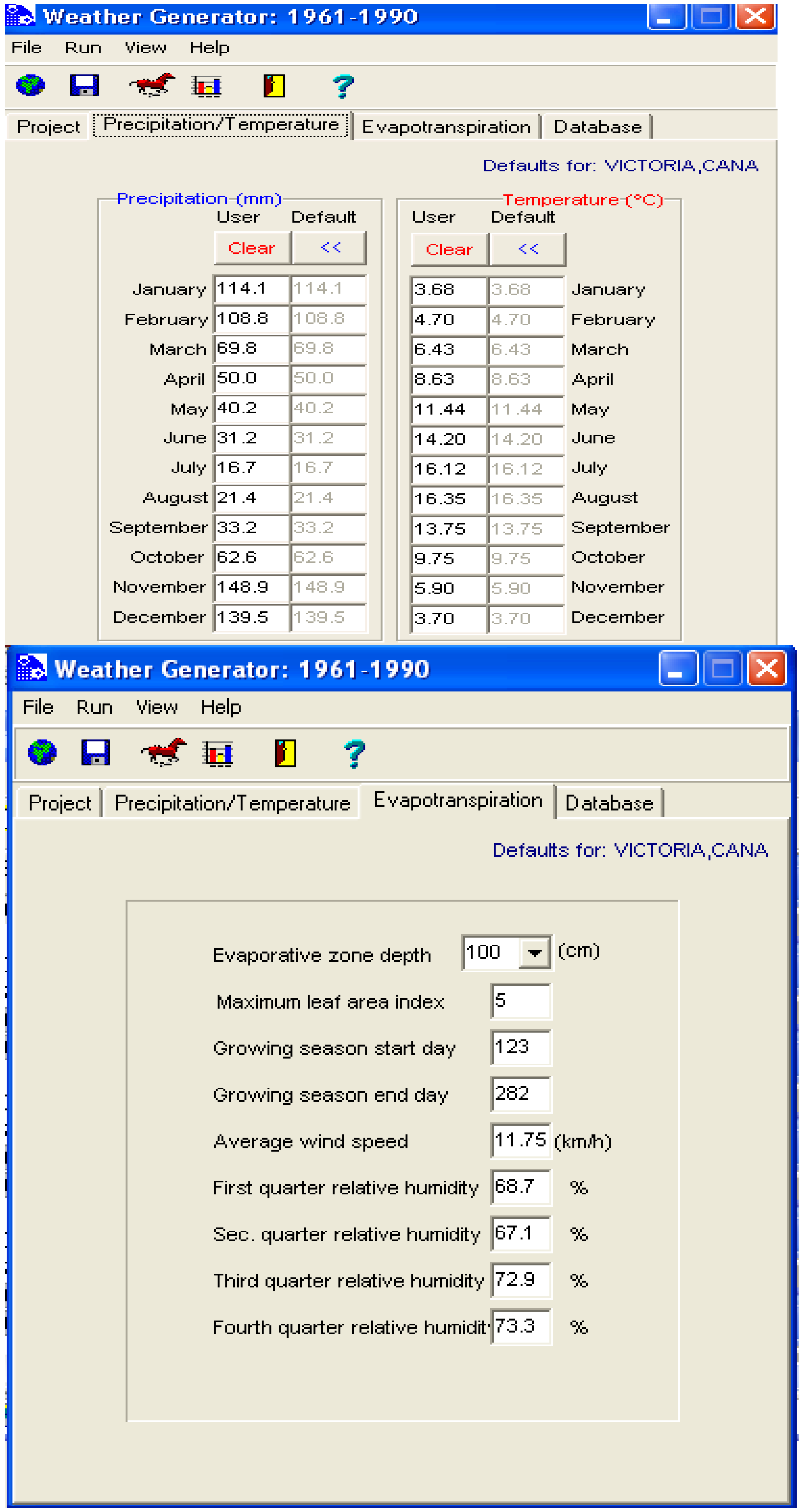

Figure B-1: Monthly climate normals and constant evapotranpspiration parameters of Victoria in HELP weather database.

a. **b.**

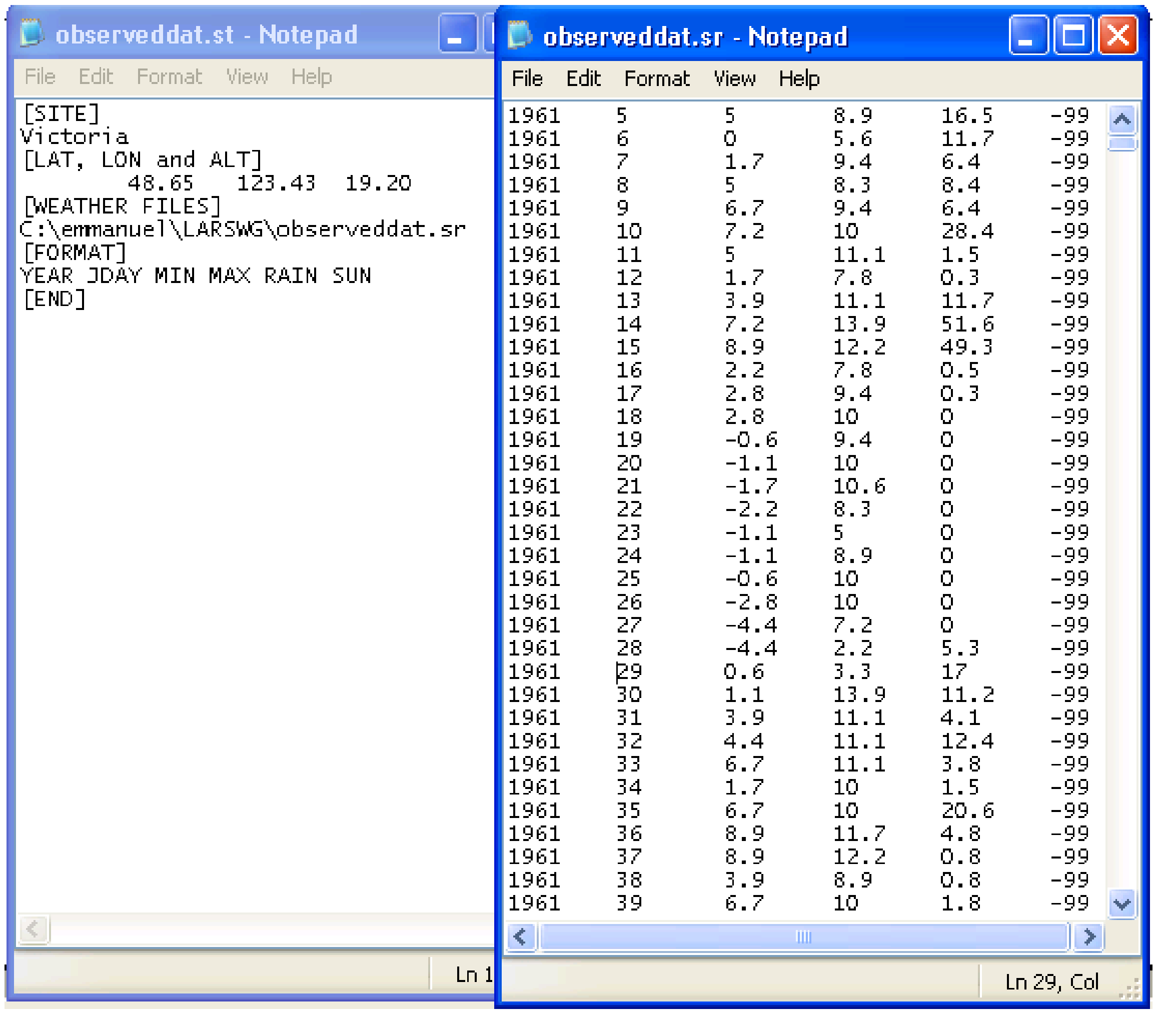

observeddat.st - Notepad

```
[SITE]
Victoria
[LAT, LON and ALT]
         48.65    123.43   19.20
[WEATHER FILES]
C:\emmanuel\LARSWG\observeddat.sr
[FORMAT]
YEAR JDAY MIN MAX RAIN SUN
[END]
```

observeddat.sr - Notepad

1961	5	5	8.9	16.5	-99
1961	6	0	5.6	11.7	-99
1961	7	1.7	9.4	6.4	-99
1961	8	5	8.3	8.4	-99
1961	9	6.7	9.4	6.4	-99
1961	10	7.2	10	28.4	-99
1961	11	5	11.1	1.5	-99
1961	12	1.7	7.8	0.3	-99
1961	13	3.9	11.1	11.7	-99
1961	14	7.2	13.9	51.6	-99
1961	15	8.9	12.2	49.3	-99
1961	16	2.2	7.8	0.5	-99
1961	17	2.8	9.4	0.3	-99
1961	18	2.8	10	0	-99
1961	19	-0.6	9.4	0	-99
1961	20	-1.1	10	0	-99
1961	21	-1.7	10.6	0	-99
1961	22	-2.2	8.3	0	-99
1961	23	-1.1	5	0	-99
1961	24	-1.1	8.9	0	-99
1961	25	-0.6	10	0	-99
1961	26	-2.8	10	0	-99
1961	27	-4.4	7.2	0	-99
1961	28	-4.4	2.2	5.3	-99
1961	29	0.6	3.3	17	-99
1961	30	1.1	13.9	11.2	-99
1961	31	3.9	11.1	4.1	-99
1961	32	4.4	11.1	12.4	-99
1961	33	6.7	11.1	3.8	-99
1961	34	1.7	10	1.5	-99
1961	35	6.7	10	20.6	-99
1961	36	8.9	11.7	4.8	-99
1961	37	8.9	12.2	0.8	-99
1961	38	3.9	8.9	0.8	-99
1961	39	6.7	10	1.8	-99

Figure B-2: Sample input files for used in LARS-WG (a) and its corresponding data file (b)

Table B-1: LARS-WG statistical out file (*.sta) for Gulf Islands observed data.

[NAME]												
Victoria												
[LAT,	LON	and	ALT]									
	48.65	123.4	19.2									
[SERIES	WET	and	DRY]									
[DJF]												
	0	1	2	3	4	5	7	10	14	19	25	
	137	93	84	62	39	63	41	15	6	1		
	0	1	2	3	4	5	6	7	9	12	16	
	252	97	61	43	22	28	11	12	14	5		
[MAM]												
	0	1	2	3	4	5	6	7	9	12	16	
233	149	72	53	30	18	13	14	8	3			
	0	1	2	3	4	5	7	10	14	19	25	
226	107	66	45	41	51	43	19	7	4			
[JJA]												
	0	1	2	3	4	5	6	7	8	9	10	
231	101	59	23	12	6	0	0	1	1			
	0	1	3	6	10	15	21	28	36	45	55	
100	103	81	62	44	21	10	8	3	1			
[SON]												
	0	1	2	3	4	5	6	8	11	15	20	
204	127	69	43	32	20	34	16	12	2			
	0	1	2	4	7	11	16	22	29	37	46	
224	87	100	63	47	13	5	0	0	2			
[WET	and	DRY	series:	mean	and	sd]						
	J	F	M	A	M	J	J	A	S	O	N	D
	4.18	3.76	3.26	2.41	2.34	2.07	1.77	1.85	2.21	2.69	4.11	3.59
	18.64	13.81	12.34	9.96	10.66	8.67	7.22	7.41	8.02	11	18.1	13.4
	2.89	2.94	3.21	3.13	4.47	4.69	9.64	6.53	5.79	3.11	2.32	2.29
	10.92	10.59	12.94	12.8	19.55	18.8	37.2	24.9	28	13	9.06	8.77
[DISTRIBUTIONS OF RAIN]												
	0	1	4	9	16	25	36	49	64	81	100	
151	171	186	109	61	28	9	4	1	1			
	0	1	3	6	10	15	21	28	36	45	55	
151	133	118	90	56	33	20	12	4	2			
	0	1	3	6	10	15	21	28	36	45	55	
169	189	118	82	42	18	12	5	1	1			
	0	1	3	6	10	15	21	28	36	45	55	
202	145	92	44	25	10	3	2	0	1			
	0	1	2	3	4	5	7	10	14	19	25	
162	84	45	37	26	31	37	11	9	2			
	0	1	2	3	4	6	9	13	18	24	31	
152	65	41	20	34	27	20	10	3	1			
	0	1	3	6	10	15	21	28	36	45	55	
	80	59	42	24	13	4	0	0	0	1		
	0	1	2	4	7	11	16	22	29	37	46	
	89	30	39	35	20	11	5	2	2	1		
	0	1	2	4	7	11	16	22	29	37	46	

102	51	50	52	27	17	13	0	0	1			
	0	1	3	6	10	15	21	28	36	46	58	
137	140	90	91	39	26	14	7	1	2			
	0	1	3	6	10	15	21	28	37	48	61	
165	148	116	117	83	53	33	15	10	4			
	0	1	3	6	11	18	27	38	51	66	83	
147	161	155	146	85	47	22	14	2	3			
[RAIN	MONTHLY	max,	min,	N,	mean	and	sd]					
	J	F	M	A	M	J	J	A	S	O	N	D
	263.9	238.6	184.5	114	99.1	80.7	67.6	96.6	84.6	207	277	295
	19	14.6	17.2	7.8	9	3.3	1.2	0	0	13.6	33.6	23
	40	40	40	40	40	40	40	40	40	40	40	40
	144	99.4	74.9	44.6	34.9	29.4	20	24	32.4	78.3	141	153
	65.58	48.74	34.75	24	18.12	18.1	14.8	22	24.2	48.4	65.7	60.3
[MAX	MONTHLY	max,	min,	N,	mean	and	sd]					
	J	F	M	A	M	J	J	A	S	O	N	D
	9.7	11.1	13.6	15.8	19.5	21.9	24.3	24.6	22.6	17	11.8	9.2
	1.4	4.1	7.8	10.8	14.3	16.4	19.6	19.1	16.7	12.6	4.1	4.2
	40	40	40	40	40	40	40	40	40	40	40	40
	6.7	8.6	10.4	13.1	16.5	19.4	21.8	21.9	19.3	14.2	9.5	7
	1.66	1.42	1.21	1.06	1.28	1.32	1.13	1.3	1.34	0.91	1.32	1.39
[MAX	DAILY	max,	min,	N,	mean	and	sd]					
	J	F	M	A	M	J	J	A	S	O	N	D
	15.4	18.3	21.4	26.3	31.5	31.7	35	32.9	30.3	27.6	18.3	15.5
	-7.8	-8.9	0	7.2	8.9	11.1	13.3	12.1	10	3.7	-8.1	-11.7
	1236	1115	1237	1199	1236	1198	1240	1238	1200	1238	1198	1243
	6.7	8.6	10.4	13.1	16.5	19.4	21.8	21.9	19.3	14.2	9.5	7
	3.36	2.94	2.62	2.83	3.43	3.34	3.35	3.31	3.38	2.93	2.92	3.32
[MIN	MONTHLY	max,	min,	N,	mean	and	sd]					
	J	F	M	A	M	J	J	A	S	O	N	D
	3.5	4	4.2	6.5	9.8	10.9	12.5	12.4	10.4	7.4	5.8	3.3
	-4.7	-3.9	0.2	2.2	5.2	7.5	9.8	8.6	6.5	3.2	-2.7	-2
	40	40	40	40	40	40	40	40	40	40	40	40
	0.6	1.4	2.2	4.1	6.8	9.4	10.8	10.8	8.5	5.5	2.7	1.1
	1.7	1.59	1.05	0.99	0.94	0.85	0.62	0.7	0.93	0.93	1.57	1.53
[MIN	DAILY	max,	min,	N,	mean	and	sd]					
	J	F	M	A	M	J	J	A	S	O	N	D
	9.4	9.1	9.1	11.4	15	15	17.2	16.2	14.4	12.9	12.4	10.2
	-15	-11.8	-10	-3.2	-0.6	2.1	4.1	4.4	-1.1	-3.9	-12.7	-14.4
	1236	1114	1237	1199	1236	1198	1240	1238	1200	1238	1198	1243
	0.6	1.4	2.2	4.1	6.8	9.4	10.8	10.8	8.5	5.5	2.7	1.1
	3.67	3.3	2.82	2.62	2.52	2.06	1.73	1.72	2.31	2.9	3.53	3.77
[SPELLS	of	FROST	and	HOT	TEMPERATURE]							
[DJF]												
	0	1	2	3	4	5	7	10	14	19	25	
	147	96	50	25	22	31	21	12	4	2		
	0	1	2	3	4	5	6	7	8	9	10	
	0	0	0	0	0	0	0	0	0	0		
[MAM]												
	0	1	2	3	4	5	6	7	8	9	10	

	94	41	12	7	5	3	2	1	0	0		
	0	1	2	3	4	5	6	7	8	9	10	
	0	1	0	0	0	0	0	0	0	0		
[JJA]												
	0	1	2	3	4	5	6	7	8	9	10	
	0	0	0	0	0	0	0	0	0	0		
	0	1	2	3	4	5	6	7	8	9	10	
	20	7	3	1	0	0	0	0	0	0		
[SON]												
	0	1	2	3	4	5	6	8	11	15	20	
	52	30	9	11	8	5	2	0	0	1		
	0	1	2	3	4	5	6	7	8	9	10	
	2	0	0	0	0	0	0	0	0	0		
[RAD	MONTHLY	max,	min,	N,	mean	and	sd]					
	J	F	M	A	M	J	J	A	S	O	N	D
	6.8	10.7	16.4	22.9	28.1	30.4	29.3	24.9	18.7	12.4	7.7	5.8
	6.8	10.6	16.4	22.9	28.1	30.4	29.3	24.8	18.6	12.3	7.7	5.8
	40	40	40	40	40	40	40	40	40	40	40	40
	6.8	10.6	16.4	22.9	28.1	30.4	29.3	24.9	18.7	12.3	7.7	5.8
	0	0.02	0.01	0	0.03	0.02	0.01	0.02	0.01	0.01	0	0
[RAD	DAILY	max,	min,	N,	mean	and	sd]					
	J	F	M	A	M	J	J	A	S	O	N	D
	8.3	13	19.6	25.7	29.8	30.6	30.4	27.5	21.8	15.3	9.4	6.2
	5.8	8.4	13.2	19.8	25.9	29.9	27.6	22	15.5	9.6	6.3	5.6
	1236	1115	1237	1199	1236	1198	1240	1238	1200	1238	1197	1243
	6.8	10.6	16.4	22.9	28.1	30.4	29.3	24.9	18.7	12.3	7.7	5.8
	0.75	1.37	1.93	1.75	1.16	0.23	0.85	1.64	1.9	1.7	0.95	0.18
[END]												

Table B-2: LARS-WG parameter out file (*.wg) for Gulf Islands observed data.

[NAME]	Victoria										
[LAT,	LON	and	ALT]								
	48.65	123.43	19.2								
[SERIES]											
	0	1	2	3	4	5	7	10	14	19	25
	46	36	35	21	13	24	17	6	4	1	
	0	1	2	3	4	5	6	7	8	10	13
	89	34	18	16	12	10	5	3	6	5	
	0	1	2	3	4	5	6	7	9	12	16
	47	23	23	19	15	13	9	10	5	2	
	0	1	2	3	4	5	6	7	9	12	16
	73	28	18	17	4	11	3	7	4	2	
	0	1	2	3	4	5	6	7	9	12	16
	66	41	22	16	14	9	7	10	4	3	
	0	1	2	3	4	5	6	8	11	15	20
	91	26	17	11	11	8	16	8	3	2	
	0	1	2	3	4	5	6	7	8	10	13
	96	49	29	14	10	4	5	2	3	2	
	0	1	2	3	4	5	6	8	11	15	20
	81	48	23	19	15	8	11	8	4	1	
	0	1	2	3	4	5	6	7	8	9	10
	69	58	23	23	6	5	2	1	0	1	
	0	1	2	3	4	5	7	10	14	19	25
	54	32	27	14	15	18	19	11	3	3	
	0	1	2	3	4	5	6	7	8	9	11
	90	39	23	14	6	2	0	0	1	2	
	0	1	2	3	4	6	9	13	18	24	31
	55	31	20	14	15	16	12	6	4	2	
	0	1	2	3	4	5	6	7	8	9	10
	70	35	15	6	4	0	0	0	0	0	
	0	1	3	6	10	15	21	28	36	45	55
	20	25	33	15	18	10	5	7	3	1	
	0	1	2	3	4	5	6	7	8	9	10
	69	28	21	3	2	4	0	0	0	0	
	0	1	2	3	4	6	9	13	18	24	31
	25	17	10	9	10	22	13	8	3	3	
	0	1	2	3	4	5	6	7	9	12	16
	70	39	17	8	6	3	1	3	0	1	
	0	1	2	4	7	11	16	22	29	37	46
	40	13	30	22	29	10	3	0	0	2	
	0	1	2	3	4	5	6	8	11	15	20
	85	52	26	15	12	4	9	4	2	1	
	0	1	2	3	4	5	7	10	14	19	25
	82	39	25	9	10	16	11	4	1	1	
	0	1	2	3	4	5	6	8	11	15	20
	54	33	26	18	13	12	22	10	9	1	
	0	1	2	3	4	5	6	7	8	9	10
102	32	23	15	7	6	2	2	5	1		
	0	1	2	3	4	5	6	7	9	12	16
	43	37	24	24	12	10	8	10	3	3	
	0	1	2	3	4	5	6	7	9	12	16
	90	38	24	10	6	7	3	1	2	1	
[RAIN]											
	0	1	4	9	16	25	36	49	64	81	100
151	171	186	109	61	28	9	4	1	1		
	0	1	3	6	10	15	21	28	36	45	55
151	133	118	90	56	33	20	12	4	2		
	0	1	3	6	10	15	21	28	36	45	55

169	189	118	82	42	18	12	5	1	1		
	0	1	3	6	10	15	21	28	36	45	55
202	145	92	44	25	10	3	2	0	1		
	0	1	2	3	4	5	7	10	14	19	25
162	84	45	37	26	31	37	11	9	2		
	0	1	2	3	4	6	9	13	18	24	31
152	65	41	20	34	27	20	10	3	1		
	0	1	3	6	10	15	21	28	36	45	55
	80	59	42	24	13	4	0	0	0	1	
	0	1	2	4	7	11	16	22	29	37	46
	89	30	39	35	20	11	5	2	2	1	
	0	1	2	4	7	11	16	22	29	37	46
102	51	50	52	27	17	13	0	0	1		
	0	1	3	6	10	15	21	28	36	46	58
137	140	90	91	39	26	14	7	1	2		
	0	1	3	6	10	15	21	28	37	48	61
165	148	116	117	83	53	33	15	10	4		
	0	1	3	6	11	18	27	38	51	66	83
147	161	155	146	85	47	22	14	2	3		
[WET	MIN]										
				-							
	12.45	-4.35	0.1	0.04							
	0	-1.99	0.72	0.06							
	5.11	0.86	0.09	0.05							
	0	0.13	-0.26	0.09							
[WET	MAX]										
				-							
	25.86	-5.39	-0.19	0.03							
	0	-2.12	0.77	0.12							
	5.07	0.42	0.29	0.12							
				-							
	0	-0.05	0.09	0.03							
[DRY	MIN]										
	8.78	-5.76	0.13	0.06							
	0	-2.02	0.71	0.16							
	4.85	0.69	0.14	0.07							
	0	0.15	-0.16	0.04							
[DRY	MAX]										
	28.72	-8.07	-0.78	0.01							
	0	-2.35	1.1	0.28							
	5.92	-0.12	0.25	0.17							
	0	0.05	0.07	0.11							
[AUTO	MIN]										
	0.574										
[AUTO	MAX]										
	0.643										
[AUTO	RAD]										
	0.762										
[WET	RAD]										
	5.8	6.1	6.3	6.6	6.8	7.1	7.3	7.6	7.8	8.1	8.3
129	127	52	99	43	66	47	69	21	68		
	8.4	8.9	9.3	9.8	10.2	10.7	11.2	11.6	12.1	12.5	13
	89	56	60	73	48	79	63	44	38	43	
	13.2	13.8	14.5	15.1	15.8	16.4	17	17.7	18.3	19	19.6
	99	56	58	75	64	53	49	73	36	74	
	19.8	20.4	21	21.6	22.2	22.8	23.3	23.9	24.5	25.1	25.7
	54	49	41	53	56	52	60	54	46	59	
	25.9	26.3	26.7	27.1	27.5	27.8	28.2	28.6	29	29.4	29.8
	59	29	41	32	45	41	33	55	58	41	
	29.9	30	30	30.1	30.2	30.2	30.3	30.4	30.5	30.5	30.6
	27	16	26	0	13	25	0	47	76	143	
	27.6	27.9	28.2	28.4	28.7	29	29.3	29.6	29.8	30.1	30.4

		6	7	13	6	13	18	22	27	49	32	
		22	22.5	23.1	23.6	24.2	24.8	25.3	25.9	26.4	27	27.5
		27	30	13	31	28	30	20	16	22	14	
		15.5	16.1	16.8	17.4	18	18.6	19.3	19.9	20.5	21.2	21.8
		46	17	38	29	35	35	25	35	20	25	
		9.6	10.2	10.7	11.3	11.9	12.5	13	13.6	14.2	14.7	15.3
		89	82	63	57	42	50	32	46	45	41	
		6.3	6.6	6.9	7.2	7.5	7.8	8.2	8.5	8.8	9.1	9.4
	153	82	69	77	69	52	61	63	55	46		
		5.6	5.7	5.7	5.8	5.8	5.9	6	6	6.1	6.1	6.2
	185	260	0	136	48	0	43	0	53	0		
[DRY		RAD]										
		5.8	6.1	6.3	6.6	6.8	7.1	7.3	7.6	7.8	8.1	8.3
	110	72	28	61	37	53	33	51	19	51		
		8.4	8.9	9.3	9.8	10.2	10.7	11.2	11.6	12.1	12.5	13
		66	67	59	47	32	41	55	36	42	37	
		13.2	13.8	14.5	15.1	15.8	16.4	17	17.7	18.3	19	19.6
		61	63	62	45	55	66	56	62	44	86	
		19.8	20.4	21	21.6	22.2	22.8	23.3	23.9	24.5	25.1	25.7
		66	53	57	67	63	68	60	66	74	101	
		25.9	26.3	26.7	27.1	27.5	27.8	28.2	28.6	29	29.4	29.8
		60	50	70	56	75	79	87	105	101	79	
		29.9	30	30	30.1	30.2	30.2	30.3	30.4	30.5	30.5	30.6
		53	24	54	0	27	53	0	73	164	377	
		27.6	27.9	28.2	28.4	28.7	29	29.3	29.6	29.8	30.1	30.4
		74	73	93	88	67	102	98	93	151	88	
		22	22.5	23.1	23.6	24.2	24.8	25.3	25.9	26.4	27	27.5
		93	90	67	105	76	89	100	104	137	106	
		15.5	16.1	16.8	17.4	18	18.6	19.3	19.9	20.5	21.2	21.8
	114	63	82	91	85	85	95	85	60	95		
		9.6	10.2	10.7	11.3	11.9	12.5	13	13.6	14.2	14.7	15.3
		71	76	57	63	78	70	48	74	75	79	
		6.3	6.6	6.9	7.2	7.5	7.8	8.2	8.5	8.8	9.1	9.4
		86	38	50	43	51	27	41	35	25	34	
		5.6	5.7	5.7	5.8	5.8	5.9	6	6	6.1	6.1	6.2
	134	138	0	71	31	0	37	0	27	0		
[END]												

Table B-3: Re-classification of soil types in the Gulf Islands.

Soil Unit	Soil Name	Soil Description	Class
ST	Beddis	Sandy Loam to Sand Fluvial, Marine or Eolian Deposits	TS
BE	Brigantine	Sandy Loam to Loamy Sand Marine Fluvial Deposits	TS
BH	Bellhouse	Gravelly Sandy Loam to Gravelly Loamy Sand Colluvial and Glacial Dr	GS
BY	Baynes	Sandy Loam to Sand Fluvial, Marine, Or Eolian Deposits	TS
CF	Crofton	Loam To Silty Loam Recent Fluvial Deposits	TS
CO	Cowichan	Silt Loam over Silty Clay Loam to Silty Clay Marine Deposits	Clay
FB	Fairbridge	Silt Loam to Loam over Silty Clay Loam to Clay Loam Marine Deposit	Clay
GA	Galiano	Shaly Loam Colluvial, Residual, and Glacial Drift Materials L	TS
HA	Haslam	Channery and Shaly Sandy Loam to Loam Colluvial, Residual, and Glacial	TS
ME	Mexicana	Loam to Sandy Loam Morainal Deposits	TS
GS	Musgrave	Gravelly Sandy Loam to Gravelly Loamy Sand Colluvial and Glacial Dr	GS
MT	Metchosin	Well Decomposed (Humic) Organic Deposits	TS
NT	Neptune	Black Colored, Calcareous Gravelly Sand Loam Gravelly Sand Marin	GS
PA	Parksville	Sandy Loam to Loamy Sand Marine or Fluvial Deposits	TS
QU	Qualicum	Gravelly Sandy Loam to Gravelly Sand Glaciofluvial, Fluvial,	GS
PD	Pender Island	Channery and Gravelly Sandy Loam Colluvial and Glacial Drift Material	GT
RO	Rock	Undifferentiated Bedrock Exposed Or Covered By Moss Or Mineral Soil	TS
RY	Rumsley	Gravely Sandy Loam to Gravelly Loamy Sand Colluvial and Glacial Dri	GS
SL	Salalakim	Gravelly Sandy Loam Colluvial and Glacial Drift Materials	GT
SM	St. Mary	Sandy Loam to Loamy Sand Marine or Fluvial Deposits	TS
ST	Saturna	Channery Sandy Loam Colluvial and Glacial Drift	GT
SU	Suffolk	Loam to Silty Clay Loam Marine Deposits Less	Clay
TL	Tolmie	Loam to Silty Clay Marine Deposits	Clay
TR	Trincomali	Gravelly Sandy Loam to Gravelly Loamy Sand	GS
CB	Coastal Beach	Present Day Coarse Textured Sand And Gravelly Beach Areas.	GS
MD	Made Land	Soils that have been artificially altered or disturbed by the Activ	TS
TF	Tidal Flat	Coastal areas with poorly drained, Saline Soils being Inundated	Clay
DA	Denman Island	Sandy Loam to Sandy Fluvial, Marine, or Eolian Deposits	TS
CH	Chemainus	Silt Loam To Loam Recent Fluvial Deposits	TS

Table B-4: Results of sensitivity analysis.

Parameters (mm)	TS	GS	Clay	GT	TS	GS	Clay	GT
	A) Default (A = 1acre; LAI = 4; EZD = 20cm; no S)				B)The same as A but Area = 2160 acres			
PRECIPITATION	818.71	818.71	818.71	818.71	818.71	818.71	818.71	818.71
RUNOFF	0.00	0.00	9.22	7.96	0.00	0.00	9.22	7.96
EVAPOTRANSPIRATION	385.10	361.09	399.37	381.74	385.10	361.09	399.37	381.74
RECHARGE	433.94	458.57	403.20	431.06	433.94	458.57	403.20	431.06
STORAGE CHANGE	-0.33	-0.95	6.92	-2.05	-0.33	-0.95	6.92	-2.05
CN	0.00	0.01	0.00	0.00	0.00	0.01	0.00	0.00
RECHARGE (% Ppt)	53.00	56.01	49.25	52.65	53.00	56.01	49.25	52.65
	C) The same as A but Area = 5900 acres				D) The same as A but LAI = 5			
PRECIPITATION	818.71	818.71	818.71	818.71	818.71	818.71	818.71	818.71
RUNOFF	0.00	0.00	9.22	7.96	0.00	0.00	9.27	7.98
EVAPOTRANSPIRATION	385.10	361.09	399.37	381.74	384.73	361.13	398.57	381.42
RECHARGE	433.94	458.57	403.20	431.06	434.34	458.53	404.11	431.39
STORAGE CHANGE	-0.33	-0.95	6.92	-2.05	-0.35	-0.95	6.76	-2.08
CN	0.00	0.01	0.00	0.00	0.00	0.01	0.00	0.00
RECHARGE (% Ppt)	53.00	56.01	49.25	52.65	53.05	56.01	49.36	52.69
	E) The same as A but EZD =100cm				F) The same as A but EZD =60cm			
PRECIPITATION	818.71	818.71	818.71	818.71	818.71	818.71	818.71	818.71
RUNOFF	0.00	0.00	5.27	0.10	0.00	0.00	7.15	0.09
EVAPOTRANSPIRATION	447.36	401.70	543.31	435.51	417.02	388.51	475.49	407.48
RECHARGE	371.52	417.94	260.38	386.40	401.97	431.11	325.94	413.11
STORAGE CHANGE	-0.16	-0.93	9.75	-3.30	-0.27	-0.90	10.13	-1.97
CN	0.00	0.01	0.00	0.00	0.00	0.01	0.00	0.00
RECHARGE (% Ppt)	45.38	51.05	31.80	47.20	49.10	52.66	39.81	50.46
	G) The same as A but Slope =15% and SL = 2856m				H) The same as A but Slope =15% and SL = 100m			
PRECIPITATION	818.71	818.71	818.71	818.71	818.71	818.71	818.71	818.71
RUNOFF	0.00	0.00	9.22	7.96	0.00	0.00	9.22	7.96
EVAPOTRANSPIRATION	385.10	361.09	399.37	381.74	385.10	361.09	399.37	381.74
RECHARGE	433.94	458.57	403.20	431.06	433.94	458.57	403.20	431.06
STORAGE CHANGE	-0.33	-0.95	6.92	-2.05	-0.33	-0.95	6.92	-2.05
CN	45.60	0.01	0.00	0.00	58.20	0.01	0.00	0.00
RECHARGE (% Ppt)	53.00	56.01	49.25	52.65	53.00	56.01	49.25	52.65
	I) The same as A but Slope =15% and SL = 10m				J) The same as A but Slope =40% and SL = 10m			
PRECIPITATION	818.71	818.71	818.71	818.71	818.71	818.71	818.71	818.71
RUNOFF	0.03	0.00	9.22	7.96	0.06	0.00	9.22	7.96
EVAPOTRANSPIRATION	385.06	361.09	399.37	381.74	385.10	361.09	399.37	381.74
RECHARGE	433.94	458.57	403.20	431.06	433.88	458.57	403.20	431.06
STORAGE CHANGE	-0.33	-0.95	6.92	-2.05	-0.33	-0.95	6.92	-2.05
CN	65.20	0.01	0.00	0.00	66.20	0.01	0.00	0.00
RECHARGE (% Ppt)	53.00	56.01	49.25	52.65	53.00	56.01	49.25	52.65

Parameters (mm)	TS	GS	Clay	GT	TS	GS	Clay	GT
	K) Specified CN but no slopes				L) S=23%; EZD=100cm, SL=25; CN specified)			
PRECIPITATION	818.71	818.71	818.71	818.71	818.71	818.71	818.71	818.71
RUNOFF	0.19	0.00	295.09	14.41	0.773	0	135.094	0.501
EVAPOTRANSPIRATION	385.20	361.09	398.38	381.36	445.106	400.706	488.915	434.24
RECHARGE	433.67	458.57	106.03	424.82	372.98042	418.92011	180.6012	387.31
STORAGE CHANGE	-0.34	-0.95	19.21	-1.88	-0.15	-0.916	14.1	-3.34
CN	70.00	50.00	77.00	55.00	74.74	60.10	80.38	63.48
RECHARGE (% Ppt)	52.97	56.01	12.95	51.89	45.56	51.17	22.06	47.31
	M) The same as A but Slope =7% and SL = 25m				N) Same as L but LAI=5			
PRECIPITATION	818.71	818.71	818.71	818.71	818.71	818.71	818.71	818.71
RUNOFF	0.002	0	9.218	7.957	6.569	0	171.766	5.519
EVAPOTRANSPIRATION	385.102	361.092	399.369	381.737	445.048	400.706	469.875	435.58
RECHARGE	433.934	458.5659	403.1991	431.06189	367.25963	418.92007	162.9795	380.82
STORAGE CHANGE	-0.327	-0.948	6.924	-2.047	-0.166	-0.916	14.089	-3.212
CN	61.30	0.01	0.00	0.00	82.30	62.79	87.05	74.74
RECHARGE (% Ppt)	53.00	56.01	49.25	52.65	44.86	51.17	19.91	46.51
	O) Same as N but S=100%				P) Same as N but S=268%			
PRECIPITATION	818.71	818.71	818.71	818.71	818.71	818.71	818.71	818.71
RUNOFF	7.811	0.005	159.915	6.82	8.727	0.015	171.407	7.772
EVAPOTRANSPIRATION	445.068	400.706	461.894	432.863	444.785	400.706	463.175	434.01
RECHARGE	366.0084	418.915	182.84383	382.22884	365.38335	418.90461	169.8242	380.17
STORAGE CHANGE	-0.177	-0.916	14.057	-3.202	-0.185	-0.916	14.304	-3.247
CN	83.70	64.89	87.50	75.90	84.03	66.23	87.89	76.65
RECHARGE (% Ppt)	44.71	51.17	22.33	46.69	44.63	51.17	20.74	46.44

APPENDIX C:

HELP RECHARGE RESULTS

Table C-1: HELP mean monthly recharge (mm/month) for current time period

Column Name	Jan	Feb	Mar	Apr	May	Jun	Jul	Aug	Sep	Oct	Nov	Dec
d1.5_LFSS_TS	129.7	90.6	49.9	30.0	16.5	16.0	6.4	3.5	2.3	1.8	13.6	84.9
d1.5_IBMS-SS_TS	129.7	90.6	50.0	30.0	16.6	15.8	6.4	3.5	2.3	1.8	13.6	84.8
d1.5_FZ_TS	129.7	90.6	49.9	30.1	16.4	16.0	6.3	3.5	2.3	1.9	13.5	85.1
d4_LFSS_TS	124.3	96.8	59.8	35.0	23.3	15.6	11.4	3.4	2.4	2.1	5.9	64.9
d4_IBMS-SS_TS	124.4	92.2	57.9	35.6	23.9	15.7	14.9	8.9	3.0	1.8	5.2	61.5
d4_FZ_TS	125.1	98.1	59.2	34.0	20.3	16.2	6.7	4.2	2.5	1.8	6.5	70.3
d7_LFSS_TS	112.2	101.5	70.9	41.7	30.9	18.4	18.8	5.2	2.3	1.8	3.0	38.8
d7_IBMS-SS_TS	112.2	101.5	70.9	41.7	30.9	18.4	18.8	5.2	2.3	1.8	3.0	38.8
d7_FZ_TS	116.4	105.6	70.1	40.4	26.8	17.2	7.5	3.5	2.2	1.8	3.6	49.8
d24_LFSS_TS	17.4	54.8	83.6	66.1	57.2	39.0	38.6	31.0	24.3	20.8	10.9	2.8
d24_IBMS-SS_TS	26.0	55.2	63.9	59.4	54.9	39.4	39.1	32.9	26.1	22.5	17.8	8.8
d24_FZ_TS	39.5	86.6	97.8	68.8	57.1	37.9	35.9	12.2	2.4	1.8	2.2	7.6
d1.5_LFSS_Clay	27.4	25.3	14.4	6.9	5.6	14.4	22.9	9.3	9.1	13.6	14.9	17.8
d7_FZ_Clay	24.5	24.8	17.4	8.7	6.3	8.5	24.8	8.4	7.9	11.9	14.1	19.1
d4_LFSS_Clay	29.3	24.3	14.9	7.4	6.3	15.2	18.5	8.0	7.2	12.8	15.5	21.1
d4_IBMS-SS_Clay	26.6	23.7	15.0	7.1	6.3	17.5	18.9	8.2	8.2	13.4	16.1	26.7
d4_FZ_Clay	32.5	27.4	15.6	7.1	6.3	18.0	17.5	8.6	7.7	12.6	13.2	20.6
d7_LFSS_Clay	25.4	21.5	18.4	11.5	7.0	7.2	22.7	11.3	8.1	10.0	14.4	16.5
d7_IBMS-SS_Clay	16.5	23.7	20.4	14.1	8.9	7.2	19.5	13.1	9.3	10.4	13.6	16.5
d24_LFSS_Clay	13.7	15.5	19.9	19.7	17.3	12.7	14.2	15.7	13.6	12.4	12.3	12.8
d24_IBMS-SS_Clay	12.2	13.0	16.7	18.9	17.5	13.3	12.7	15.7	13.7	12.7	11.8	12.6
d1.5_LFSS_GT	132.8	82.7	38.0	20.6	6.7	2.0	0.0	0.0	0.0	0.1	41.3	111.3
d1.5_IBMS-SS_GT	133.0	82.3	38.2	21.2	8.1	2.4	0.0	0.0	0.0	0.0	40.0	110.9
d1.5_FZ_GT	132.7	82.9	37.6	20.3	6.6	1.4	0.0	0.0	0.0	0.3	42.1	112.0
d4_LFSS_GT	86.6	101.8	77.0	45.0	33.5	21.3	18.1	17.1	12.3	10.0	7.8	23.5
d4_IBMS-SS_GT	87.0	101.4	75.2	45.0	33.7	22.0	17.6	17.3	12.6	10.4	8.5	23.3
d4_FZ_GT	87.2	102.3	77.1	44.8	33.3	20.0	19.2	16.4	12.2	10.0	8.2	23.4
d7_LFSS_GT	124.6	96.3	63.2	35.4	21.6	6.4	0.1	0.0	0.1	0.1	10.4	77.0
d7_IBMS_SS_GT	124.5	86.7	57.7	36.8	25.6	16.6	10.6	2.2	0.0	0.0	7.2	69.1
d7_FZ_GT	125.9	99.5	61.9	29.9	10.9	2.1	0.0	0.0	0.0	0.0	16.2	89.7
d24_LFSS_GT	36.3	76.0	90.2	64.9	53.8	38.6	31.0	24.1	12.6	1.7	1.0	6.7
d24_IBMS-SS_GT	37.4	65.6	68.9	58.5	52.1	39.8	32.8	25.9	20.6	18.1	11.9	5.8
d24_FZ_GT	65.7	98.8	97.9	65.3	52.1	28.5	4.2	0.0	0.0	0.0	2.2	22.1
d1.5_LFSS_GS	133.1	87.1	43.2	26.4	15.3	12.8	5.7	3.9	3.4	4.1	45.4	114.9
d1.5_IBMS-SS_GS	122.6	103.0	64.7	36.7	26.4	17.5	15.4	10.8	7.6	5.9	9.9	73.6
d4_LFSS_GS	122.9	102.5	64.8	37.1	26.8	17.4	15.8	10.9	7.4	5.8	9.9	73.0
d4_IBMS-SS_GS	123.0	101.6	63.4	37.4	26.8	17.6	15.9	11.4	8.2	6.4	9.5	73.0
d7_LFSS_GS	114.7	105.8	75.5	43.5	33.4	22.1	18.5	15.3	9.4	5.4	5.9	44.8
d7_IBMS-SS_GS	114.0	101.2	67.9	44.5	33.5	23.0	18.7	15.7	12.1	10.2	8.6	45.1
d24_LFSS_GS	21.8	60.3	91.4	71.9	59.2	45.1	36.9	31.9	26.4	23.3	18.2	9.6
d24_IBMS-SS_GS	35.4	70.6	68.6	63.3	56.7	45.5	38.0	33.2	27.6	24.9	20.0	11.5
d4_FZ_GS	122.6	103.0	64.7	36.7	26.4	17.5	15.4	10.8	7.6	5.9	9.9	73.6
d24_FZ_Clay	16.7	19.9	24.1	16.6	9.6	6.7	20.9	13.6	8.7	9.8	12.5	14.5
d7_FZ_GS	117.4	108.6	75.3	42.8	32.6	19.5	16.8	9.6	6.9	5.3	6.6	52.9
d24_FZ_GS	37.3	86.3	102.9	73.3	58.5	43.1	35.6	28.1	12.8	5.5	4.9	8.0

Table C-2: HELP mean monthly recharge (mm/month) for 2010-2039 time period.

Column Name	Jan	Feb	Mar	Apr	May	Jun	Jul	Aug	Sep	Oct	Nov	Dec
d1.5_LFSS_TS	146.7	136.9	96.8	66.5	36.1	20.2	10.0	4.3	2.6	6.1	101.9	231.4
d1.5_IBMS-SS_TS	146.6	136.9	96.8	66.5	36.1	20.2	10.0	4.3	2.6	6.0	102.0	231.4
d1.5_FZ_TS	146.7	136.8	96.8	66.5	36.1	20.1	10.0	4.3	2.6	6.1	102.1	231.4
d4_LFSS_TS	151.6	136.2	103.0	69.4	45.3	22.6	19.1	4.9	2.6	3.8	74.3	226.5
d4_IBMS-SS_TS	148.5	136.3	100.0	69.0	43.9	23.1	20.3	11.3	5.4	3.5	72.2	226.0
d4_FZ_TS	152.5	136.6	103.6	69.4	44.6	21.8	13.1	4.7	3.2	4.2	77.5	227.9
d7_LFSS_TS	155.3	135.7	110.9	73.8	54.2	29.1	25.4	12.9	2.6	2.6	45.2	211.6
d7_IBMS-SS_TS	155.3	135.7	110.9	73.8	54.2	29.1	25.4	12.9	2.6	2.6	45.2	211.6
d7_FZ_TS	159.0	135.6	112.6	74.5	52.9	27.4	17.4	4.3	2.6	3.0	53.0	216.3
d24_LFSS_TS	137.1	126.9	130.6	98.5	86.4	60.2	50.9	40.0	29.9	24.1	12.2	62.8
d24_IBMS-SS_TS	137.5	134.2	107.5	81.6	69.0	55.3	49.6	41.1	31.6	25.9	16.5	109.4
d24_FZ_TS	165.6	134.4	143.2	101.3	86.0	57.9	48.8	35.3	8.1	2.7	6.7	84.1
d1.5_LFSS_Clay	31.8	30.5	23.0	13.1	6.0	6.1	37.1	13.9	17.3	16.3	21.9	31.0
d7_FZ_Clay	30.7	30.4	24.5	16.2	7.0	6.4	27.2	15.5	16.3	14.5	22.9	27.7
d4_LFSS_Clay	26.0	24.8	14.7	11.7	6.5	6.3	26.0	12.3	15.6	12.0	21.5	32.8
d4_IBMS-SS_Clay	30.9	30.2	19.8	13.0	6.2	6.6	24.7	12.6	16.3	13.5	25.5	31.2
d4_FZ_Clay	31.3	34.0	22.0	14.5	6.5	7.1	31.3	13.7	16.3	13.6	30.0	36.8
d7_LFSS_Clay	39.4	36.7	26.6	18.6	10.4	7.0	19.4	18.9	13.2	14.3	15.6	28.0
d7_IBMS-SS_Clay	32.7	31.7	25.0	17.3	10.9	7.4	14.9	17.2	14.1	15.2	15.9	24.2
d24_LFSS_Clay	19.4	21.4	28.8	26.5	25.8	18.9	14.3	18.9	15.8	17.4	16.3	15.3
d24_IBMS-SS_Clay	18.0	18.2	23.3	23.3	23.1	18.1	13.7	17.1	14.1	15.3	14.4	15.9
d1.5_LFSS_GT	136.9	133.2	88.5	59.8	21.9	6.1	0.1	0.0	0.1	17.9	146.7	228.7
d1.5_IBMS-SS_GT	136.6	133.2	88.2	60.6	23.1	7.9	0.3	0.0	0.1	16.9	146.4	228.6
d1.5_FZ_GT	137.3	133.4	88.5	60.0	21.2	5.3	0.1	0.0	0.0	18.7	148.2	228.8
d4_LFSS_GT	167.0	132.8	116.9	78.2	56.9	34.0	23.4	20.8	14.3	11.8	29.0	172.9
d4_IBMS-SS_GT	166.3	133.0	115.8	77.7	56.5	34.0	23.4	21.0	14.9	12.1	29.5	173.7
d4_FZ_GT	167.7	132.4	117.5	78.1	56.8	33.3	23.9	20.2	13.7	11.7	29.3	173.3
d7_LFSS_GT	148.2	132.8	103.2	68.8	46.7	22.2	4.6	0.1	0.1	2.9	88.4	221.4
d7_IBMS_SS_GT	140.0	132.9	96.5	66.9	44.3	25.2	18.1	9.6	1.0	1.9	84.1	221.0
d7_FZ_GT	151.7	133.5	104.9	68.3	42.9	9.8	0.2	0.0	0.0	4.8	99.2	224.6
d24_LFSS_GT	143.6	128.5	126.7	94.3	83.9	56.8	43.5	31.5	23.7	14.2	5.8	86.5
d24_IBMS-SS_GT	134.9	132.4	103.9	78.9	69.2	53.7	44.6	33.2	25.4	20.0	14.1	131.6
d24_FZ_GT	169.6	134.0	136.1	95.5	82.7	54.1	33.5	4.1	0.0	0.6	15.1	114.7
d1.5_LFSS_GS	144.9	137.0	92.6	63.7	31.0	19.9	6.8	4.8	4.8	24.3	154.6	246.0
d1.5_IBMS-SS_GS	163.5	135.8	110.1	71.5	49.2	27.7	21.9	13.0	8.6	8.5	86.6	234.4
d4_LFSS_GS	162.9	136.0	109.9	71.5	49.3	27.9	22.3	13.4	8.4	8.5	86.1	234.4
d4_IBMS-SS_GS	162.3	135.9	109.0	71.0	48.8	28.1	22.5	13.8	9.3	9.1	86.1	234.8
d7_LFSS_GS	167.3	135.4	116.1	77.2	56.0	34.0	27.2	19.6	12.9	7.3	56.8	220.7
d7_IBMS-SS_GS	162.6	136.1	111.7	74.5	53.4	34.7	27.7	20.4	14.3	11.5	61.1	224.3
d24_LFSS_GS	155.2	131.8	134.3	102.6	86.1	64.6	50.8	42.1	32.8	27.2	16.0	87.1
d24_IBMS-SS_GS	155.8	135.6	114.0	85.1	67.6	58.4	49.7	42.8	34.0	28.9	23.3	135.4
d4_FZ_GS	163.5	135.8	110.1	71.5	49.2	27.7	21.9	13.0	8.6	8.5	86.6	234.4
d24_FZ_Clay	24.3	25.5	31.5	29.1	23.1	11.4	14.5	23.6	16.6	14.0	14.5	19.3
d7_FZ_GS	170.9	134.0	118.1	77.4	55.5	33.0	27.1	13.2	7.8	7.0	63.6	222.7
d24_FZ_GS	173.8	134.7	145.9	105.1	86.0	62.2	48.9	40.1	29.0	11.0	8.1	86.3

Table C-3: HELP mean monthly recharge (mm/month) for 2040-2069 time period.

Column Name	Jan	Feb	Mar	Apr	May	Jun	Jul	Aug	Sep	Oct	Nov	Dec
d1.5_LFSS_TS	170.2	141.3	94.2	67.9	40.7	20.7	10.1	4.4	2.8	14.8	132.6	236.1
d1.5_IBMS-SS_TS	170.2	141.3	94.1	67.9	40.8	20.8	10.0	4.4	2.8	14.8	132.5	236.2
d1.5_FZ_TS	170.2	141.4	94.1	67.9	40.8	20.7	9.9	4.4	2.8	14.8	132.8	236.0
d4_LFSS_TS	171.1	145.0	99.4	72.8	48.0	23.3	19.5	4.8	2.8	8.8	105.2	235.2
d4_IBMS-SS_TS	170.6	143.0	97.2	70.9	47.2	23.8	20.3	11.2	5.6	8.5	103.4	234.0
d4_FZ_TS	171.7	146.2	100.4	72.3	47.9	21.7	13.7	4.9	3.2	9.7	108.6	235.5
d7_LFSS_TS	173.2	147.8	107.9	76.0	56.0	30.2	25.7	13.0	2.7	4.5	68.7	230.0
d7_IBMS-SS_TS	173.2	147.8	107.9	76.0	56.0	30.2	25.7	13.0	2.7	4.5	68.7	230.0
d7_FZ_TS	174.6	150.2	111.1	76.0	55.6	28.0	17.9	4.3	2.8	5.3	78.2	231.8
d24_LFSS_TS	160.6	154.7	134.4	96.9	85.2	61.6	51.8	40.4	30.0	23.8	11.6	83.8
d24_IBMS-SS_TS	165.3	145.2	108.5	78.0	70.0	56.4	50.4	41.5	31.8	25.6	14.1	148.8
d24_FZ_TS	175.1	161.8	150.9	102.6	85.1	59.4	49.8	36.0	8.8	2.6	9.0	107.8
d1.5_LFSS_Clay	39.2	21.7	16.4	10.7	5.5	6.3	30.7	18.4	17.2	21.2	27.4	40.4
d7_FZ_Clay	44.2	32.8	26.9	15.4	8.6	6.8	27.3	19.6	17.1	18.4	18.8	39.1
d4_LFSS_Clay	40.9	26.9	20.6	12.3	7.4	7.2	29.4	15.7	16.3	20.4	28.5	39.3
d4_IBMS-SS_Clay	41.7	28.8	21.8	13.2	7.2	7.3	30.0	15.6	16.4	18.7	25.5	41.7
d4_FZ_Clay	39.4	25.5	22.4	14.0	7.6	7.6	29.3	15.0	15.8	21.3	20.9	37.7
d7_LFSS_Clay	48.3	37.6	27.6	20.0	10.6	7.1	17.7	21.1	15.5	19.5	20.5	36.3
d7_IBMS-SS_Clay	45.9	32.3	21.6	15.9	11.5	7.6	13.5	17.9	14.0	18.1	22.3	40.0
d24_LFSS_Clay	22.5	30.6	33.0	29.9	26.3	19.1	13.8	17.9	15.9	18.1	18.4	18.6
d24_IBMS-SS_Clay	18.2	25.7	30.1	28.9	26.4	20.6	15.2	16.1	15.0	16.1	17.0	17.0
d1.5_LFSS_GT	167.3	134.6	88.5	60.9	26.2	5.7	0.0	0.1	0.0	33.8	173.4	228.0
d1.5_IBMS-SS_GT	167.2	134.3	88.5	61.5	27.6	7.2	0.0	0.1	0.0	33.4	172.5	227.8
d1.5_FZ_GT	167.8	134.6	88.6	60.6	25.6	5.0	0.0	0.0	0.1	35.1	174.2	228.3
d4_LFSS_GT	177.2	149.4	120.7	77.9	59.0	34.9	24.7	19.8	15.4	13.0	41.6	206.5
d4_IBMS-SS_GT	176.8	149.1	119.7	77.3	58.6	35.1	24.7	20.0	15.7	13.4	42.6	207.1
d4_FZ_GT	177.9	149.3	121.2	78.1	58.9	34.2	24.9	19.4	15.0	12.9	41.9	206.5
d7_LFSS_GT	169.6	144.4	99.4	72.6	49.0	22.7	4.2	0.1	0.0	9.5	120.8	226.2
d7_IBMS_SS_GT	168.4	138.1	93.7	69.3	47.4	26.5	17.7	8.9	0.9	8.3	116.3	224.3
d7_FZ_GT	171.4	146.1	102.1	71.5	45.7	10.2	0.0	0.0	0.0	12.7	130.9	228.6
d24_LFSS_GT	165.5	155.3	128.0	95.6	83.4	58.4	43.9	31.6	23.9	14.0	7.5	111.3
d24_IBMS-SS_GT	164.1	141.1	102.1	79.5	69.5	55.5	44.7	33.1	25.3	19.8	16.7	168.1
d24_FZ_GT	177.4	159.3	142.6	99.5	82.8	55.8	33.9	4.8	0.0	1.0	21.4	141.1
d1.5_LFSS_GS	170.4	139.9	91.2	64.5	36.5	18.7	7.1	5.2	5.3	43.0	179.5	246.3
d1.5_IBMS-SS_GS	175.9	148.2	109.8	72.6	51.9	28.9	20.9	12.6	8.8	15.6	116.8	245.4
d4_LFSS_GS	175.4	148.1	109.5	72.5	52.0	29.2	21.3	13.2	8.6	15.3	116.7	245.7
d4_IBMS-SS_GS	174.9	147.9	108.5	71.8	51.7	29.3	21.5	13.5	9.4	16.4	116.8	245.7
d7_LFSS_GS	177.9	150.6	117.4	76.1	58.4	36.1	26.6	19.1	12.9	11.0	80.9	240.3
d7_IBMS-SS_GS	175.0	148.3	112.3	72.8	57.2	36.5	27.2	20.0	14.0	15.4	87.1	243.1
d24_LFSS_GS	175.1	158.5	140.8	99.5	85.4	65.9	52.3	42.1	32.5	26.5	14.9	113.8
d24_IBMS-SS_GS	170.6	149.0	118.2	79.4	69.8	59.4	51.3	42.9	33.8	28.3	23.7	180.9
d4_FZ_GS	175.9	148.2	109.8	72.6	51.9	28.9	20.9	12.6	8.8	15.6	116.8	245.4
d24_FZ_Clay	25.2	30.5	28.6	24.7	19.9	11.1	12.6	21.6	18.9	18.0	17.5	23.2
d7_FZ_GS	179.8	151.3	119.8	76.9	58.0	35.1	25.8	13.0	8.0	10.8	87.9	241.2
d24_FZ_GS	183.2	162.0	155.8	106.6	84.9	64.1	50.4	40.1	29.1	10.9	10.7	109.2

Table C-4: HELP mean monthly recharge (mm/month) for 2070-2099 time period.

Column Name	Jan	Feb	Mar	Apr	May	Jun	Jul	Aug	Sep	Oct	Nov	Dec
d1.5_LFSS_TS	133.1	159.9	175.6	114.8	41.5	24.0	8.5	4.2	2.8	11.2	160.7	180.8
d1.5_IBMS-SS_TS	133.1	159.8	175.6	114.8	41.6	23.9	8.5	4.2	2.8	11.2	160.6	180.8
d1.5_FZ_TS	133.1	159.9	175.5	114.8	41.4	23.9	8.4	4.2	2.8	11.2	160.8	180.8
d4_LFSS_TS	135.2	156.6	174.6	126.1	51.5	28.1	18.0	4.4	2.8	6.6	134.8	178.5
d4_IBMS-SS_TS	134.0	158.6	175.6	118.7	50.5	28.5	20.1	10.5	5.0	6.4	131.8	177.1
d4_FZ_TS	136.3	155.9	173.4	129.1	50.7	27.2	11.1	4.5	3.2	7.0	139.1	179.7
d7_LFSS_TS	137.4	153.0	175.1	135.0	63.3	34.8	27.6	11.7	2.8	4.1	104.3	168.4
d7_IBMS-SS_TS	137.4	153.0	175.1	135.0	63.3	34.8	27.6	11.7	2.8	4.1	104.3	168.4
d7_FZ_TS	140.1	150.3	173.9	141.4	62.5	33.4	17.4	4.2	2.7	4.4	113.4	174.1
d24_LFSS_TS	108.8	131.9	175.5	153.6	109.8	71.0	58.9	42.6	31.1	25.0	22.8	86.3
d24_IBMS-SS_TS	117.0	154.8	175.4	123.1	75.9	61.4	56.1	43.4	32.6	26.8	41.2	109.1
d24_FZ_TS	134.9	131.3	169.0	174.4	116.8	69.7	56.5	39.5	11.2	2.3	23.5	106.5
d1.5_LFSS_Clay	39.6	39.5	43.5	17.3	7.6	12.0	29.9	14.3	15.5	22.7	20.0	32.0
d7_FZ_Clay	36.6	37.1	34.1	20.6	8.6	6.9	26.5	14.2	16.0	20.9	18.3	27.2
d4_LFSS_Clay	39.8	36.4	34.9	15.9	8.1	11.3	27.4	14.6	15.4	23.8	23.1	45.1
d4_IBMS-SS_Clay	40.6	33.8	34.4	12.9	7.3	10.6	23.7	14.4	14.3	23.5	20.3	38.5
d4_FZ_Clay	39.7	35.0	37.6	16.2	7.8	10.8	24.0	13.1	15.1	23.1	22.5	36.8
d7_LFSS_Clay	39.5	40.6	38.0	25.5	11.2	7.4	19.4	17.8	15.4	21.8	19.5	31.9
d7_IBMS-SS_Clay	26.1	27.6	27.2	21.2	11.7	7.6	13.5	14.3	13.8	18.2	19.5	21.7
d24_LFSS_Clay	20.1	23.9	28.8	36.0	31.7	22.1	17.0	20.6	18.7	17.8	19.7	18.2
d24_IBMS-SS_Clay	18.2	22.5	28.2	36.9	33.8	24.8	18.6	21.5	18.8	18.0	19.8	16.1
d1.5_LFSS_GT	129.4	157.2	176.3	95.3	27.6	6.8	0.0	0.0	0.0	31.2	194.1	177.1
d1.5_IBMS-SS_GT	129.2	156.9	176.3	94.5	29.2	8.1	0.0	0.1	0.0	31.2	192.1	176.7
d1.5_FZ_GT	129.5	157.6	176.4	95.2	26.8	6.0	0.0	0.0	0.0	32.3	195.4	177.1
d4_LFSS_GT	143.5	144.0	168.0	149.4	70.3	38.4	28.6	20.5	14.7	11.4	71.9	153.9
d4_IBMS-SS_GT	143.1	144.6	167.9	148.4	68.8	38.6	28.7	20.8	14.8	12.3	72.6	154.1
d4_FZ_GT	143.4	143.7	167.9	150.2	70.4	37.9	28.7	20.0	14.0	11.5	72.4	154.6
d7_LFSS_GT	133.3	153.1	171.8	123.7	54.0	26.3	5.0	0.1	0.0	6.3	143.4	178.1
d7_IBMS_SS_GT	130.6	155.3	175.0	106.6	51.6	29.7	18.4	9.7	1.0	5.8	137.0	174.5
d7_FZ_GT	28.7	30.9	50.2	68.5	98.1	76.3	33.4	37.6	44.8	38.1	23.4	24.9
d24_LFSS_GT	120.6	135.1	171.0	151.3	104.2	67.3	48.2	34.0	25.3	17.6	22.3	99.8
d24_IBMS-SS_GT	120.1	153.2	173.7	114.6	76.7	60.8	48.0	35.0	26.5	20.5	45.3	120.8
d24_FZ_GT	142.8	132.6	160.4	171.0	108.2	65.1	43.5	8.8	0.0	0.5	40.0	126.0
d1.5_LFSS_GS	131.1	162.2	178.9	108.1	38.2	20.3	6.1	4.7	4.5	38.0	215.4	184.7
d1.5_IBMS-SS_GS	139.7	152.5	173.7	141.0	57.6	33.6	21.9	12.4	8.2	10.8	155.1	188.0
d4_LFSS_GS	139.3	153.0	173.5	140.3	57.7	33.8	22.5	13.0	8.1	10.6	154.7	187.9
d4_IBMS-SS_GS	139.0	153.9	173.1	139.0	56.9	33.9	22.8	13.5	9.0	11.3	154.7	187.3
d7_LFSS_GS	141.7	148.7	175.2	146.2	69.0	40.6	30.4	19.6	12.5	7.5	123.9	179.1
d7_IBMS-SS_GS	139.8	153.1	174.0	139.5	63.1	40.8	31.2	20.4	13.8	12.8	128.9	178.2
d24_LFSS_GS	121.9	136.9	174.6	157.6	116.1	76.0	60.4	46.3	34.7	28.3	33.3	107.6
d24_IBMS-SS_GS	130.3	152.1	173.6	140.0	75.8	64.2	57.6	46.6	35.8	30.1	60.9	127.3
d4_FZ_GS	139.7	152.5	173.7	141.0	57.6	33.6	21.9	12.4	8.2	10.8	155.1	188.0
d24_FZ_Clay	22.8	28.1	33.1	35.1	27.7	14.9	15.7	20.0	15.8	19.0	17.8	18.3
d7_FZ_GS	143.0	147.5	174.1	151.1	69.0	39.5	29.5	12.7	7.6	7.6	129.2	184.2
d24_FZ_GS	139.6	130.9	165.9	173.4	125.2	74.5	58.5	44.0	31.8	12.4	24.9	113.6

Table C-5: HELP mean annual water balance for the current time period.

HELP Column	Precipitation (mm)	Runoff (mm)	Evapotranspiration (mm)	Recharge (mm)	Storage (mm)	Recharge (% Ppt)
d1.5_LFSS_TS	880.48	4.50	430.46	445.27	0.25	50.57
d1.5_IBMS-SS_TS	880.48	4.50	430.64	445.09	0.25	50.55
d1.5_FZ_TS	880.48	4.50	430.51	445.22	0.25	50.57
d1.5_Clay	880.48	204.68	494.32	181.70	-0.22	20.64
d1.5_LFSS_GT	880.48	5.57	439.15	435.53	0.22	49.47
d1.5_IBMS-SS_GT	880.48	5.73	438.27	436.25	0.22	49.55
d1.5_FZ_GT	880.48	5.44	438.76	435.98	0.30	49.52
d1.5_GS	880.48	0.05	384.64	495.49	0.30	56.28
d4_LFSS_TS	880.48	4.50	430.64	444.94	0.41	50.53
d4_IBMS-SS_TS	880.48	4.50	430.64	445.04	0.30	50.55
d4_FZ_TS	880.48	4.50	430.64	444.93	0.42	50.53
d4_LFSS_Clay	880.48	193.62	491.39	180.56	14.91	20.51
d4_IBMS-SS_Clay	880.48	190.26	487.60	187.87	14.75	21.34
d4_FZ_Clay	880.48	189.32	489.31	187.12	14.74	21.25
d4_LFSS_GT	880.48	5.23	422.59	454.10	-1.44	51.57
d4_IBMS-SS_GT	880.48	5.23	422.59	454.05	-1.39	51.57
d4_FZ_GT	880.48	5.23	422.59	454.07	-1.41	51.57
d4_LFSS_GS	880.48	0.05	385.65	494.19	0.58	56.13
d4_IBMS-SS_GS	880.48	0.05	385.65	494.26	0.51	56.14
d4_FZ_GS	880.48	0.05	385.65	494.19	0.58	56.13
d7_LFSS_TS	880.48	4.50	430.64	445.30	0.04	50.57
d7_IBMS-SS_TS	880.48	4.50	430.64	445.30	0.04	50.57
d7_FZ_TS	880.48	4.50	430.64	444.96	0.39	50.54
d7_FZ_Clay	880.48	195.76	492.83	176.44	15.45	20.04
d7_LFSS_GT	880.48	5.57	439.32	435.21	0.38	49.43
d7_IBMS_SS_GT	880.48	5.73	437.55	436.99	0.21	49.63
d7_FZ_GT	880.48	5.49	438.45	436.19	0.35	49.54
d7_LFSS_GS	880.48	0.05	385.65	494.39	0.38	56.15
d7_IBMS-SS_GS	880.48	0.00	385.49	494.71	0.28	56.19
d7_FZ_GS	880.48	0.05	385.65	494.23	0.54	56.13
d24_LFSS_TS	880.48	4.50	430.64	446.65	-1.31	50.73
d24_IBMS-SS_TS	880.48	4.50	430.64	446.09	-0.75	50.66
d24_FZ_TS	880.48	1.53	430.37	449.80	-1.23	51.09
d24_LFSS_Clay	880.48	194.40	490.76	179.66	15.66	20.40
d24_IBMS-SS_Clay	880.48	200.21	491.32	170.57	18.38	19.37
d24_FZ_Clay	880.48	199.33	491.97	173.59	15.59	19.72
d24_LFSS_GT	880.48	5.58	438.95	437.14	-1.19	49.65
d24_IBMS-SS_GT	880.48	5.73	437.79	437.38	-0.42	49.68
d24_FZ_GT	880.48	5.43	438.94	436.95	-0.84	49.63
d24_LFSS_GS	880.48	0.05	385.65	495.88	-1.11	56.32
d24_IBMS-SS_GS	880.48	0.05	385.65	495.18	-0.40	56.24
d24_FZ_GS	880.48	0.05	385.65	496.29	-1.52	56.37
D7_LFSS_Clay	880.48	197.86	494.00	173.77	14.85	19.74
D7_IBMS-SS_Clay	880.48	201.84	489.66	173.21	15.77	19.67

Table C-6: HELP mean annual water balance for the 2010-2039 time period.

HELP Column	Precipitation (mm)	Runoff (mm)	Evapotranspiration (mm)	Recharge (mm)	Storage (mm)	Recharge (% Ppt)
d1.5_LFSS_TS	1413.97	30.10	523.27	859.60	1.01	60.79
d1.5_IBMS-SS_TS	1413.97	30.09	523.46	859.42	1.00	60.78
d1.5_FZ_TS	1413.97	30.09	523.46	859.41	1.01	60.78
d1.5_Clay	1413.97	612.62	553.43	247.93	0.00	17.53
d1.5_LFSS_GT	1413.97	43.56	529.83	839.93	0.66	59.40
d1.5_IBMS-SS_GT	1413.97	44.23	527.31	841.82	0.62	59.54
d1.5_FZ_GT	1413.97	42.66	529.18	841.43	0.70	59.51
d1.5_GS	1413.97	2.22	480.33	930.60	0.82	65.81
d4_LFSS_TS	1413.97	30.09	523.46	859.32	1.11	60.77
d4_IBMS-SS_TS	1413.97	30.09	523.46	859.41	1.02	60.78
d4_FZ_TS	1413.97	30.09	523.46	859.06	1.36	60.76
d4_LFSS_Clay	1413.97	619.77	572.63	210.21	11.37	14.87
d4_IBMS-SS_Clay	1413.97	605.81	566.29	230.51	11.38	16.30
d4_FZ_Clay	1413.97	594.18	551.30	257.13	11.36	18.18
d4_LFSS_GT	1413.97	41.44	512.30	857.99	2.24	60.68
d4_IBMS-SS_GT	1413.97	41.44	512.30	857.98	2.25	60.68
d4_FZ_GT	1413.97	41.44	512.30	857.92	2.31	60.67
d4_LFSS_GS	1413.97	2.22	479.35	930.59	1.81	65.81
d4_IBMS-SS_GS	1413.97	2.22	479.35	930.58	1.82	65.81
d4_FZ_GS	1413.97	2.22	479.35	930.59	1.81	65.81
d7_LFSS_TS	1413.97	30.09	523.46	859.20	1.22	60.77
d7_IBMS-SS_TS	1413.97	30.09	523.46	859.20	1.22	60.77
d7_FZ_TS	1413.97	30.09	523.46	858.61	1.81	60.72
d7_FZ_Clay	1413.97	609.64	553.03	239.44	11.87	16.93
d7_LFSS_GT	1413.97	43.58	530.10	839.31	0.99	59.36
d7_IBMS_SS_GT	1413.97	44.24	527.60	841.51	0.63	59.51
d7_FZ_GT	1413.97	43.00	529.47	839.90	1.61	59.40
d7_LFSS_GS	1413.97	2.22	479.35	930.62	1.78	65.82
d7_IBMS-SS_GS	1413.97	0.09	479.68	932.38	1.82	65.94
d7_FZ_GS	1413.97	2.22	479.35	930.28	2.12	65.79
d24_LFSS_TS	1413.97	30.09	523.46	859.65	0.77	60.80
d24_IBMS-SS_TS	1413.97	30.09	523.46	859.40	1.02	60.78
d24_FZ_TS	1413.97	15.28	523.34	874.11	1.25	61.82
d24_LFSS_Clay	1413.97	606.04	556.67	238.71	12.56	16.88
d24_IBMS-SS_Clay	1413.97	619.33	563.89	214.50	16.26	15.17
d24_FZ_Clay	1413.97	601.77	552.48	247.36	12.37	17.49
d24_LFSS_GT	1413.97	43.64	530.06	839.03	1.24	59.34
d24_IBMS-SS_GT	1413.97	44.19	527.28	841.87	0.64	59.54
d24_FZ_GT	1413.97	42.65	529.56	840.08	1.68	59.41
d24_LFSS_GS	1413.97	2.22	479.35	930.62	1.78	65.82
d24_IBMS-SS_GS	1413.97	2.22	479.35	930.58	1.82	65.81
d24_FZ_GS	1413.97	2.22	479.35	931.14	1.26	65.85
d7_LFSS_Clay	1413.97	593.36	560.95	247.94	11.73	17.53
d7_IBMS-SS_Clay	1413.97	609.01	566.41	226.37	12.19	16.01

Table C-7: HELP mean annual water balance for the 2040-2069 time period.

HELP Column	Precipitation (mm)	Runoff (mm)	Evapotranspiration (mm)	Recharge (mm)	Storage (mm)	Recharge (% Ppt)
d1.5_LFSS_TS	1517.24	26.21	557.77	935.76	-2.50	61.68
d1.5_IBMS-SS_TS	1517.24	26.21	557.83	935.70	-2.50	61.67
d1.5_FZ_TS	1517.24	26.21	557.83	935.70	-2.50	61.67
d1.5_Clay	1517.24	649.81	612.30	255.14	-0.02	16.82
d1.5_LFSS_GT	1517.24	37.97	563.30	918.58	-2.60	60.54
d1.5_IBMS-SS_GT	1517.24	38.67	560.95	920.21	-2.59	60.65
d1.5_FZ_GT	1517.24	37.10	562.78	919.96	-2.61	60.63
d1.5_GS	1517.24	1.50	511.18	1007.42	-2.86	66.40
d4_LFSS_TS	1517.24	26.21	557.83	935.74	-2.54	61.67
d4_IBMS-SS_TS	1517.24	26.21	557.83	935.70	-2.50	61.67
d4_FZ_TS	1517.24	26.21	557.83	935.74	-2.54	61.67
d4_LFSS_Clay	1517.24	646.41	592.75	264.83	13.24	17.45
d4_IBMS-SS_Clay	1517.24	645.46	590.66	267.88	13.24	17.66
d4_FZ_Clay	1517.24	657.70	589.83	256.47	13.24	16.90
d4_LFSS_GT	1517.24	35.80	544.11	940.09	-2.75	61.96
d4_IBMS-SS_GT	1517.24	35.80	544.11	940.08	-2.75	61.96
d4_FZ_GT	1517.24	35.80	544.11	940.11	-2.77	61.96
d4_LFSS_GS	1517.24	1.50	511.24	1007.45	-2.95	66.40
d4_IBMS-SS_GS	1517.24	1.50	511.24	1007.43	-2.93	66.40
d4_FZ_GS	1517.24	1.50	511.24	1007.47	-2.97	66.40
d7_LFSS_TS	1517.24	26.21	557.83	935.79	-2.59	61.68
d7_IBMS-SS_TS	1517.24	26.21	557.83	935.79	-2.59	61.68
d7_FZ_TS	1517.24	26.21	557.83	935.81	-2.61	61.68
d7_FZ_Clay	1517.24	643.42	584.68	274.91	14.24	18.12
d7_LFSS_GT	1517.24	37.95	563.48	918.42	-2.62	60.53
d7_IBMS_SS_GT	1517.24	38.66	561.31	919.80	-2.54	60.62
d7_FZ_GT	1517.24	37.42	563.37	919.07	-2.63	60.58
d7_LFSS_GS	1517.24	1.50	511.24	1007.46	-2.96	66.40
d7_IBMS-SS_GS	1517.24	0.06	511.16	1008.95	-2.93	66.50
d7_FZ_GS	1517.24	1.50	511.24	1007.54	-3.04	66.41
d24_LFSS_TS	1517.24	26.21	557.83	934.75	-1.55	61.61
d24_IBMS-SS_TS	1517.24	26.21	557.83	935.70	-2.50	61.67
d24_FZ_TS	1517.24	12.40	557.66	948.90	-1.72	62.54
d24_LFSS_Clay	1517.24	636.71	600.51	264.10	15.92	17.41
d24_IBMS-SS_Clay	1517.24	640.21	612.04	246.35	18.63	16.24
d24_FZ_Clay	1517.24	654.43	597.00	251.66	14.15	16.59
d24_LFSS_GT	1517.24	37.98	562.74	918.42	-1.90	60.53
d24_IBMS-SS_GT	1517.24	38.65	561.60	919.51	-2.53	60.60
d24_FZ_GT	1517.24	37.11	562.47	919.44	-1.79	60.60
d24_LFSS_GS	1517.24	1.50	511.24	1007.48	-2.98	66.40
d24_IBMS-SS_GS	1517.24	1.50	511.24	1007.42	-2.92	66.40
d24_FZ_GS	1517.24	1.50	511.24	1006.78	-2.28	66.36
d7_LFSS_Clay	1517.24	626.53	595.51	281.68	13.52	18.57
d7_IBMS-SS_Clay	1517.24	633.25	609.51	260.51	13.97	17.17

Table C-8: HELP mean annual water balance for the 2040-2069 time period.

HELP Column	Precipitation (mm)	Runoff (mm)	Evapotranspiration (mm)	Recharge (mm)	Storage (mm)	Recharge (% Ppt)
d1.5_LFSS_TS	1599.06	34.07	549.05	1016.99	-1.06	63.60
d1.5_IBMS-SS_TS	1599.06	34.07	549.15	1016.88	-1.05	63.59
d1.5_FZ_TS	1599.06	34.07	549.15	1016.90	-1.06	63.59
d1.5_Clay	1599.06	721.32	583.75	293.84	0.15	18.38
d1.5_LFSS_GT	1599.06	50.12	554.72	994.99	-0.77	62.22
d1.5_IBMS-SS_GT	1599.06	50.94	554.46	994.41	-0.75	62.19
d1.5_FZ_GT	1599.06	48.98	554.58	996.26	-0.76	62.30
d1.5_GS	1599.06	2.54	505.60	1091.90	-0.97	68.28
d4_LFSS_TS	1599.06	34.07	549.15	1017.19	-1.35	63.61
d4_IBMS-SS_TS	1599.06	34.07	549.15	1016.91	-1.07	63.59
d4_FZ_TS	1599.06	34.07	549.15	1017.28	-1.44	63.62
d4_LFSS_Clay	1599.06	712.40	580.28	295.78	10.60	18.50
d4_IBMS-SS_Clay	1599.06	713.70	600.29	274.44	10.62	17.16
d4_FZ_Clay	1599.06	710.06	596.65	281.77	10.58	17.62
d4_LFSS_GT	1599.06	47.98	539.02	1014.73	-2.67	63.46
d4_IBMS-SS_GT	1599.06	47.98	539.02	1014.66	-2.60	63.45
d4_FZ_GT	1599.06	47.98	539.02	1014.74	-2.68	63.46
d4_LFSS_GS	1599.06	2.54	504.11	1094.38	-1.96	68.44
d4_IBMS-SS_GS	1599.06	2.54	504.11	1094.35	-1.93	68.44
d4_FZ_GS	1599.06	2.54	504.11	1094.44	-2.03	68.44
d7_LFSS_TS	1599.06	34.07	549.15	1017.42	-1.58	63.63
d7_IBMS-SS_TS	1599.06	34.07	549.15	1017.42	-1.58	63.63
d7_FZ_TS	1599.06	34.07	549.15	1017.81	-1.97	63.65
d7_FZ_Clay	1599.06	736.57	584.62	267.14	10.73	16.71
d7_LFSS_GT	1599.06	50.10	555.31	995.20	-1.55	62.24
d7_IBMS_SS_GT	1599.06	50.95	553.77	995.24	-0.90	62.24
d7_FZ_GT	1599.06	49.37	554.88	996.60	-1.79	62.32
d7_LFSS_GS	1599.06	2.54	504.11	1094.50	-2.09	68.45
d7_IBMS-SS_GS	1599.06	0.27	504.95	1095.76	-1.92	68.53
d7_FZ_GS	1599.06	2.54	504.11	1094.97	-2.56	68.48
d24_LFSS_TS	1599.06	34.07	549.15	1017.26	-1.43	63.62
d24_IBMS-SS_TS	1599.06	34.07	549.15	1017.04	-1.21	63.60
d24_FZ_TS	1599.06	16.83	549.15	1035.63	-2.56	64.76
d24_LFSS_Clay	1599.06	729.16	581.71	274.56	13.62	17.17
d24_IBMS-SS_Clay	1599.06	719.85	585.96	276.96	16.29	17.32
d24_FZ_Clay	1599.06	723.62	595.23	268.24	11.96	16.77
d24_LFSS_GT	1599.06	50.15	554.95	996.74	-2.78	62.33
d24_IBMS-SS_GT	1599.06	50.98	554.04	995.21	-1.18	62.24
d24_FZ_GT	1599.06	48.96	554.77	998.84	-3.52	62.46
d24_LFSS_GS	1599.06	2.54	504.11	1093.74	-1.33	68.40
d24_IBMS-SS_GS	1599.06	2.54	504.11	1094.32	-1.91	68.44
d24_FZ_GS	1599.06	2.54	504.11	1094.70	-2.29	68.46
d7_LFSS_Clay	1599.06	707.92	590.77	287.99	12.37	18.01
d7_IBMS-SS_Clay	1599.06	755.87	609.36	222.37	11.46	13.91